

QA: QA

**Civilian Radioactive Waste Management System  
Management & Operating Contractor**

**Evaluation of Codisposal Viability for Th/U Oxide (Shippingport LWBR)  
DOE-Owned Fuel**

**TDR-EDC-NU-000005 REV 00**

**September 2000**

Prepared for:

U.S. Department of Energy  
Yucca Mountain Site Characterization Office  
P.O. Box 30307  
North Las Vegas, Nevada 89036-0307

Prepared By:

TRW Environmental Safety Systems Inc.  
1180 Town Center Drive  
Las Vegas, Nevada 89144

Under Contract Number  
DE-AC08-91RW00134

#### **DISCLAIMER**

This report was prepared as an account of work sponsored by an agency of the United States Government. Neither the United States Government nor any agency thereof, nor any of their employees, nor any of their contractors, subcontractors or their employees, makes any warranty, express or implied, or assumes any legal liability or responsibility for the accuracy, completeness, or any third party's use or the results of such use of any information, apparatus, product, or process disclosed, or represents that its use would not infringe privately owned rights. Reference herein to any specific commercial product, process, or service by trade name, trademark, manufacturer, or otherwise, does not necessarily constitute or imply its endorsement, recommendation, or favoring by the United States Government or any agency thereof or its contractors or subcontractors. The views and opinions of authors expressed herein do not necessarily state or reflect those of the United States Government or any agency thereof.

**Civilian Radioactive Waste Management System  
Management & Operating Contractor**

**Evaluation of Codisposal Viability for Th/U Oxide (Shippingport LWBR)  
DOE-Owned Fuel**

**TDR-EDC-NU-000005 REV 00**

**September 2000**

Prepared By:

*Horia R. Radulescu*

\_\_\_\_\_  
Horia R. Radulescu  
DOE Fuel Analysis, Waste Package Department

*09/18/2000*

\_\_\_\_\_  
Date

Checked by:

*S.F. Alex Deng*

\_\_\_\_\_  
S.F. Alex Deng  
DOE Fuel Analysis, Waste Package Department

*09/18/2000*

\_\_\_\_\_  
Date

Approved By:

*J. Wesley Davis*

\_\_\_\_\_  
J. Wesley Davis, Manager  
DOE Fuel Analysis, Waste Package Department

*9/19/00*

\_\_\_\_\_  
Date



## HISTORY OF CHANGE

**Revision Number**  
00

**Description of Change**  
Initial Issue

INTENTIONALLY LEFT BLANK

## EXECUTIVE SUMMARY

### INTRODUCTION

This report provides the technical information that supports the disposal, in the potential Monitored Geologic Repository (MGR) at Yucca Mountain, of the spent nuclear fuel (SNF) owned by the U.S. Department of Energy (DOE) that was removed from the Shippingport light water breeder reactor (LWBR).

There are more than 250 forms of DOE-owned SNF. Due to the variety of the SNF, the National Spent Nuclear Fuel Program (NSNFP) has designated nine representative fuel groups for disposal criticality analyses based on fuel matrix, primary fissile isotope, and enrichment. The SNF from the Shippingport LWBR has been designated as the representative fuel for the thorium-uranium oxide (Th/U oxide) SNF group, which is a mixture of thorium and uranium oxides clad with Zircaloy-4. The uranium concentration in the mixture is maximum 5.2 wt.%, whereas the U-233 content is 5.11 wt.%. The Shippingport LWBR fuel is a “seed and blanket” type fuel. This technical report addresses the seed type fuel assemblies that are presently the only candidates for intact disposal. The blanket and reflector assemblies may be subject to deroding or partial disassembly to meet both dimensional constraints and/or fissile limits for existing standard SNF canister design (DOE 1999a). Therefore, this report does not specifically address the disposal of blanket and reflector assemblies in the MGR. Demonstration that other fuels in this group are bounded by the Shippingport LWBR analysis remains to be performed in the future before acceptance of these fuel forms.

The results of the analyses will be used to develop waste acceptance criteria. The parameters and conditions that are important to criticality control are identified herein based on the analysis needs and sensitivities of the results. Prior to acceptance of fuel from the Th/U oxide fuel group for disposal, the criticality control items for the fuel types that are being considered for disposal under the Th/U oxide fuel group must be demonstrated to satisfy the conditions determined in this report.

The intact and degraded component criticality analyses have been performed following the disposal criticality analysis methodology, which has been documented in *Disposal Criticality Analysis Methodology Topical Report* (YMP 1998) and submitted to the U.S. Nuclear Regulatory Commission. The methodology includes the analysis of the geochemical and physical processes that can breach the waste package and degrade the waste forms and other internal components. One or more addenda to the topical report will be required to establish the critical limit for DOE SNF once sufficient critical benchmarks are identified and performed.

The waste package (WP) that holds the DOE SNF canister with Shippingport LWBR SNF also contains five high-level waste (HLW) glass pour canisters and a carbon steel basket assembly. The Shippingport LWBR DOE SNF canister is placed in a carbon steel support tube that becomes the center of the waste package (see Figure ES-1). The DOE SNF canister is surrounded by five 4.5-meter long Hanford HLW glass canisters, which has a cylindrical stainless steel shell with an outer diameter of approximately 610 mm (24 in.). The waste

package carbon steel basket height is 4607 mm. The five HLW glass canisters are evenly spaced around the Shippingport LWBR DOE SNF canister. The Shippingport LWBR DOE SNF canister is designed for one intact Shippingport LWBR fuel assembly placed in the center position of the 4107-mm-long stainless steel basket. The canister basket consists of a 295 by 257-mm rectangular grid of stainless steel plate (Type 316L) 9.5-mm thick.

The 5-Defense High Level Waste (DHLW)/DOE SNF-long waste package is based on the Enhanced Design Alternative (EDA) II for the waste packages. The outer barrier is made of corrosion-resistant material, 25-mm-thick Alloy 22. The inner barrier is fabricated from a 50-mm thick 316 NG stainless steel. Both the top and bottom lids are also based on the two-barrier principle and are fabricated from the same materials.

This report presents the results of analyzing the 5-DHLW/DOE SNF-long waste package for structural, thermal, shielding, and intact- and degraded-mode criticality performance compared to the respective design criteria. Section 2.2 provides the criteria, and Section 2.3 provides the essential assumptions for the various analyses. This report does not address codisposal waste packages with HLW glass canisters that contain immobilized plutonium.

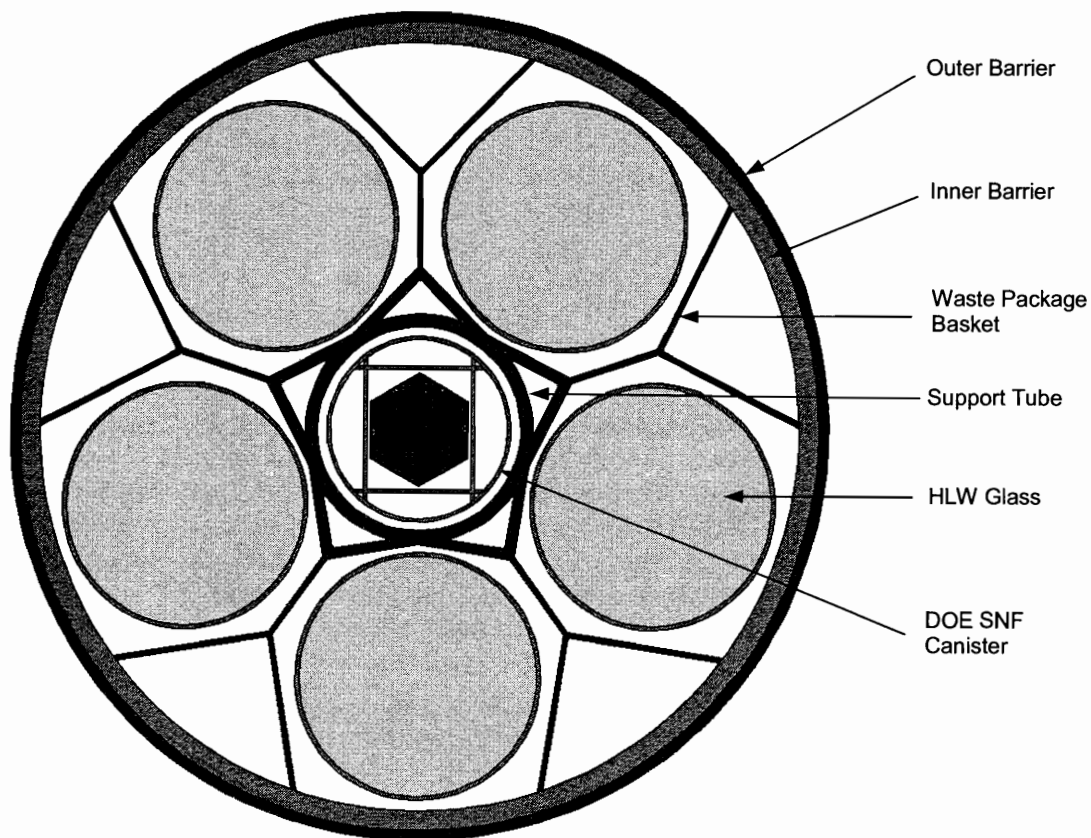


Figure ES-1. 5-DHLW/DOE SNF Waste Package with Shippingport LWBR SNF

## STRUCTURAL ANALYSES

ANSYS Version 5.4 – a finite-element analysis (FEA) computer code – was used for the structural analysis of the 5-DHLW/DOE SNF-long waste package with the Shippingport LWBR DOE SNF canister in the center. A two-dimensional (2-D) finite-element representation of the 5-DHLW/DOE SNF-long waste package was developed to determine the effects of loads on container's structural components due to a waste package tipover design-basis event (DBE). Calculations of maximum potential energy for each waste package handling accident scenario (2.4-m horizontal drop, 2.0-m vertical drop, and tipover DBEs) show that the bounding dynamic load results from a tipover case in which the rotating top end of the waste package experiences the highest impact load. Therefore, tipover structural evaluations are bounding for all handling accident scenarios under the above constraints of 2.4-m horizontal drop, 2.0-m vertical drop, and tipover considered in the DBEs document (CRWMS M&O 1997a).

The results show that the cavity between the Shippingport LWBR fuel assembly and the basket plates does not close, but on the contrary, becomes larger because of the dynamic load applied on the bottom plate by the Shippingport LWBR fuel assembly. Hence, there will be no interference between the fuel assembly and the basket plates because of tipover DBE. The maximum stress in the DOE SNF canister structural components, including internals is determined to be 243.6 MPa. This magnitude of stress is less than 0.9 or 0.7 of the ultimate tensile strength of 316L stainless steel, 483 MPa, therefore the allowable stress-limit criteria presented in Section 3.2 are met.

The calculations also show that the maximum bending stress on the spacer base plate due to the weight of the structural components and the fuel is 16.6 MPa, which is less than the yield strength of 316L stainless steel (172 MPa). Finally, the critical stress for buckling to take place on the spacer tube is 1.43 GPa, whereas the compressive stress is only 2.06 MPa. Therefore, the Shippingport LWBR fuel assembly will not be crushed within the basket structure.

## THERMAL ANALYSES

ANSYS Version 5.4 was used for the thermal analysis of the 5-DHLW/DOE SNF-long waste package with the Shippingport LWBR DOE SNF canister in the center. The maximum heat generation from a Hanford 15-foot HLW glass canister is projected to be 1473.4 watts at the projected year of emplacement, 2010. Although this maximum heat generation may be reduced, which will result in even lower temperatures than the temperatures calculated in this report, the analysis was based on heat output of 1473.4 watts. The thermal conductivity of the HLW glass is approximated as that of pure borosilicate glass, whereas the properties of density and specific heat are approximated as those of Pyrex glass. Only the axial cross section of the waste package at the center of the DOE SNF canister is represented in this 2-D calculation. The Shippingport LWBR DOE SNF canister is analyzed with helium (He) and argon (Ar) as fill gases, whereas the waste package is filled with He. Separate analyses were performed for the Viability Assessment (VA) and the EDA II waste package designs and emplacement parameters.

The thermal analyses show that the Shippingport LWBR waste package satisfies applicable criteria under normal conditions (accident fire condition is not within the scope of this analysis). The highest HLW glass temperature in the waste package for the EDA II design is same for

helium or argon fill gas in the DOE SNF canister, and is 300.04 °C. For the VA design, the highest HLW glass temperature is also the same for both fill gases in the DOE SNF canister, and is 220.34 °C. Both results are below the 400 °C maximum HLW glass temperature criterion in *Defense High Level Waste Disposal Container System Description Document* (CRWMS M&O 2000j) (see Section 2.2.2). The highest total thermal output for the waste package 8007.1 W for the VA and EDA II designs and emplacement parameters. For both designs the thermal output is below the 11.8 kW maximum limit for the waste package.

## SHIELDING ANALYSES

The Monte Carlo radiation transport code, MCNP, Version 4B2, was used to calculate average dose rates on segments of the radial and axial surfaces of the waste package. Dose rate calculations were performed for a waste package containing the 4.5-m long Hanford HLW glass canisters and Shippingport LWBR SNF. The maximum dose rate, calculated on a radial outer surface segment of the waste package, was  $81.33 \pm 1.72$  rem/h. The dose rates on the bottom and top surfaces of the waste package are one and two orders of magnitude, respectively, smaller than the maximum dose rate on the outer radial surface.

Although the gamma spectra and intensities of each 4.5-m-long HLW glass canister and the Shippingport LWBR SNF assembly are similar, the dose generated by the HLW glass dominates the dose at the external surfaces of the waste package. The Shippingport LWBR assembly makes a small contribution to the dose rate at the external surfaces of the waste package because of the fuel self-shielding and the central position that the DOE SNF canister occupies inside the waste package.

The highest dose rate on the outer surfaces segment of the waste package design described herein is 83.05 rem/h ( $81.33 + 2\sigma$ ). The maximum dose rate on the outer surfaces of the waste package is below the criterion-limiting value of 1450 rem/h (TBV-248, Section 2.2.3) for the cases investigated by about a factor of 18. The dose rates from primary gamma rays dominate the neutron dose rates by approximately three orders of magnitude.

## DEGRADATION AND GEOCHEMISTRY ANALYSES

The degradation analyses follow the general methodology developed for application to all waste forms containing fissile material. This methodology evaluates potential critical configurations from the intact waste package (geometrically intact components in a breached waste package assumed to be flooded with water as a moderator) through the completely degraded waste package. The waste package design is used as the starting point for the intact configuration. Sequences of events and/or processes of component degradation are developed. Standard scenarios from the master scenario list in the *Disposal Criticality Analysis Methodology Topical Report* (YMP 1998) are refined using unique fuel characteristics. Potentially critical configurations are identified for further analysis.

The geochemistry analyses are performed using the EQ3/6 Version 7.2B geochemistry code in the solid-centered flow-through mode. A principal objective of these analyses is to assess the chemical circumstances that could lead to removal of neutron absorber material (Gd) from the

waste package, while fissile materials remain behind. Such circumstances could increase the probability of a nuclear criticality occurrence within the waste package. Gadolinium is initially present as  $GdPO_4$  that is combined with aluminum shot to produce Gd-doped aluminum shot, which is distributed in the void space inside the DOE SNF canister. Water with the composition of J-13 well water is assumed to drip in through an opening at the top of the waste package, pooling inside and eventually overflowing, allowing soluble components to be removed through continual dilution. Twenty six EQ3/6 cases have been selected and examined to identify the reasons for the chemical composition changes during the degradation of waste package materials and the flushing by J-13 well water. The results show that loss of Gd was insignificant ( $< 3.7\%$ ), when it is present in the package as  $GdPO_4$ . EQ3/6 cases are constructed to span the range of possible fuel corrosion. The effects of steel corrosion, glass degradation, and fluid influx rate on thorium and uranium oxide dissolution are also investigated. Uranium losses from the spent nuclear fuel only, varied from 0.09 to 100% for the full range of corrosion, degradation and fluid influx rates considered, and for the failure of the fuel cladding considered as well. At a given glass dissolution rate, uranium loss varies inversely with the influx of water. Thorium oxide is very stable for the time range studied (up to 300000 years) and the loss is very small ( $< 0.03\%$ ).

## **INTACT- AND DEGRADED-MODE CRITICALITY ANALYSES**

The criticality calculations were performed using the MCNP code, Version 4B2, for the internal configurations that can be created during degradation of the codisposal waste package containing Shippingport LWBR SNF.

The intact and degraded component criticality analyses consider a single Shippingport LWBR seed assembly inside the DOE SNF canister, which contains a stainless steel Type 316L basket. Analyses consider optimum moderation, optimum distribution of fissile material and degradation products, and optimum reflection to determine the highest  $k_{eff}$  attainable by the system. Intact cases represent breached but otherwise intact waste package and DOE SNF canister. Degraded cases cover range of degradation of waste package internals, HLW glass canisters, DOE SNF canister, and the fuel assembly.

For one Shippingport LWBR seed assembly in the DOE SNF canister the results from the intact criticality analysis show that  $k_{eff} + 2\sigma$  (at 95% confidence) are less than or equal to 0.92. This configuration does not need any neutron absorber in the DOE SNF canister or elsewhere in the waste package. The results from the degraded criticality analysis for the intact SNF, but degraded DOE SNF canister shell show that all configurations with at least 10.12 kg  $GdPO_4$  included in the aluminum shot that fills all void spaces in the DOE SNF canister, result in  $k_{eff} + 2\sigma$  of less than or equal to 0.92.

The second part of the degraded criticality analysis considers configurations with full degradation of the DOE SNF canister along with degradation of HLW glass and waste package internals. The results for these configurations are less than or equal to 0.92 with at least 10.12 kg  $GdPO_4$  present in the initial DOE SNF canister void space, including the space within the assembly. Additional critical benchmark experiments must be evaluated to establish the critical limit for Shippingport LWBR fuel.

## CONCLUSIONS

In summary, the structural, shielding and thermal design criteria are met for a DOE SNF canister containing Shippingport LWBR SNF. Each waste package can contain one DOE SNF canister containing one seed fuel assembly and falls below the interim critical limit of 0.92 with at least 10.12 kg GdPO<sub>4</sub> present in the DOE SNF canister with the filler material. 10 kg or more of additional GdPO<sub>4</sub> should be loaded to provide extra margin (defense in depth). With this design, there will be approximately 12 DOE SNF canisters loaded with Shippingport LWBR SNF. This corresponds to 12 waste packages.

# CONTENTS

	<b>Page</b>
EXECUTIVE SUMMARY .....	vii
ACRONYMS AND ABBREVIATIONS.....	xxi
1. INTRODUCTION AND BACKGROUND.....	1
1.1 OBJECTIVE.....	2
1.2 SCOPE .....	2
1.3 QUALITY ASSURANCE .....	3
2. DESIGN INFORMATION.....	5
2.1 DESIGN PARAMETERS .....	5
2.1.1 Codisposal Waste Package.....	5
2.1.2 HLW Glass Pour Canisters .....	7
2.1.3 DOE SNF Canister .....	8
2.1.4 Shippingport LWBR DOE SNF.....	11
2.1.4.1 Description of SNF from the Seed Region.....	12
2.1.5 Structural.....	18
2.1.6 Thermal.....	18
2.1.7 Shielding Source Terms .....	20
2.1.7.1 Radiation Source Terms of the Shippingport LWBR SNF.....	20
2.1.7.2 Radiation Source Terms for the Glass Canisters .....	21
2.1.8 Material Compositions .....	22
2.1.9 Degradation and Geochemistry .....	23
2.1.9.1 Physical and Chemical Forms of Shippingport LWBR Waste Package.....	24
2.1.9.2 Chemical Composition of J-13 Well Water.....	27
2.1.9.3 Drip Rate of J-13 Well Water into a Waste Package .....	29
2.2 FUNCTIONS AND DESIGN CRITERIA.....	29
2.2.1 Structural.....	30
2.2.2 Thermal.....	31
2.2.3 Shielding.....	31
2.2.4 Degradation and Geochemistry .....	31
2.2.5 Intact and Degraded Criticality.....	31
2.3 ASSUMPTIONS .....	31
2.3.1 Structural.....	32
2.3.2 Thermal.....	32
2.3.3 Shielding.....	33
2.3.4 Degradation and Geochemistry .....	33
2.3.5 Intact and Degraded Mode Criticality .....	34
2.3.6 General.....	34
2.4 BIAS AND UNCERTAINTY IN CRITICALITY CALCULATIONS.....	35
2.4.1 Benchmarks Related to Intact Waste Package Configurations.....	35
2.4.2 Benchmarks Related to Degraded Waste Package Configurations .....	36

## CONTENTS (Continued)

	Page
2.4.3 Critical Limit .....	36
3. STRUCTURAL ANALYSIS .....	37
3.1 USE OF COMPUTER SOFTWARE .....	37
3.2 DESIGN ANALYSIS .....	37
3.3 CALCULATIONS AND RESULTS .....	37
3.3.1 Description of the Finite-Element Representation .....	37
3.3.2 Results .....	39
3.4 SUMMARY .....	40
4. THERMAL ANALYSIS .....	41
4.1 USE OF COMPUTER SOFTWARE .....	41
4.2 THERMAL DESIGN ANALYSIS .....	41
4.3 CALCULATIONS AND RESULTS .....	42
4.4 SUMMARY .....	46
5. SHIELDING ANALYSIS .....	47
5.1 USE OF COMPUTER SOFTWARE .....	47
5.2 SHIELDING DESIGN ANALYSIS .....	47
5.3 CALCULATIONS AND RESULTS .....	47
5.4 SUMMARY .....	50
6. DEGRADATION AND GEOCHEMISTRY ANALYSIS .....	51
6.1 USE OF COMPUTER SOFTWARE .....	51
6.2 DESIGN ANALYSIS .....	51
6.2.1 Systematic Investigation of Degradation Scenarios and Configurations .....	51
6.2.1.1 Most Likely Scenario for Shippingport LWBR SNF .....	58
6.2.1.2 Degraded DOE SNF Canister Basket and Intact SNF .....	60
6.2.1.3 Intact DOE SNF Canister and Degraded Waste Package Internals .....	60
6.2.1.4 Degraded DOE SNF Canister and Waste Package Internals, Intact SNF .....	60
6.2.1.5 Degraded SNF with Intact DOE Canister or Waste Package .....	60
6.2.1.6 Partially or Completely Degraded DOE SNF Canister and Waste Package Internals .....	60
6.2.2 Basic Design Approach for Geochemistry Analysis .....	61
6.3 CALCULATIONS AND RESULTS .....	61
6.3.1 Results of EQ6 Runs .....	62
6.4 SUMMARY .....	64
7. INTACT- AND DEGRADED-MODE CRITICALITY ANALYSIS .....	65
7.1 USE OF COMPUTER SOFTWARE .....	65
7.2 DESIGN ANALYSIS .....	65

## CONTENTS (Continued)

	Page
7.3 CALCULATIONS AND RESULTS–PART I: INTACT-MODE CRITICALITY ANALYSIS .....	66
7.3.1 Intact Mode.....	66
7.4 CALCULATIONS AND RESULTS–PART II: SCENARIOS WITH FISSILE MATERIAL RETAINED IN THE DOE SNF CANISTER.....	68
7.4.1 Intact Fuel Assembly in Partially Degraded DOE SNF Canister .....	68
7.4.2 Partially Degraded Fuel Assembly in Intact DOE SNF Canister .....	69
7.4.3 Partially to Totally Degraded Internal Structures of DOE SNF Canister with Intact Fuel Pins .....	70
7.4.4 Degraded Waste Package and DOE SNF Canister Internal Structures with Intact DOE SNF Canister Shell .....	73
7.5 CALCULATIONS AND RESULTS–PART III: SCENARIOS WITH FISSILE MATERIAL DISTRIBUTED IN WASTE PACKAGE .....	75
7.5.1 Degraded Waste Package Internal Structures with Intact Fuel Assembly.....	75
7.5.2 Degraded Waste Package Internal Structures with Intact Fuel Pins .....	77
7.5.3 Degraded DOE SNF Canister Mixture Settled at the Bottom of the Waste Package .....	79
7.6 CALCULATIONS AND RESULTS–PART IV: ADDITIONAL TOPICS OF INTEREST .....	81
7.6.1 Axial Redistribution of Degraded DOE SNF in the Canister and in the Waste Package .....	81
7.6.2 Results for Uranium Decay Effects .....	81
7.7 SUMMARY.....	82
8. CONCLUSIONS.....	83
8.1 STRUCTURAL ANALYSIS.....	83
8.2 THERMAL ANALYSIS.....	83
8.3 SHIELDING ANALYSIS.....	84
8.4 GEOCHEMISTRY ANALYSIS.....	84
8.5 INTACT- AND DEGRADED-MODE CRITICALITY ANALYSIS.....	85
8.6 ITEMS IMPORTANT TO CRITICALITY CONTROL.....	85
9. REFERENCES.....	87
9.1 DOCUMENTS CITED.....	87
9.2 CODES, STANDARDS, REGULATIONS, AND PROCEDURES.....	92
9.3 SOURCE DATA.....	93
APPENDIX A SHIPPINGPORT LWBR DOE SNF CANISTER AND BASKET ASSEMBLY .....	A-1
APPENDIX B 5DHLW/DOE SNF-LONG SINGLE CRM DISPOSAL CONTAINER .....	B-1

INTENTIONALLY LEFT BLANK

## FIGURES

	Page
ES-1. 5-DHLW/DOE SNF Waste Package with Shippingport LWBR SNF.....	viii
1. Cross Section of 5-DHLW/DOE SNF-Long Waste Package.....	6
2. HLW Glass Pour Canister .....	7
3. Plan View of the 18-in.-Diameter DOE SNF Canister.....	9
4. Cross-Section of the Shippingport LWBR DOE SNF Canister .....	10
5. Isometric View of the Shippingport LWBR DOE SNF Canister .....	10
6. Schematic Representation of Seed Fuel Assembly and Rods.....	12
7. Layout of Fuel Rods in a Seed Assembly .....	17
8. Stresses in the 5-DHLW/DOE SNF-Long Waste Package.....	39
9. Stresses in the DOE SNF Canister .....	40
10. Finite-Element Representation of the 5-DHLW/DOE SNF-Long Waste Package .....	41
11. Finite-Element Representation of the Shippingport LWBR Seed Assembly Fuel (one-sixth section).....	42
12. DHLW Peak Temperature versus Time.....	44
13. Radial Temperature Profile of the Waste Package .....	45
14. Vertical and Horizontal Cross Sections of the MCNP Geometry Representation .....	48
15. Surfaces and Segments Used for Dose-Rate Calculations .....	49
16. Internal Criticality Master Scenarios, Part 1 (YMP 1998).....	54
17. Internal Criticality Master Scenarios, Part 2 (YMP 1998).....	55
18. Examples of Degraded Configurations from Class 1 .....	56
19. Examples of Degraded Configurations from Class 2.....	56
20. Example of Degraded Configuration from Class 3.....	56
21. Example of Degraded Configuration from Class 4.....	57
22. Examples of Degraded Configurations from Class 5.....	57
23. Example of Degraded Configuration from Class 6.....	57
24. Cross-Sectional View of the Waste Package Showing the Contents of the DOE SNF Canister for the Intact-Mode Analysis.....	66
25. Intact Assembly Surrounded by Degraded Contents of the DOE SNF Canister in an Intact Waste Package.....	69
26. Different Arrangements of Fuel Pins Inside DOE SNF Canister.....	71
27. Cross-Sectional View of the Degraded Configuration with Intact Fuel Pins Dispersed within the DOE Canister Shell.....	72
28. Cross-Sectional View of the Breached Intact DOE SNF Canister Containing Fully Degraded Fuel.....	74
29. Cross-Sectional View of the Intact Fuel Assembly with Degraded DOE SNF Canister and Degraded Contents of the Waste Package .....	76
30. Cross-Sectional View of Loose Fuel Pins (compact arrangement) in the Waste Package.	78
31. Cross-Sectional View of Loose, Spread Out Fuel Pins in the Waste Package.....	78
32. Fully Degraded DOE SNF Canister Settled at the Bottom of Waste Package.....	80

INTENTIONALLY LEFT BLANK

## TABLES

	Page
1. List of Supporting Documents .....	2
2. Codisposal Waste Package Dimensions and Material Specifications .....	6
3. Geometry and Material Specifications for HLW Glass Canisters.....	7
4. Isotopic Composition of the Uranium.....	11
5. Characteristics of Pellets in the Seed Region.....	13
6. As-Built Characteristics of Seed Fuel Rods.....	14
7. Further As-Built Characteristics of Fuel Rods in the Seed Region.....	14
8. Average As-Built Cladding Dimensions for all Core Regions.....	14
9. Plenum Spring Dimensions for all Core Regions .....	15
10. Estimated Masses of Unirradiated Fuel Rod Components for all Core Regions .....	15
11. Average As-Built Fissile Loading of Assemblies from All Core Regions.....	15
12. Composition of the Seed Assembly with Maximum Fissile Loading.....	17
13. Heat Output of Each Waste Package Component .....	18
14. Axial Peaking Factors Estimated from Peak and Average Burnups .....	19
15. Thermal Conductivity of UO <sub>2</sub> and Thoria Fuel .....	20
16. Gamma Source Terms of a Shippingport LWBR SNF Seed Assembly at Year 2005.....	20
17. Gamma and Neutron Sources for a SRS HLW Glass Canister at Day One after Pouring.....	21
18. Gamma and Neutron Sources for a 4.5-m Long HLW Glass Canister .....	21
19. Chemical Composition of Zircaloy-4 (UNS R60804) .....	22
20. Chemical Composition of ASTM B 575 (Alloy 22 or UNS N06022).....	22
21. Chemical Composition of ASTM A 516 Grade 70 Carbon Steel (UNS K02700) .....	23
22. Chemical Composition of Stainless Steel Type 304L (UNS S30403) .....	23
23. Chemical Composition of Stainless Steel Type 316L (UNS S31603).....	23
24. HLW Glass Composition, Density, and Degradation Rates.....	24
25. Steel Degradation Rates and Rate Constants .....	25
26. Shippingport LWBR (Th/U Oxide) SNF Elemental Composition and Degradation Rates ...	26
27. Elemental Composition, Degradation Rate Constant, and Density of Aluminum Fill Material.....	27
28. Composition of J-13 Well Water.....	28
29. Containment Structure Allowable Stress-limit Criteria .....	37
30. Peak Temperature versus Time for Various Components .....	43
31. Dose Rates on the Waste Package Outer Radial Surface .....	49
32. Dose Rates on the Waste Package Axial Surfaces .....	49
33. Materials and Thicknesses .....	59
34. Summary of Geochemistry Results.....	63
35. Results of the Intact-Mode Criticality Analysis.....	67
36. Results of the Intact Assembly with Degraded Basket Plates.....	68
37. Results of the Degraded Assembly with the Components in the DOE SNF Canister Intact .	70
38. Results for Loose Fuel Pins with Intact Basket Plates in the DOE SNF Canister .....	71
39. Results for Loose Fuel Pins with Degraded Internal Structures of the DOE SNF Canister ..	73
40. Results for Fully Degraded Waste Package Internals and Degraded SNF Contents in the Intact DOE SNF Canister.....	74

**TABLES (Continued)**

	<b>Page</b>
41. Results for Intact Fuel Assembly with Degraded DOE SNF Canister and Degraded Contents of the Waste Package (Prebreach Clay) .....	76
42. Results for Intact Fuel Assembly with Degraded SNF Canister and Degraded Contents of the Waste Package (Post-Breach Clay).....	77
43. Results for Fully Degraded Fuel with Degraded SNF Canister and Degraded Contents in the Waste Package with Post-Breach Clay.....	81
44. Shippingport LWBR Codisposal Waste Package Thermal Results and Governing Criteria..	83

## ACRONYMS AND ABBREVIATIONS

ASME	American Society of Mechanical Engineers
ASTM	American Society for Testing and Materials
BPVC	Boiler and Pressure Vessel Code
CRM	corrosion resistant material
CRWMS	Civilian Radioactive Waste Management System
CSCI	Computer Software Configuration Item
DBE	design basis event
DHLW	defense high-level waste
DOE	U.S. Department of Energy
DTN	Data Tracking Number
EDA	Enhanced Design Alternative
FEA	finite-element analysis
HEU	highly enriched uranium
HLW	high-level (radioactive) waste
INEEL	Idaho National Engineering & Environmental Laboratory
IP	internal to the package
$k_{\text{eff}}$	effective multiplication factor
LCE	laboratory critical experiment
LWBR	Light Water Breeder Reactor
M&O	Management and Operating Contractor
MGR	Monitored Geologic Repository
NSNFP	National Spent Nuclear Fuel Program
OCRWM	Office of Civilian Radioactive Waste Management
PC	personal computer
PPF	power peaking factor
QARD	Quality Assurance Requirements and Description
SCM	Software Configuration Management
SDD	System Description Document
SNF	spent nuclear fuel

## ACRONYMS AND ABBREVIATIONS (Continued)

SQR	Software Qualification Report
SRP	Savannah River Plant
SRS	Savannah River Site
SS	stainless steel
TBD	to be determined
TBV	to be verified
UNS	Unified Numbering System
VA	Viability Assessment
WF	Waste Form
WP	Waste Package
2-D	two-dimensional
3-D	three-dimensional

## 1. INTRODUCTION AND BACKGROUND

As part of the criticality licensing strategy, NSNFP has provided a reviewed data report (DOE 1999b) with traceable data for the representative fuel type. The results of the analyses performed by using the information from this reviewed data report will be used to develop waste acceptance criteria which must be met by all fuel forms within the Th/U oxide fuel group including Shippingport LWBR SNF.

The Shippingport LWBR was a small water-cooled, U-233/Th-232 cycle breeder reactor developed by Pittsburgh Naval Reactors to improve utilization of the nation's nuclear fuel resources in light water reactors. The LWBR core was operated successfully from September 1977 to October 1, 1982 at Shippingport Atomic Power Station, which was a Department of Energy (DOE)-owned reactor plant. At full power, the thermal power output of the reactor was 236.6 MW. The core operated for 29,047 effective full power hours over the five-year period of operation.

The different aspects of the analyses reported in this document have been performed by following the disposal criticality analysis methodology as documented in the topical report submitted to U.S. Nuclear Regulatory Commission (YMP 1998). The methodology includes analyzing the geochemical and physical processes that degrade the waste package internals and the waste forms after the waste package is breached. Addenda to the topical report will be required to establish the critical limit for the DOE SNF once sufficient critical benchmarks are identified and run. In this report, a conservative and simplified bounding approach is employed to designate an interim critical limit.

The analyses performed also include structural, thermal, shielding, and intact- and degraded-mode criticality analyses. This report is in support of the work outlined in Civilian Radioactive Waste Management System (CRWMS) Management & Operating Contractor (M&O) *DOE SNF Analysis Plan for FY 2000* (CRWMS 2000a).

In this technical report, there are numerous references to "codisposal container" and "waste package." Since the use of these two terms may be confusing, a definition of the terms is included here:

"(Co)disposal container" means the container barriers or shells, spacing structures and baskets, shielding integral to the container, packing contained within the container, and other absorber materials designed to be placed internal to the container or immediately surrounding the disposal container (i.e., attached to the outer surface of the disposal container). The disposal container is designed to contain SNF and high-level waste (HLW), but exists only until the outer weld is complete and accepted. The disposal container does not include the waste form or the encasing containers or canisters (e.g., HLW pour canisters, DOE SNF codisposal canisters, multi-purpose canisters of SNF, etc.).

"Waste package" means the waste form and any containers (i.e., disposal container barriers and other canisters), spacing structures or baskets, shielding integral to the container, packing contained within the container, and other absorbent materials immediately surrounding an individual waste container placed internally to the container or attached to the outer surface of

the disposal container. The waste package begins its existence when the outer lid weld of the disposal container is complete and accepted.

“5-DHLW/DOE SNF-long waste package” is the waste package that can accommodate a 15-ft long (18-in. diameter) DOE SNF canister and five 15-ft HLW glass canisters.

## 1.1 OBJECTIVE

The objective of this technical report is to provide sufficient detail to establish the technical viability for disposing of Th/U oxide (Shippingport LWBR) SNF in the potential Monitored Geologic Repository (MGR). This technical report sets limits and establishes values that if and when these limits are met by a specific fuel type under the Th/U oxide fuel group, the results for that fuel will be bounded by the results reported in this technical report.

Section 2, Design Information, describes the design of the codisposal container (Section 2.1, Design Parameters), with both requirements and assumptions identified (Section 2.2, Functions and Design Criteria, and Section 2.3, Assumptions). Analytical results to demonstrate the adequacy of the design and evaluate the feasibility of codisposing the Th/U oxide (Shippingport LWBR) SNF in the MGR are presented in Section 3 for Structural Analysis, Section 4 for Thermal Analysis, Section 5 for Shielding Analysis, Section 6 for Degradation and Geochemistry Analysis, and Section 7 for Intact and Degraded Mode Criticality Analysis. For purposes of this report, these five items may be collectively designated as waste package performance. Section 8, Conclusions, provides the connections between the design criteria and analytical results to establish technical viability. References are given in Section 9.

This technical document summarizes and analyzes the results of the detailed calculations that were performed in support of determining the evaluation of codisposal viability of Th/U oxide (Shippingport LWBR) fuel. These calculation documents and the section of this report in which they are summarized and analyzed are shown in Table 1.

Table 1. List of Supporting Documents

Discipline	Document Title	Summarized/ Analyzed in	Reference
Structural	<i>Structural Calculations for the Codisposal of Shippingport LWBR Spent Nuclear Fuel in a Waste Package</i>	Section 3	CRWMS M&O 1999a
Thermal	<i>Thermal Evaluation of the Shippingport LWBR SNF Codisposal Waste Package</i>	Section 4	CRWMS M&O 2000b
Shielding	<i>Dose Calculations for the Codisposal WP of HLW Glass and the Shippingport LWBR SNF</i>	Section 5	CRWMS M&O 1999b
Degradation and Geochemistry	<i>EQ6 Calculation for Chemical Degradation of Shippingport LWBR (Th/U Oxide) Spent Nuclear Fuel Waste Packages</i>	Section 6	CRWMS M&O 2000c
Intact- and Degraded-Mode Criticality Analysis	<i>Intact and Degraded Criticality Calculations for the Codisposal of Shippingport LWBR Spent Nuclear Fuel in a Waste Package</i>	Section 7	CRWMS M&O 2000d

## 1.2 SCOPE

This technical report, *Evaluation of Codisposal Viability for Th/U Oxide (Shippingport LWBR) DOE-Owned Fuel*, evaluates the performance of Th/U oxide (Shippingport LWBR) SNF in a waste package. This technical report summarizes the evaluation of viability of the

5-DHLW/DOE SNF-long waste package design with Th/U oxide (Shippingport LWBR) SNF, which is the representative fuel for Th/U oxide fuel group. The remaining fuels in the same group must be demonstrated to be bounded by the values in the Shippingport LWBR SNF data report (DOE 1999b).

### 1.3 QUALITY ASSURANCE

This technical report was prepared in accordance with AP-3.11Q, *Technical Reports*. The responsible manager for DOE Fuel Analysis has evaluated this report development activity in accordance with QAP-2-0, *Conduct of Activities*. The evaluations (CRWMS M&O 1999h and CRWMS M&O 1999i) concluded that the development of this report is subject to the DOE Office of Civilian Radioactive Waste Management Quality Assurance Requirements and Description (QARD) controls (DOE 2000). Though QAP-2-0, *Conduct of Activities*, has been replaced by AP-2.21Q, *Quality Determinations and Planning for Scientific, Engineering, and Regulatory Compliance Activities*, these activity evaluations remain in effect. The information provided in this report is to be used to evaluate the codisposal viability of U/Th Oxide fuel. AP-SV.1Q, *Control of the Electronic Management of Data* does not apply because there are no electronic data generated from the creation of this report.

There is no determination of importance evaluation developed in accordance with Nevada Line Procedure, NLP-2-0, *Determination of Importance Evaluations*, since the report does not involve any field activity.

This technical report is based in part on unqualified data. However, the unqualified data is only used to determine the bounding values and items that are important to safety for the fuel group by establishing the limits based on the representative fuel type (Shippingport LWBR) for this group (Th/U oxide fuel). Hence, the input values used for evaluation of codisposal viability of Th/U oxide (Shippingport LWBR) SNF do not constitute data that have to be qualified in this application. They only establish the bounds for acceptance (Assumption 2.3.6.1). Since the input values are not relied upon directly to address criticality control and waste isolation issues and since the design inputs do not affect a system characteristic that is critical for satisfactory performance, according to the governing procedure (AP-3.11Q, *Technical Reports*), the data do not need to be controlled as TBV (to be verified) (AP-3.15Q, *Managing Technical Product Inputs*). However, prior to acceptance of the fuel for disposal, the items that are identified as important to criticality control in Section 8.6 must be qualified by any means identified in the QARD (i.e., experiment, non-destructive test, chemical assay, qualification under a program subject to the QARD requirements).

INTENTIONALLY LEFT BLANK

## 2. DESIGN INFORMATION

Data and technical information were obtained from the following codes and standards: ASTM (American Society for Testing and Materials) B 575-97, *Standard Specification for Low-Carbon Nickel-Molybdenum-Chromium, Low-Carbon Nickel-Chromium-Molybdenum, Low-Carbon Nickel-Chromium-Molybdenum-Copper and Low-Carbon Nickel-Chromium-Molybdenum-Tungsten Alloy Plate, Sheet, and Strip*; ASTM A 516/A 516M-90, *Standard Specification for Pressure Vessel Plates, Carbon Steel, for Moderate- and Lower-Temperature Service*; ASTM A 276-91a, *Standard Specification for Stainless and Heat-Resisting Steel Bars and Shapes*; ASTM B 811-90, *Standard Specification for Wrought Zirconium Alloy Seamless Tubes for Nuclear Reactor Fuel Cladding*; ASTM G 1-90, *Standard Practice for Preparing, Cleaning, and Evaluating Corrosion Test Specimens*; ASTM A 240/A 240M-97a, *Standard Specification for Heat-Resisting Chromium and Chromium-Nickel Stainless Steel Plate, Sheet, and Strip for Pressure Vessels*; and ASME (American Society of Mechanical Engineers) 1995, *1995 ASME Boiler and Pressure Vessel Code*.

The number of digits in the values cited herein may be the result of a calculation or may reflect the input from another source; consequently, the number of digits should not be interpreted as an indication of accuracy. In most tables, three to four digits after the decimal place have been retained to reduce the round-off errors in subsequent calculations.

The information provided by the sketches appended to this technical report is that of the potential design of the type of waste package considered in the technical report.

### 2.1 DESIGN PARAMETERS

Each of the following sections either describes the design of the waste package or identifies the basis of major parameters.

#### 2.1.1 Codisposal Waste Package

The codisposal waste package contains five defense high-level waste (DHLW) canisters surrounding a DOE standardized 18-inch-diameter SNF canister. The 5-DHLW/DOE SNF-long waste package design is based on the EDA II (Wilkins 1999, see also Figure 1 and Appendix B). The barrier materials of the waste package are typical of those used for commercial SNF waste packages. The inner barrier is composed of 50 mm of stainless steel SS 316 NG. The outer barrier comprises 25 mm of high-nickel alloy ASTM B 575 (Alloy 22). The outside diameter of the waste package is 2030 mm and the length of the inside cavity is 4617 mm, which is designed to accommodate Hanford 15-foot HLW glass canisters. The lids of the inner barrier are 105-mm thick; those of the outer barrier, 25-mm thick. There is a 30-mm gap between the inner and outer barrier upper lids. Each end of the waste package has a 225-mm-long skirt. Table 2 summarizes the dimensions and materials of the waste package as depicted in Appendix B.

The DOE SNF canister is placed in a 31.75-mm-thick carbon steel (ASTM A 516 Grade 70) support tube with a nominal outer diameter of 565 mm. The support tube is connected to the inside wall of the waste package by a web-like structure of carbon steel (ASTM A 516 Grade 70)

basket plates to support five long HLW glass canisters, as shown in Figure 1. The support tube and the plates are 4607-mm long.

Table 2. Codisposal Waste Package Dimensions and Material Specifications

Component	Material	Parameter	Dimension (mm)
Outer barrier shell	ASTM B 575 (Alloy 22)	Thickness	25
		Outer diameter	2030
Inner barrier shell	SS 316 NG	Thickness	50
		Inner length	4617
Top and bottom outer barrier lids	ASTM B 575 (Alloy 22)	Thickness	25
Top and bottom inner barrier lids	SS 316 NG	Thickness	105
Gap between the upper inner and outer closure lids	Air	Thickness	30
Support tube	ASTM A 516 Grade 70	Outer diameter	565
		Inner diameter	501.5
		Length	4607

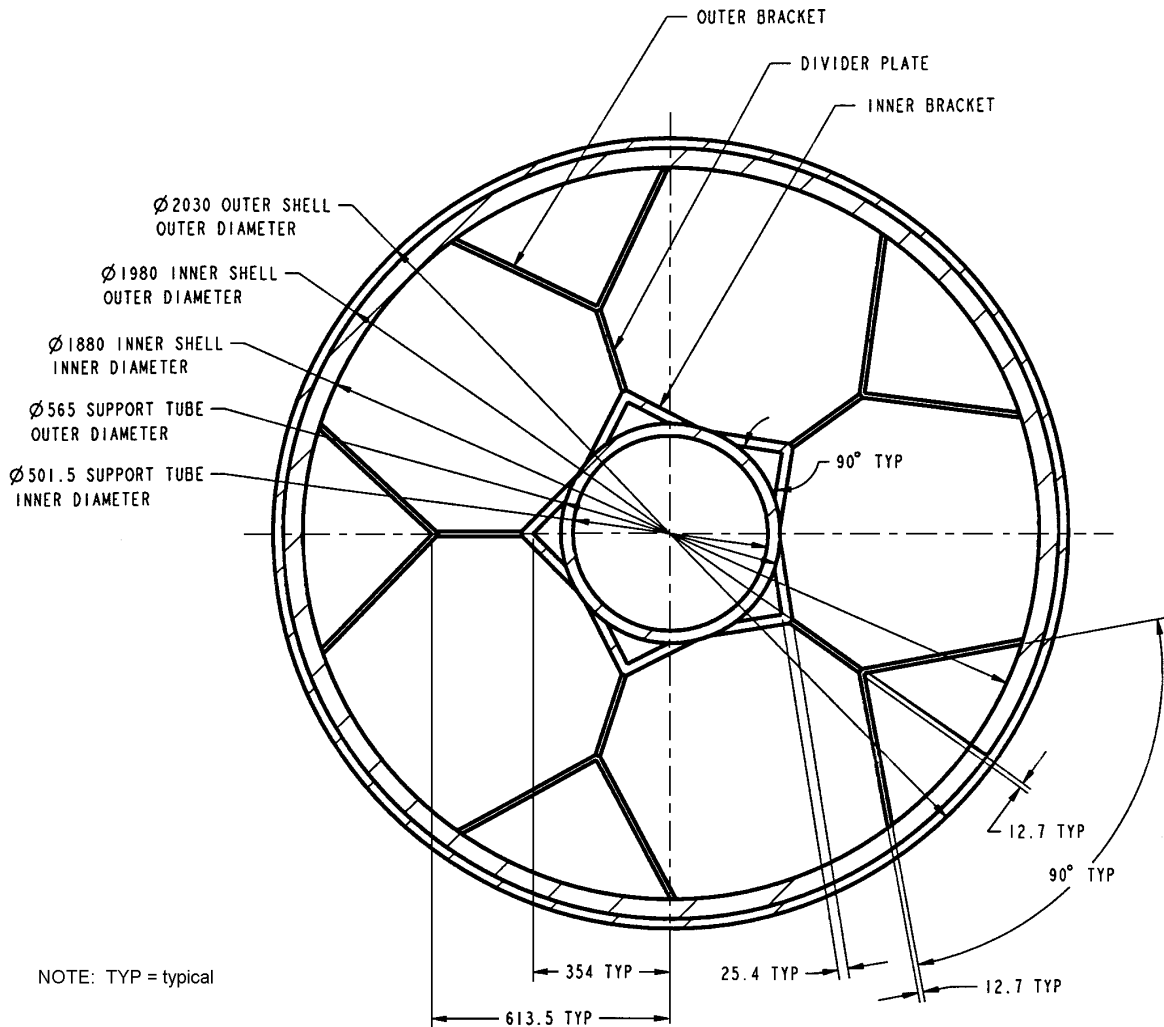


Figure 1. Cross Section of 5-DHLW/DOE SNF-Long Waste Package

## 2.1.2 HLW Glass Pour Canisters

There is no long Savannah River Site (SRS) HLW glass canister. Therefore, the Hanford 15-foot HLW glass canister, shown in Figure 2, is used in the Shippingport LWBR waste package. Since the specific composition of the Hanford HLW glass is not known at this time, the SRS glass composition is used in all analyses (Table 24, see also Assumption 2.3.6.2). The Hanford 15-foot HLW glass canister is 4500-mm long stainless steel Type 304L canister with an outer diameter of 610 mm (24.00 in.) (Taylor 1997). The wall thickness is 10.5 mm. The maximum loaded canister weight is 4200 kg and the fill volume is 87% (Taylor 1997). The heat output from a single Hanford 15-foot HLW canister for the year 2010 is 1473.4 W (see Table 13 in Section 2.1.6). The geometry and material specifications for HLW glass canisters are given in Table 3.

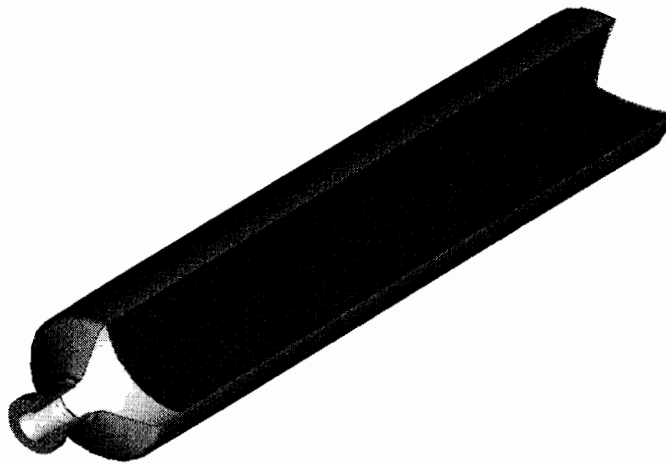


Figure 2. HLW Glass Pour Canister

Table 3. Geometry and Material Specifications for HLW Glass Canisters

Component	Material	Parameter	Value
Hanford 15-ft canister	Stainless Steel 304L	Outer diameter	610 mm
		Wall thickness	10.5 mm
		Length	4500 mm
		Total weight of canister and glass	4200 kg
		Fill volume of glass in canister	87%

Source: Taylor (1997).

### 2.1.3 DOE SNF Canister

The conceptual design for the standardized 18-in.-diameter DOE SNF canister is taken from DOE 1999a, p. 5, A-2, and A-3. The canister is a right circular cylinder of stainless steel (Type 316L) that contains a stainless steel (Type 316L) basket. The basket is not a standard part of the DOE SNF canister. The basket design is modified for each specific fuel type. The basket provides structural support and acts as a guide for the fuel assembly during loading. The dimensions for the DOE SNF canister are a 457-mm (18.00-in.) outer diameter with a 9.525-mm (0.375-in.) wall thickness. The nominal internal length of the canister is 4115 mm (162.0 in.) and the nominal overall length is 4570 mm (179.92 in.). There is a curved carbon-steel impact plate, which varies in thickness from 15.24 mm (0.60 in.) to 50.80 mm (2.0 in.) at the top and bottom boundaries of the canister. In addition, there are 9.525-mm (0.375-in.)-thick ASME (American Society of Mechanical Engineers) flanged and dished heads and 12.70-mm (0.5 in.)-thick lifting rings at each end of the canister. The maximum loaded weight of the canister is 2721 kg (DOE 1999a, Table 3.2). A drawing of the canister is shown in Figure 3.

The standardized 18-inch-diameter DOE SNF canister (15-ft-long) is used for disposal of Shippingport LWBR fuels, and holds a single Shippingport LWBR SNF seed assembly in a specially designed basket. A cross-sectional and an isometric view of the DOE SNF canister containing one Shippingport LWBR assembly are shown in Figures 4 and 5, respectively. The basket consists of a 295 mm by 257 mm rectangular grid. The basket plate is stainless steel (Type 316L) with a 9.5-mm thickness. Inside the basket is placed a spacer that has the role of limiting the length of space available for the Shippingport LWBR seed assembly to 3,350 mm that is slightly greater than the maximum length of the intact assemblies, including the shipping plates (3327.4 mm). The purpose of this limitation is to avoid significant movements of the assembly within the space available, during the handling of the DOE SNF canister, with the potential of damaging the assembly and the DOE SNF canister components. The spacer consists of a 293 mm by 255 mm rectangular tube made of 9.5-mm-thick plates that has a 19.1-mm-thick plate attached at the end closer to the assembly location. The spacer plates are made of stainless steel type 316L.

The void space inside the DOE SNF canister will be filled with shot consisting of a mixture of Al and GdPO<sub>4</sub>. This mixture has the role of a neutron absorber intended to prevent criticality inside the codisposal waste package.

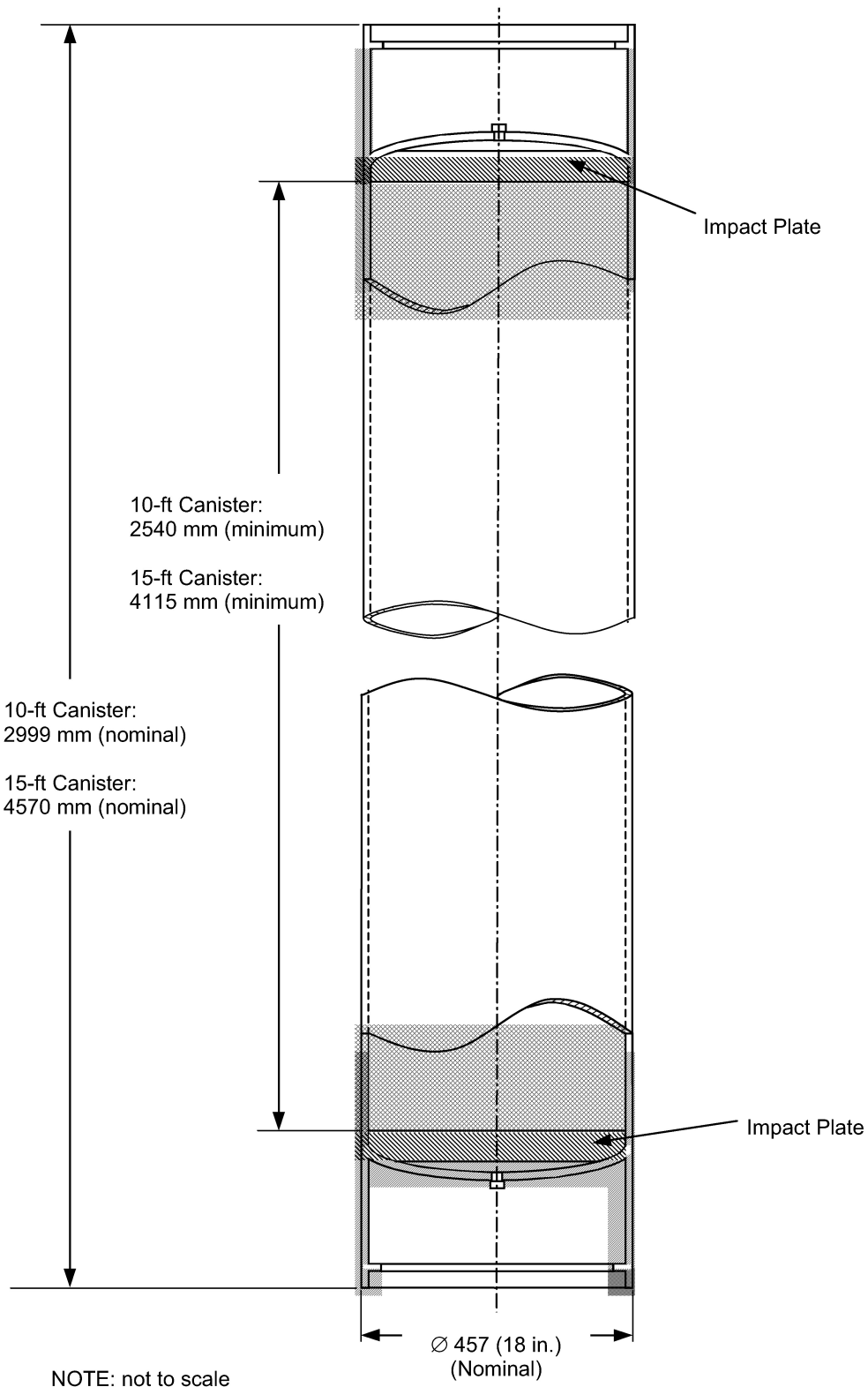


Figure 3. Plan View of the 18-in.-Diameter DOE SNF Canister

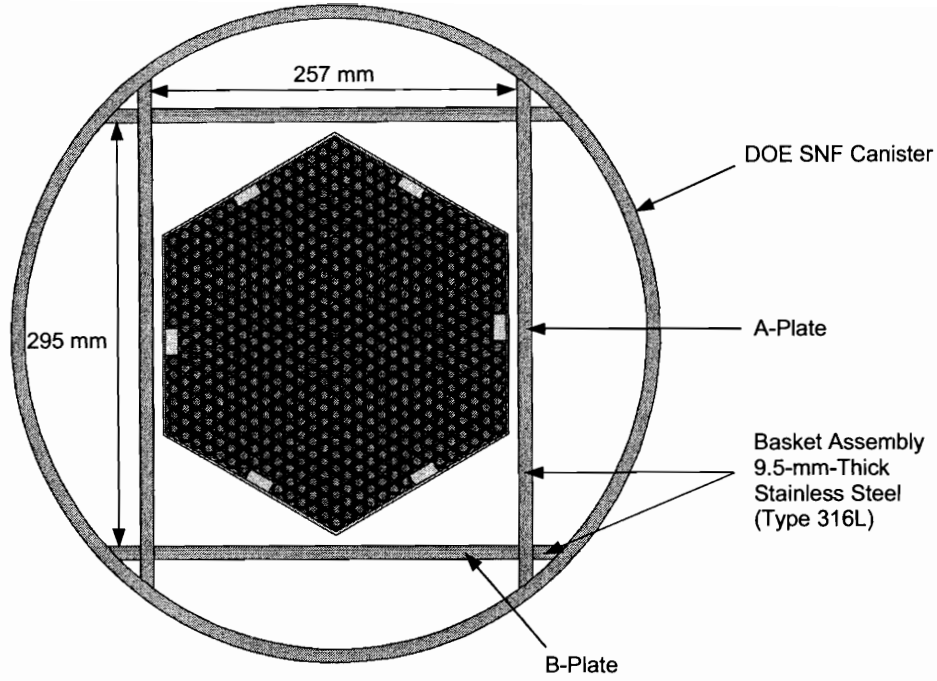


Figure 4. Cross-Section of the Shippingport LWBR DOE SNF Canister

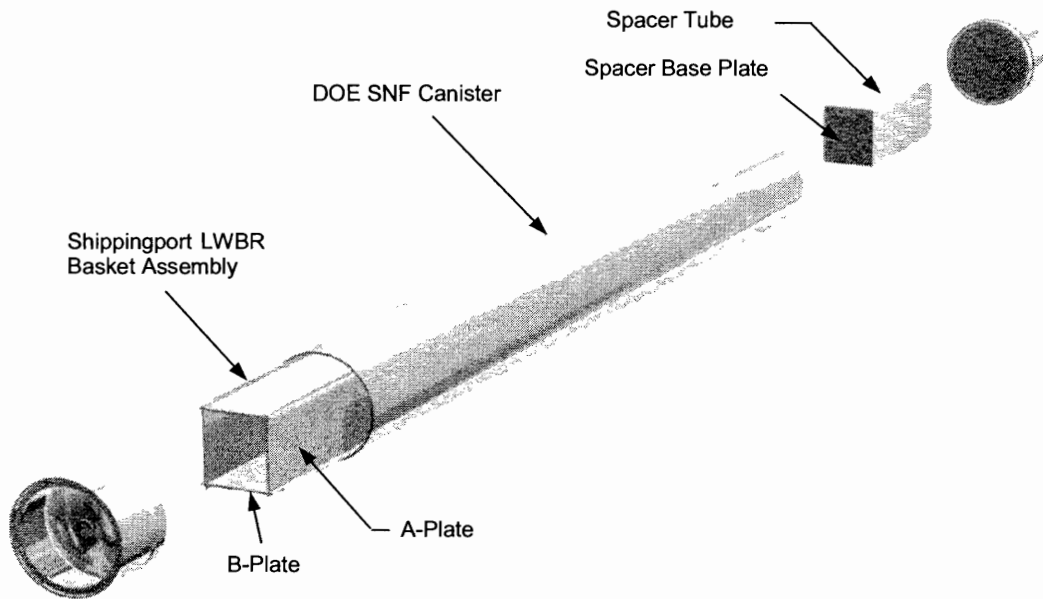


Figure 5. Isometric View of the Shippingport LWBR DOE SNF Canister

#### 2.1.4 Shippingport LWBR DOE SNF

The Shippingport LWBR was a “seed and blanket” reactor that used the movable seed fuel assemblies for the core reactivity control. The method of shipping and handling the blankets is yet to be decided. Therefore, this report does not specifically address the disposal of blanket assemblies in the MGR.

The source of the information in this section is DOE 1999b.

The Shippingport LWBR seed fuel assembly is shown in Figure 6 (DOE 1999b, p. 21). The LWBR core was fueled with fertile Th-232 and fissile U-233, the relative concentrations of which varied axially and radially across the core to promote high neutron economy. The uranium that was used in fabricating the fuel was mostly U-233, but some isotopic impurities were also present (Table 4). The design called for vertical fuel rods on a triangular pitch (i.e., the distance between the centers of two adjacent rods) with the space between taken up by circulating cooling water. The fuel rods featured cladding tubes loaded with cylindrical fuel pellets of thoria (ThO<sub>2</sub>) or a binary mixture of thoria and UO<sub>2</sub> and backfilled with helium at 1 atmosphere during welding. The binary fuel is a solid solution fabricated from the two oxides in powder form. Processing of the well-mixed powder preparation achieved a nearly homogeneous structure owing to diffusion at elevated temperature during sintering. Axial variation in fissile material concentration was achieved by loading individual fuel rods such that part of the length bore a binary mixture of fissile and fertile material and the rest bore only fertile material. Radial variation was achieved by the arrangement of fuel rods that differed in their axial loading and by using binary pellets of different binary mixtures, depending on the radial location of the rod. Zircaloy-4 with hafnium content less than 40 ppm was used for the cladding tubes and all other structures in the fuel region, except the grids, which were made of AM-350 stainless steel. The fuel and fuel components suffered minimal damage during operation. Extensive destructive and non-destructive examinations after shutdown confirmed that the fuel was in good condition with minimal deformation of the cladding and minimal cracking of fuel pellets.

Table 4. Isotopic Composition of the Uranium

Isotope	Weight Percent (wt.%)
U-232	<0.001
U-233	98.23
U-234	1.29
U-235	0.09
U-236	0.02
U-238	0.37

Source: DOE 1999b, p. 4.

The as-built core was conceptually segregated into four regions. Although the relative concentrations of fissile and fertile material varied axially and radially within each region, the regions can be broadly described as follows: (1) the Seed Region constituted islands of fuel initially rich in U-233; (2) the Standard Blanket Region surrounded the islands of concentrated seed material with a fuel initially less rich in U-233, and consequently richer in Th-232; (3) the Power Flattening Blanket Region enveloped the Seed and Standard Blanket Regions with fuel of initially somewhat higher fissile concentration than the Standard Blanket; and (4) the Reflector

Region surrounded the other regions with fertile material that was initially free of fissile material. The scope of this report is limited to the analysis of the codisposal of Seed Region spent nuclear fuel.

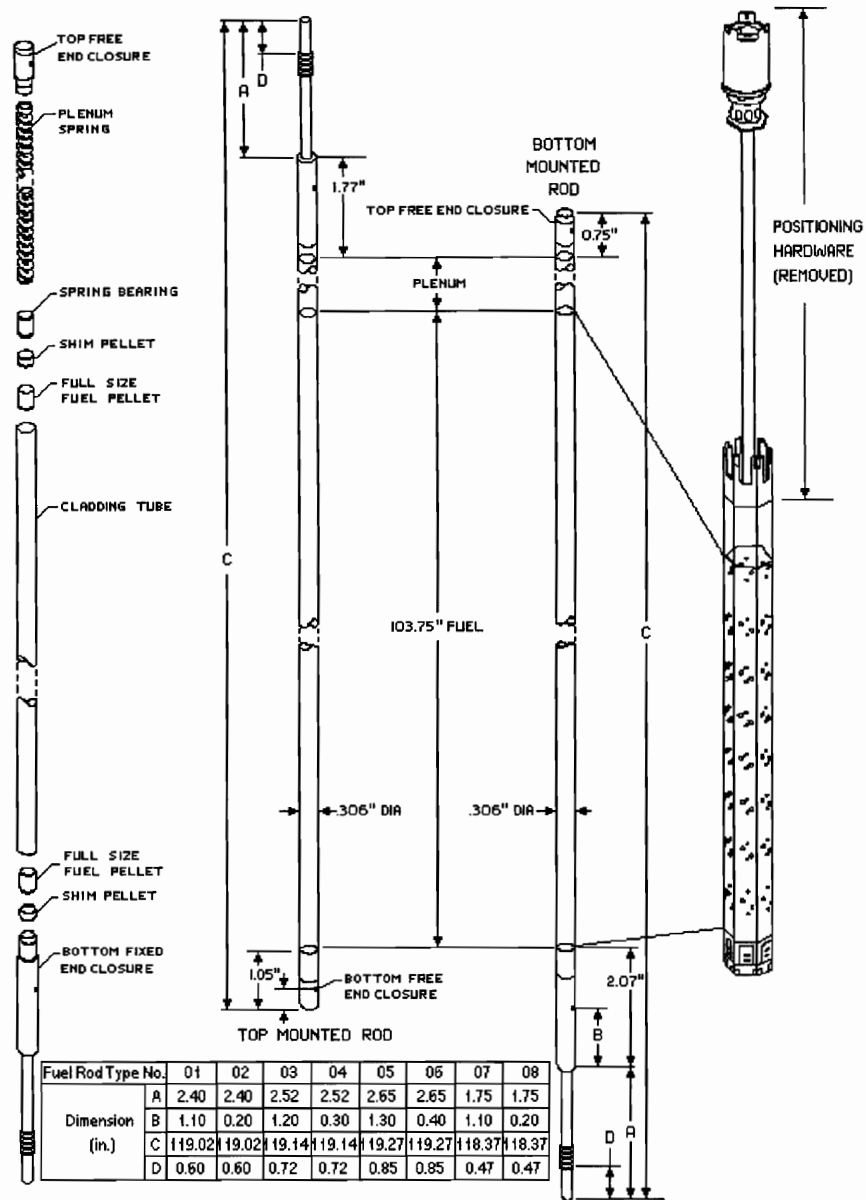


Figure 6. Schematic Representation of Seed Fuel Assembly and Rods

#### 2.1.4.1 Description of SNF from the Seed Region

Two different binary mixtures were used to fabricate the fuel in the Seed Region, resulting in binary fuel of higher and lower fissile concentrations. The tops and bottoms of the fuel rods were stacked with  $\text{ThO}_2$  pellets. Between the two fertile end stacks was a variable length binary

ThO<sub>2</sub>-UO<sub>2</sub> stack, which began 254 mm (10 in.) from the bottom of the stack. Any given fuel rod contained fuel that was fabricated from only one of the two binary mixtures. Rods in the Seed Region were grouped into movable hexagonal seed assemblies, each of which contained 619 fuel rods. The twelve Seed assemblies together initially contained 198.59 kg of fissile material, with 61.28 kg in rods of the lower fissile concentration (low zone) and 137.31 kg in rods of the higher fissile concentration (high zone).

**Fuel Pellets** - Seed pellets were right circular cylinders, with chamfers (bevels) on both ends. The seed pellets had dished ends to reduce axial expansion of the stack. Fuel pellets in the Seed Region were smaller in diameter than pellets elsewhere in the core. Binary pellets of two different lengths and two different binary mixtures were used in the Seed Region. The shorter pellets were made of the binary mixture with the lower fissile concentration, while the longer pellets were made of the binary mixture of greater fissile concentration. The length of the thoria pellets was about midway between the two different lengths of the binary pellets. Much shorter thoria shim pellets were used near the top and bottom of the fuel stack to make up the desired stack length. A spring-bearing thoria pellet with only one dished end was used at the top of the fuel stack. During fabrication, the pellets were sintered to a large fraction of their theoretical densities to ensure dimensional stability. Table 5 gives dimensions and other characteristics for seed fuel pellets. The void fraction listed in Table 5 and elsewhere is defined as the fraction of the volume of a right circular cylindrical pellet of the nominal dimensions that is missing due to end dishes, chamfers, and pellet chips.

Table 5. Characteristics of Pellets in the Seed Region

Property (units)	Seed Region Enrichment Zone		
	High	Low	ThO <sub>2</sub>
Diameter <sup>a</sup> (mm [in.])	6.4008 (0.2520)	6.4008 (0.2520)	6.49224 (0.2556)
Diameter <sup>b</sup> (mm [in.])	6.4008 ± .0127 (0.252 ± 0.0005)	6.4008 ± .0127 (0.252 ± 0.0005)	6.4897 ± .0127 (0.2555 ± .0005)
Length <sup>a</sup> (mm [in.])	15.621 (0.615)	11.2776 (0.444)	13.462 (0.530)
Length <sup>b</sup> (mm [in.])	15.621 ± .508 (0.615 ± .020)	11.303 ± .508 (0.445 ± .020)	13.462 ± .508 (0.530 ± .020)
Taper or Chamfer Depth <sup>b</sup> (mm [in.])	0.381 ± 0.127 (0.015 ± 0.005)	0.381 ± 0.127 (0.015 ± 0.005)	0.381 ± 0.127 (0.015 ± 0.005)
Taper or Chamfer Length <sup>b</sup> (mm [in.])	0.381 ± 0.127 (0.015 ± 0.005)	0.381 ± 0.127 (0.015 ± 0.005)	0.381 ± 0.127 (0.015 ± 0.005)
End Dish Spherical Radius <sup>b</sup> (mm [in.])	9.144 (0.360)	9.144 (0.360)	7.5692 (0.298)
End Shoulder Width <sup>b</sup> (mm [in.])	1.1684 ± 0.20 (0.046 ± 0.008)	1.1684 ± 0.20 (0.046 ± 0.008)	1.397 ± 0.254 (0.055 ± 0.010)
End Face Dish Depth <sup>b</sup> (mm [in.])	0.2286 ± 0.0762 (0.009 ± 0.003)	0.2286 ± 0.0762 (0.009 ± 0.003)	0.2286 ± 0.0762 (0.009 ± 0.003)
Void Fraction <sup>a</sup> (of chamfers, dishes, and chip defects)	0.01172	0.01704	0.01253
Percent Theoretical Density <sup>a</sup>	97.554	97.712	98.013
Theoretical Density (g/cm <sup>3</sup> )	10.042	10.035	9.999

Source: DOE 1999b, Table 3-5.

NOTES: <sup>a</sup> Average as built.

<sup>b</sup> Design specification.

**Fuel Rods** - Fuel rods from the Seed Region differed amongst themselves in several ways. A classification based on differences in the overall length of the rod and whether the rod was fixed to the seed assembly at the top or the bottom yields eight rod types (Figure 6, Table 6). Rods with odd type numbers were fixed to the bottom of the assembly, while even numbered rods were fixed at the top. The bottom 254 mm (10.0 in.) of each stack consists of thorium pellets. The binary stack begins at the 254-mm level. Thorium pellets make up the rest of the stack above the binary stack. Total pellet stack length is 2635.25 mm (103.75 in.). Other as-built characteristics of the Seed Region fuel rods are given in Table 7. The diameter of the mounting stems is not precisely known but historical documents imply that it does not exceed 5.7658 mm (0.227 in.). The seamless cladding tubes were welded at both ends to solid end plugs of Zircaloy-4. Cladding dimensions are given in Table 8. The cladding tubes in the Seed Region are freestanding; that is, they were designed to withstand operating pressures and temperatures without collapsing onto the pellet stack. However, irradiation of the rods caused a reduction in diameter of 0.03 to 0.06 mm (1.2 to 2.5 mils). Within the tube and above the pellet stack there is a  $254 \pm 2.54$ -mm ( $10.0 \pm 0.1$ -in.) plenum at the top of the fuel stack to accommodate fission gases. The plenum houses an Inconel X-750 wire compression spring (Table 9). The approximate weights of unirradiated fuel rod components for all core regions are given in Table 10.

Table 6. As-Built Characteristics of Seed Fuel Rods

Fuel Rod Type	Number per Assembly	Overall Length (mm [in.])	Length of Fixed-End Plug (mm [in.])	Length of Mounting Stem (mm [in.])	Length of Free-End Plug (mm [in.])
01	30	3023.108 (119.02)	52.578 (2.07)	60.96 (2.40)	19.05 (0.75)
02	84	3023.108 (119.02)	44.958 (1.77)	60.96 (2.40)	26.67 (1.05)
03	72	3026.156 (119.14)	52.578 (2.07)	64.008 (2.52)	19.05 (0.75)
04	66	3026.156 (119.14)	44.958 (1.77)	64.008 (2.52)	26.67 (1.05)
05	181	3029.458 (119.27)	52.578 (2.07)	67.31 (2.65)	19.05 (0.75)
06	150	3029.458 (119.27)	44.958 (1.77)	67.31 (2.65)	26.67 (1.05)
07	30	3006.598 (118.37)	52.578 (2.07)	44.45 (1.75)	19.05 (0.75)
08	6	3006.598 (118.37)	44.958 (1.77)	44.45 (1.75)	26.67 (1.05)

Table 7. Further As-Built Characteristics of Fuel Rods in the Seed Region

Rod Type	Initial Fissile Mass Loading (g/rod)	Fissile Concentration of the Binary Stack <sup>a</sup> (wt.% fissile)	Length of Binary Stack (mm [in.])
01, 02, 07, 08	14.33	4.337	1066.8 (42)
03	19.14	4.337	1422.4 (56)
04	23.92	4.337	1778 (70)
05,06	34.57	5.202	2133.6 (84)

NOTE: <sup>a</sup> Weight percent fissile (U-233+U-235)/(ThO<sub>2</sub>+UO<sub>2</sub>).

Table 8. Average As-Built Cladding Dimensions for all Core Regions

Core Region	Outside Diameter (mm [in.])	Thickness (mm [in.])
Seed	7.78002 (0.3063)	0.563118 (0.02217)
Standard Blanket	14.52118 (0.5717)	0.713232 (0.02808)
Power Flattening Blanket	13.39596 (0.5274)	0.671068 (0.02642)
Reflector	21.14042 (0.8323)	1.06426 (0.0419)

Table 9. Plenum Spring Dimensions for all Core Regions

Core Region	Number of Coils	Wire Diameter (mm [in.])	Spring Diameter (mm [in.])
Seed	190	1.0795 (0.0425)	5.2578 (0.207)
Standard Blanket	125	1.81102 (0.0713)	9.1694 (0.361)
Power Flattening Blanket	135	1.66624 (0.0656)	8.4328 (0.332)
Reflector	33	2.7686 (0.109)	13.3858 (0.527)

Table 10. Estimated Masses of Unirradiated Fuel Rod Components for all Core Regions

Core Region	Mass per Rod (kg)			
	Fuel Pellets	Cladding and End Caps	Internal Hardware	Total
Seed	0.83	0.27	0.02	1.12
Standard Blanket	3.38	0.69	0.14	4.21
Power Flattening Blanket	2.85	0.59	0.12	3.56
Reflector	6.94	1.47	0.12	8.53

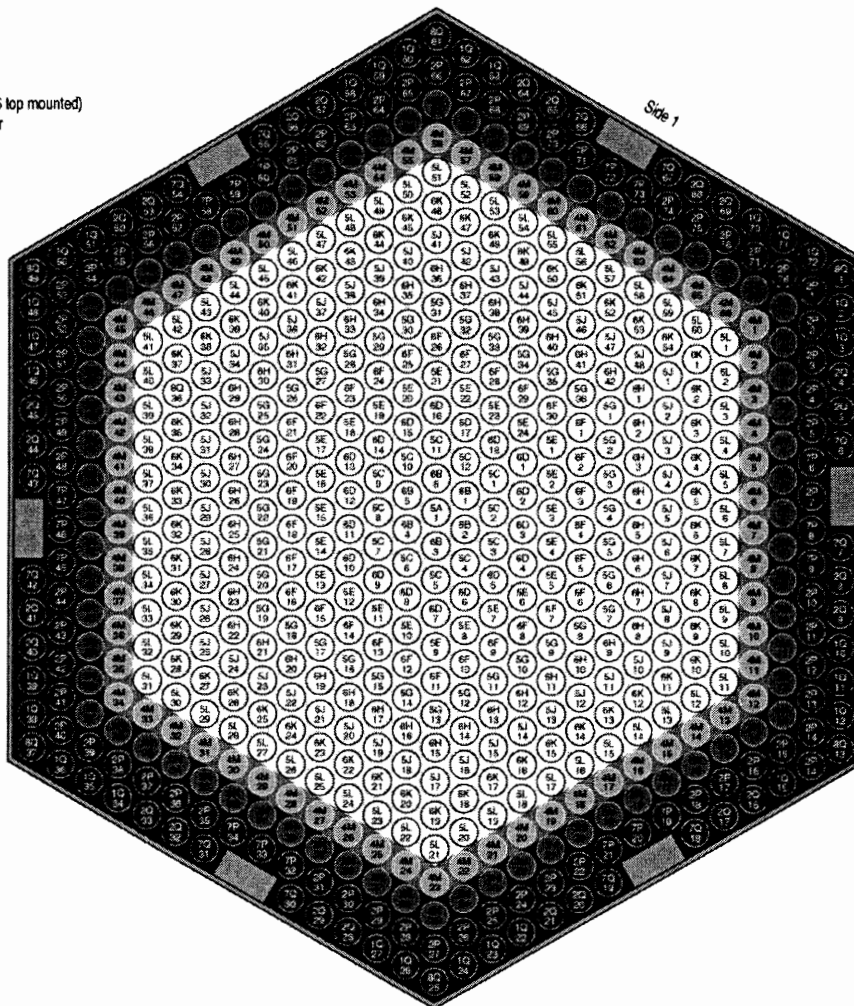
**Seed Assemblies** - There were twelve nominally identical seed assemblies, or modules, in the Shippingport LWBR documentation. The categorization of modules into Types I through IV refers to the blanket and reflector assemblies, although seed assemblies can be categorized according to the same system due to their unique associations with particular blanket assemblies. The numbering of assemblies by Arabic numerals within each type gives each assembly a unique identifier. Key dimensions of the horizontal cross sections of the various types of fuel assembly are given in DOE 1999b, p.22. Figure 7 (DOE 1999b, p.6) depicts the layout of the different types of fuel rod in the seed assemblies. The fuel rod in the center of a seed assembly is said to occupy the first row. Each successive hexagonal layer of rods wrapping around the central fuel rod forms another consecutively numbered row. The fuel of higher fissile concentration occupied the central eleven rows of the seed assemblies, where the binary stack length was at its maximum. Fuel rods bearing fuel of the lower fissile concentration occupied the remaining four outer rows. In the four outer rows, the binary stack length declined toward the edges of the assemblies. Base plates of Inconel 600 alloy held the fuel rods in position axially. Approximately half of the fuel rods were secured to the top base plate and the others were secured to the bottom base plate. The base plates were 38.1-mm (1.5-in.) thick and were perforated to accept the rod mounting stems and to allow the flow of cooling water. Average as-built fissile masses in assemblies from all core regions are given in Table 11. The Seed assembly with the maximum fissile loading contained the quantities of thorium and isotopes of uranium is shown in Table 12.

Table 11. Average As-Built Fissile Loading of Assemblies from All Core Regions

Core Region	Average As-Built Fissile Loading (kg)		
	Type I	Type II	Type III
Seed	16.53	16.55	16.56
Blanket	16.18	25.00	29.85

	Rod Type <sup>1</sup>	Binary Stack Length
	05, 06	84"
	04	70"
	03	56"
	01, 02, 07, 08	42"

619 Rods (306 top mounted)  
.306" Diameter  
.369" Pitch



NOTE: <sup>a</sup> Rod type: First two digits of a rod serial number correspond to the rod type number (Illegibility does not impact the technical meaning or content of the record).

Figure 7. Layout of Fuel Rods in a Seed Assembly

Table 12. Composition of the Seed Assembly with Maximum Fissile Loading

Nuclide	Mass (g)
<sup>232</sup> Th	434090
<sup>232</sup> U	0.10
<sup>233</sup> U	16568.7
<sup>235</sup> U	215.20
<sup>235</sup> U	11.49
<sup>236</sup> U	2.49
<sup>238</sup> U	45.85
<sup>233</sup> U + <sup>235</sup> U	16580.2

A nominal 9.36244-mm (0.3686-in.) center-to-center spacing between fuel rods was maintained along the length of each seed assembly by nine stainless steel (AM-350) grids. The uppermost grid was entirely above the fuel, and half of the lowermost grid was below the fuel. Leaving out the portions of the grids above and below pellet stacks, the grids displaced 2.130 cm<sup>3</sup> (0.130 in.<sup>3</sup>) of cooling water for each fuel rod in the seed assemblies. Grids in the seed region weighed, on average, 1542 g each grid, while the assembly with the most massive grids had an average grid mass of 1557 g.

The outer support shell of the seed assemblies was a 2.032-mm (0.080-in.) thick hexagonal shell of Zircaloy-4. The length of the support shell may be taken to be 3302 mm (130.00 in.), though this length includes that of the bottom cover plate. The distance between the inner surfaces of the top and bottom base plates was 3009.9 mm (118.500 in.). The distance between the bottom of the assembly and the inner surface of the bottom base plate was greater than 111.76 mm (4.4 in.) and less than 254 mm (10 in.); halfway between the bounds (182.88 mm) is a reasonable approximation. For top- and bottom-mounted fuel rods, the distance to the bottom of the pellet stack from the inner surface of the bottom base plate is 52.578 mm (2.07 in.). Therefore, the total distance between the bottom of the fuel assembly and the bottom of the fuel stack is approximately 235 mm. The maximum corner-to-corner width of the seed assemblies was 281.432 mm (11.08 in.).

Hardware removed from the seed assembly tops included the support shaft, the uppermost hexagonal portion of the assembly, the cover plate, and the top base plate bolts. The removal of mounting hardware from the assemblies necessitated the attachment of shipping plates at the tops so that the assemblies could be picked up. The shipping plates on the seed assemblies consist of 2-in. (50.8 mm) thick rings of Type 304 stainless steel with inner diameter 6.140 in. (155.956 mm) and outer diameter 9.628 in. (244.5512 mm). There are a number of holes and recessions in the shipping plates. Of the many holes and recessions, the 9 largest are: 6 holes 14.224 mm (0.560 in.) in diameter and 3 holes 25.4 mm (1.00 in.) in diameter. Records of the total weights of intact assemblies in storage are available (DOE 1999b, Table 3-4). The intact assemblies, including attached shipping plates, are between 3302 mm (130 in.) and 3327.4 mm (131 in.) long, allowing for the 1-in. maximum extent that the studs and nuts for attaching the shipping plates were allowed to protrude beyond the Zircaloy-4 support shell.

## 2.1.5 Structural

A two-dimensional (2-D) finite-element representation of the 5-DHLW DOE SNF-long waste package was developed to determine the effects of loads on the structural components due to a tipover design basis event (DBE). Calculations of maximum potential energy for each waste package handling accident scenario (horizontal drop, vertical drop, and tipover DBE) showed that the bounding dynamic load is obtained from a tipover case in which the rotating end of the waste package experiences the highest impact load. Therefore, for the 18-in. diameter DOE SNF canister and its structural components, the structural evaluations presented in this document are bounding for all handling-accident scenarios. The finite-element representation was developed using the dimensions provided in DOE 1999b.

## 2.1.6 Thermal

Table 13 lists the heat output of each waste package component. The data in second column is obtained by multiplying the DHLW short canister (3-m) heat output in CRWMS M&O (2000b), Table 13, with a factor of 1.69124. The method used to calculate this factor is explained in Taylor (1997), p. 2. The time of emplacement is year 2010. The thermal properties of the Shippingport LWBR fuel are determined as described in CRWMS M&O 2000b.

Table 13. Heat Output of Each Waste Package Component

Time After Emplacement (years)	Hanford 15-foot DHLW Canister (W)	Shippingport LWBR Seed SNF Assembly (W)	Waste Package Total (W)
0	1473.4	640.0	8007.1
0.1	1427.9	638.8 <sup>a</sup>	7778.4
0.2	1386.3	637.7 <sup>a</sup>	7569.3
0.3	1348.1	636.5 <sup>a</sup>	7377.0
0.4	1313.1	635.4 <sup>a</sup>	7200.8
0.5	1280.9	634.2 <sup>a</sup>	7038.9
0.6	1251.4	633.0 <sup>a</sup>	6889.6
0.7	1224.0	631.9 <sup>a</sup>	6751.7
0.8	1198.9	630.7 <sup>a</sup>	6625.3
0.9	1175.8	629.6 <sup>a</sup>	6508.4
1	1154.3	628.4 <sup>a</sup>	6399.8
2	1009.2	616.8 <sup>a</sup>	5662.6
3	933.7	605.2 <sup>a</sup>	5273.9
4	887.7	593.6 <sup>a</sup>	5032.3
5	854.9	582.0	4856.6
6	828.5	571.6 <sup>a</sup>	4714.3
7	805.7	561.2 <sup>a</sup>	4589.7
8	785.2	550.8 <sup>a</sup>	4477.0
9	766.0	540.4 <sup>a</sup>	4370.2
10	747.7	530.0	4268.5
15	666.0	482.0	3812.1
20	594.5	442.0	3414.4
30	475.1	442.0 <sup>b</sup>	2817.4
40	381.2	442.0	2348.1
50	307.1	442.0	1977.7
60	249.0	442.0	1686.8
70	202.9	442.0	1456.7
80	166.8	442.0	1275.8
90	138.0	442.0	1132.0

Table 13. Heat Output of Each Waste Package Component (Continued)

Time After Emplacement (years)	DHLW Canister (W)	Shippingport LWBR Seed SNF Assembly (W)	Waste Package Total (W)
100	115.5	442.0	1019.6
200	35.9	442.0	621.3
300	24.2	442.0	562.9
400	19.3	442.0	538.4
500	15.9	442.0	521.5
600	13.0	442.0	507.1
700	10.7	442.0	495.3
800	8.8	442.0	486.0
900	7.3	442.0	478.4
1000	5.9	442.0	471.6

NOTE: <sup>a</sup> Value derived from linear interpolation between given values.

The thermal conductivity of the HLW glass is approximated as that of pure borosilicate glass, while the properties of density and specific heat are approximated as those of Pyrex glass. Only the axial cross section of the waste package at the center of the DOE SNF canister is represented in the calculations. The values of thermal conductivity, specific heat, and density for borosilicate glass are 1.1 W/m/K, 835.0 J/kg/K, and 2,225.0 kg/m<sup>3</sup> respectively. The thermal conductivity is the mid-range value for a temperature range of 100 °C to 500 °C (CRWMS M&O 2000b, p. 28). The density and specific heat are taken to be the same as that of Pyrex glass at 27 °C (300 K) (CRWMS M&O 2000b, p. 28).

Decay heat for intact assemblies can be estimated from predicted decay heat curves that were developed for the Shippingport LWBR. The decay heat curves represent the decay heat generation rates as a function of cooling time for the hottest intact seed, blanket, and reflector assemblies. The maximum estimated heat generation rates for the various assemblies in 1992 (ten years after shutdown) are (DOE 1999b, p.34) for:

Seed Assemblies (assuming 619 rods): 630 W (2,150 BTU/hr)  
 Blanket Assemblies (assuming 564 rods): 527 W (1,800 BTU/hr)  
 Reflector Assemblies (assuming 228 rods): 175 W (600 BTU/hr).

Estimates of axial thermal peaking factors can be derived from average and peak burnup data for individual fuel rods (see Table 14). Estimates of the thermal conductivity of the two components of the unirradiated fuel at elevated temperatures as a function of temperature are presented in Table 15.

Table 14. Axial Peaking Factors Estimated from Peak and Average Burnups

Core Region	Peak Burnup (MWd/MTHM)	Maximum Rod Average Burnup (MWd/MTHM)	Estimated Axial Peaking Factor
Seed	53400	29800	1.79
Standard Blanket	23200	13200	1.76
Power Flattening Blanket	25200	14700	1.71
Reflector	4500	2200	2.05

Source: DOE 1999b, Table 3-22.

Table 15. Thermal Conductivity of UO<sub>2</sub> and Thoria Fuel

Temperature (°F)	Thermal Conductivity (Btu/hr/ft <sup>2</sup> /°F)	
	UO <sub>2</sub>	ThO <sub>2</sub>
500	3.4	4.1
1000	2.7	3.2
2000	1.8	2.1
3000	1.4	1.6
4000	1.1	1.2

Source: DOE 1999b, Table 3-23.

## 2.1.7 Shielding Source Terms

The source terms used in shielding calculations consist of gamma and neutron source terms of a Shippingport LWBR SNF assembly and gamma and neutron source terms of the five HLW glass canisters. This section presents the radiation source terms used to evaluate the dose rates at the external surfaces of the waste package.

### 2.1.7.1 Radiation Source Terms of the Shippingport LWBR SNF

A burnup and decay simulation of the Shippingport LWBR seed assembly provided the radiation source terms as a function of cooling time (DOE 1999b, p. 34). The initial fissile loading of the simulated assembly is 16892.84 g, which is approximately 2% greater than the actual initial fissile loading. The simulated burnup for the assembly is 10,269.14 MWd. Table 16 presents the gamma radiation source terms of a Shippingport LWBR SNF seed assembly at year 2005. The total neutron intensity at year 2005 is 5.770E+08 neutrons/s (DOE 1999b, p. B-4). Estimates of axial radiation peaking factors can be derived from average and peak burnup data for individual fuel rods (Table 14).

Table 16. Gamma Source Terms of a Shippingport LWBR SNF Seed Assembly at Year 2005

Mean Photon Energy (MeV)	Gamma Intensity (photons/s)		
	Activation Products	Actinides and Daughters	Fission Products
1.50E-02	1.208E+11	1.546E+13	1.123E+15
2.50E-02	1.034E+11	1.215E+12	2.340E+14
3.75E-02	6.585E+10	9.808E+11	2.006E+14
5.75E-02	1.967E+10	1.159E+12	2.185E+14
8.50E-02	1.187E+10	7.029E+12	1.322E+14
1.25E-01	5.647E+10	5.412E+11	8.913E+13
2.25E-01	1.869E+10	9.856E+12	1.143E+14
3.75E-01	4.747E+10	7.169E+11	4.979E+13
5.75E-01	7.054E+10	6.543E+12	7.568E+14
8.50E-01	6.130E+10	3.041E+12	1.275E+13
1.25E+00	3.202E+12	1.741E+11	7.310E+12
1.75E+00	1.979E+09	5.637E+11	3.450E+11
2.25E+00	1.662E+07	3.567E+05	2.293E+07
2.75E+00	5.144E+04	5.682E+12	1.706E+04
3.50E+00	1.468E-06	2.298E+04	2.219E+03
5.00E+00	5.276E-09	7.014E+03	2.227E-05
7.00E+00	3.423E-10	5.310E+02	1.445E-06
1.10E+01	2.165E-11	4.255E+01	9.138E-08
<b>Total</b>	3.781E+12	5.296E+13	2.939E+15

Source: DOE 1999b, pp. B-2 and B-3.

### 2.1.7.2 Radiation Source Terms for the Glass Canisters

The radiation source terms of the SRS HLW glass are bounding values for all HLW glass forms. The gamma and neutron source spectra and intensities of the SRS HLW glass per 3-m long canister (CRWMS M&O 1997b, Attachment IX, p. 1, and Attachment X, p. 1) are given in Table 17. These source terms were scaled up to correspond to the 4.5-m long HLW canister that will be placed in the 5-DHLW/DOE SNF-long waste package (CRWMS M&O 1998h, Attachment III, p. 1). Table 18 presents the gamma and neutron source terms for a 4.5-m long HLW glass canister.

The source terms for the SRS HLW glass were obtained by decaying the radionuclides that compose the SRS HLW. The radionuclide compositions were provided in *Characteristics of Potential Repository Wastes* (DOE 1992).

Table 17. Gamma and Neutron Sources for a SRS HLW Glass Canister at Day One after Pouring

Gamma Source		Neutron Source	
Upper Energy Boundary (MeV)	Intensity (photons/s)	Upper Energy Boundary (MeV)	Intensity (neutrons/s)
0.05	1.32E+15	0.10	1.97E+05
0.10	3.96E+14	0.40	1.89E+06
0.20	3.10E+14	0.90	6.34E+06
0.30	8.74E+13	1.40	6.92E+06
0.40	6.39E+13	1.85	6.12E+06
0.60	8.83E+13	3.00	2.61E+07
0.80	1.35E+15	6.43	3.42E+07
1.00	2.13E+13	20.00	3.07E+05
1.33	2.96E+13		
1.66	6.42E+12		
2.00	5.14E+11		
2.50	2.94E+12		
3.00	2.04E+10		
4.00	2.28E+09		
5.00	5.25E+05		
6.50	2.11E+05		
8.00	4.13E+04		
10.00	8.75E+03		
<b>Totals</b>	3.68E+15		8.21E+07

Source: CRWMS M&O 1997b, Attachment IX, p. IX-1, and Attachment X, p. X-1.

Table 18. Gamma and Neutron Sources for a 4.5-m Long HLW Glass Canister

Gamma Source		Neutron Source	
Upper Energy Boundary (MeV)	Intensity (photons/s)	Upper Energy Boundary (MeV)	Intensity (neutrons/s)
0.05	2.0480E+15	0.10	3.0535E+05
0.10	6.1351E+14	0.40	2.9342E+06
0.20	4.7986E+14	0.90	9.8224E+06
0.30	1.3546E+13	1.40	1.0724E+07
0.40	9.9093E+13	1.85	9.4907E+06
0.60	1.3681E+14	3.00	4.0517E+07
0.80	2.0891E+15	6.43	5.2948E+07
1.00	3.3083E+13	20.00	4.7557E+05
1.33	4.5956E+13		
1.66	9.9450E+12		

Table 18. Gamma and Neutron Sources for a 4.5-m Long HLW Glass Canister (Continued)

Gamma Source		Neutron Source	
Upper Energy Boundary (MeV)	Intensity (photons/s)	Upper Energy Boundary (MeV)	Intensity (neutrons/s)
2.00	7.9634E+11		
2.50	4.5524E+12		
3.00	3.1682E+10		
4.00	3.5394E+09		
5.00	8.1428E+09		
6.50	3.2640E+05		
8.00	6.3958E+04		
10.00	1.3569E+04		
<b>Totals</b>	5.6962E+15		1.2722E+08

Source: CRWMS M&O 1998h, Attachment III, p. 1.

### 2.1.8 Material Compositions

The chemical compositions of the materials used in the analyses are given in Tables 19 through 23.

Table 19. Chemical Composition of Zircaloy-4 (UNS R60804)

Element	Composition (wt.%) <sup>a</sup>	Value Used (wt.%)
Iron (Fe)	0.18-0.24	0.20
Chromium (Cr)	0.7-0.13	0.10
Iron and Chromium (Fe+Cr)	0.28-0.37	0.00
Tin (Sn)	1.2-1.7	1.40
Oxygen (O)	0.09-0.16	0.12
Zirconium (Zr)	Balance	98.18
Density <sup>b</sup> = 6.56 g/cm <sup>3</sup>		

Sources: <sup>a</sup> ASTM B 811-90, p. 2.

<sup>b</sup> ASM International 1990, p. 666.

Table 20. Chemical Composition of ASTM B 575 (Alloy 22 or UNS N06022)

Element	Composition (wt.%)	Value Used (wt.%)
Carbon (C)	0.015 (max)	0.015
Manganese (Mn)	0.50 (max)	0.50
Silicon (Si)	0.08 (max)	0.08
Chromium (Cr)	20.0 - 22.5	21.25
Molybdenum (Mo)	12.5 - 14.5	13.5
Cobalt (Co)	2.50 (max)	2.50
Tungsten (W)	2.5 - 3.5	3.0
Vanadium (V)	0.35 (max)	0.35
Iron (Fe)	2.0 - 6.0	4.0
Phosphorus (P)	0.02 (max)	0.02
Sulfur (S)	0.02 (max)	0.02
Nickel (Ni)	Balance	54.765
Density = 8.69 g/cm <sup>3</sup>		

Source: ASTM B 575-97, p. 2.

Table 21. Chemical Composition of ASTM A 516 Grade 70 Carbon Steel (UNS K02700)

Element	Composition (wt.%)	Value Used (wt.%)
Carbon (C)	0.30 (max)	0.30
Manganese (Mn)	0.85-1.20	1.025
Phosphorus (P)	0.035 (max)	0.035
Sulfur (S)	0.035 (max)	0.035
Silicon (Si)	0.15-0.40	0.275
Iron (Fe)	Balance	98.33
Density <sup>a</sup> = 7.86 g/cm <sup>3</sup>		

Source: ASTM A 516/A 516M-90, Table 1.

NOTE: <sup>a</sup> ASTM G 1-90, p. 7.

Table 22. Chemical Composition of Stainless Steel Type 304L (UNS S30403)

Element	Composition (wt.%)	Value Used (wt.%)
Carbon (C)	0.03 (max)	0.03
Manganese (Mn)	2.00 (max)	2.00
Phosphorus (P)	0.045 (max)	0.045
Sulfur (S)	0.03 (max)	0.03
Silicon (Si)	0.75 (max)	0.75
Chromium (Cr)	18.00 - 20.00	19.00
Nickel (Ni)	8.00 - 12.00	10.00
Nitrogen (N)	0.10	0.10
Iron (Fe)	Balance	68.045
Density <sup>a</sup> = 7.94 g/cm <sup>3</sup>		

Source: ASTM A 240/A 240M-97a, p. 2.

NOTE: <sup>a</sup> Density of this material is given as 7.94 g/cm<sup>3</sup> in ASTM G 1-90, p. 7.

Table 23. Chemical Composition of Stainless Steel Type 316L (UNS S31603)

Element	Composition (wt.%)	Value Used (wt.%)
Carbon (C)	0.03 (max)	0.03
Manganese (Mn)	2.00 (max)	2.00
Phosphorus (P)	0.045 (max)	0.045
Sulfur (S)	0.03 (max)	0.03
Silicon (Si)	1.00 (max)	1.0
Chromium (Cr)	16.00 - 18.00	17.00
Nickel (Ni)	10.00 - 14.00	12.00
Molybdenum (Mo)	2.00 - 3.00	2.50
Nitrogen (N)	0.10 (max)	0.10
Iron (Fe)	Balance	65.295
Density <sup>a</sup> = 7.98 g/cm <sup>3</sup>		

Source: ASTM A 276-91a, p. 2.

NOTE: <sup>a</sup> ASTM G 1-90, p. 7.

### 2.1.9 Degradation and Geochemistry

This section identifies the degradation rate of the principal alloys, the chemical composition of J-13 well water, and the drip rate of J-13 well water into a waste package. These rates are used in Section 6, Degradation and Geochemistry Analysis.

### 2.1.9.1 Physical and Chemical Forms of Shippingport LWBR Waste Package

Table 24 gives the composition of the HLW glass used in the calculations. The composition in CRWMS M&O 1999b was simplified to produce the values of weight percent listed in Table 24 (see Attachment 1 of CRWMS M&O 2000c). Minor elements or elements with questionable thermodynamic data were removed (Ag, Cr, Cs, Cu, Li, Mn, Ni, Pb, Th, Ti, Zn), and shorter half-life Pu isotopes were "predecayed" to longer half-life U isotopes:  $^{242}\text{Pu}$  was converted to  $^{238}\text{U}$ ;  $^{241}\text{Pu}$  was converted to  $^{237}\text{Np}$ , which was converted to  $^{233}\text{U}$ ;  $^{240}\text{Pu}$  was converted to  $^{236}\text{U}$ ;  $^{239}\text{Pu}$  was converted to  $^{235}\text{U}$ ; and  $^{238}\text{Pu}$  was converted to  $^{234}\text{U}$ . Since small amounts of neutron absorbers (Ag, Th, Zn) were removed in the simplified glass composition, this approach is conservative for internal criticality analyses.

Table 24. HLW Glass Composition, Density, and Degradation Rates

Element	Wt %	Moles, Normalized <sup>a</sup>
O	4.3928E+01	2.8079E+00
U	1.8574E+00	7.9811E-03
Ba	1.5007E-01	1.1211E-03
Al	2.3300E+00	8.8317E-02
S	1.2702E-01	4.0512E-03
Ca	6.4944E-01	1.6572E-02
P	1.3795E-02	4.5548E-04
Si	2.1820E+01	7.9455E-01
B	3.1503E+00	2.9802E-01
F	3.1253E-02	1.6824E-03
Fe	8.9370E+00	1.7623E-01
K	2.9325E+00	7.6706E-02
Mg	8.0925E-01	3.4052E-02
Na	1.3264E+01	5.9006E-01
<b>Total</b>	<b>1.0000E+02</b>	<b>4.8977E+00</b>
Density = 2.85 g/cm <sup>3</sup>		
<b>Total VA Rate Constant = <math>K_1[\text{H}^+]^{-0.4721} + K_2[\text{H}^+]^{0.6381}</math> (mol/cm<sup>2</sup>·s)</b>		
<b>Moderate Rate Constant (K<sub>1</sub>)</b>	1.98373E-19 liter/cm <sup>2</sup> ·s	
<b>High Rate Constant (K<sub>1</sub>)</b>	2.92353E-18 liter/cm <sup>2</sup> ·s	
<b>Moderate Rate Constant (K<sub>2</sub>)</b>	6.14458E-12 liter/cm <sup>2</sup> ·s	
<b>High Rate Constant (K<sub>2</sub>)</b>	3.67106E-11 liter/cm <sup>2</sup> ·s	
<b>Total Ebert Rate Constant = <math>K_3[\text{H}^+]^{-0.4} + K_4[\text{H}^+]^{0.6}</math> (mol/cm<sup>2</sup>·s)</b>		
<b>Moderate Rate Constant (K<sub>3</sub>)</b>	8.85753E-19 liter/cm <sup>2</sup> ·s	
<b>High Rate Constant (K<sub>3</sub>)</b>	1.07560E-17 liter/cm <sup>2</sup> ·s	
<b>Moderate Rate Constant (K<sub>4</sub>)</b>	7.97555E-13 liter/cm <sup>2</sup> ·s	
<b>High Rate Constant (K<sub>4</sub>)</b>	4.87424E-12 liter/cm <sup>2</sup> ·s	

Source: CRWMS M&O 2000c, p. 21.

NOTE: <sup>a</sup> One mole = 100g HLW glass

The actual HLW glass composition used in the HLW glass pour containers may vary significantly from these values, since the sources of the HLW glass and melting processes are not currently fixed. The silica and the alkali contents of the HLW glass have perhaps the most

significant bearing on EQ3/6 calculations. The amount of silica in the HLW glass strongly controls the amount of clay that forms in the waste package, and the silica activity controls the presence of insoluble uranium phases, such as soddyite ( $(\text{UO}_2)_2\text{SiO}_4 \cdot 2\text{H}_2\text{O}$ ). The alkali – sodium (Na), lithium (Li), and potassium (K) – content increase can cause pH to rise in the early stages of the EQ3/6 run, as HLW glass degrades. The silica and alkali contents shown in Table 24 are typical for proposed DOE glasses (CRWMS M&O 1999d).

Table 24 also lists the HLW glass density and degradation rates. A pH-dependent rate for HLW glass degradation was derived from CRWMS M&O 1998I (Section 6.3.3.2, Figure 6-31), and normalized. The first rate constant ( $K_1$ ) in Table 24 is dominant at pH values above 7, while the second rate constant ( $K_2$ ) is dominant at pH values below 7. The high glass degradation rate constants in Table 24 are those predicted at 50 °C, while the moderate rate constants are those predicted for degradation at 25°C (CRWMS M&O 1998I, Section 6.3.3.2, Figure 6-31).

For EQ6 cases 22 through 25 (Table 34) run for this calculation, a different set of pH dependent glass degradation rates, a slightly different glass composition and a different EQ6 database were used (CRWMS M&O 2000c, Attachment I). These rates were also derived from Equations 7 and 8 in CRWMS M&O 2000e (Section 6.2.3.3) and normalized. The third rate constant ( $K_3$ ) in Table 24 is dominant at pH values above 7, while the fourth rate constant ( $K_4$ ) is dominant at pH values below 7. As for the other HLW glass degradation rates, the high glass degradation rate constants in Table 24 are those predicted at 50 °C, while the moderate rate constants are those predicted for degradation at 25 °C.

Table 25 summarizes the degradation rates of the principal alloys used in the degradation and geochemistry calculations. For a comparable specific surface area, the carbon steel (Type A 516) is expected to degrade much more rapidly than the stainless steels (Type 316L and Type 304L). In addition, the stainless steels contain significant amounts of chromium (Cr) and molybdenum (Mo), and under the assumption of complete oxidation, would produce more acid, per unit volume, than the carbon steel.

Table 25. Steel Degradation Rates and Rate Constants

	<b>A 516 Carbon Steel</b>	<b>AM350 Stainless Steel</b>	<b>304L Stainless Steel</b>	<b>316L Stainless Steel</b>
<b>Low Rate (<math>\mu\text{m}/\text{yr}</math>)</b>	35	0.1	0.1	0.1
<b>Low Rate Constant (<math>\text{mol}/\text{cm}^2/\text{sec}</math>)</b>	8.706E-12	2.503E-14	2.516E-14	2.529E-14
<b>Moderate Rate (<math>\mu\text{m}/\text{yr}</math>)</b>	100.0	1.0	1.0	1.0
<b>Moderate Rate Constant (<math>\text{mol}/\text{cm}^2/\text{sec}</math>)</b>	2.488E-11	2.503E-13	2.516E-13	2.529E-13
<b>Average Rate (<math>\mu\text{m}/\text{yr}</math>)</b>	72.271364	1.9996307	34.405015	1.9996307
<b>Average Rate Constant (<math>\text{mol}/\text{cm}^2/\text{sec}</math>)</b>	1.79776E-11	5.00579E-13	8.65642E-12	5.05648E-13
<b>High Rate (<math>\mu\text{m}/\text{yr}</math>)</b>	131.12667	33.274895	207.53885	33.274895
<b>High Rate Constant (<math>\text{mol}/\text{cm}^2/\text{sec}</math>)</b>	3.2618E-11	8.32990E-12	5.22175E-11	8.41425E-12

Source: CRWMS M&O 2000c, Table 2.

Table 26 (CRWMS M&O 2000c) summarizes the characteristics of the three enrichment zones in the seed assemblies of Shippingport LWBR nuclear fuel. Because no fission product inventory is available, the calculations used the composition of fresh fuel. Use of fresh fuel is

conservative, since most fission products have significant neutron absorption cross sections, and the unirradiated fuel has a higher fissile content than partially spent fuel (note that the properties of the spent fuel do not affect the criticality results presented in this report because the fissile material was retained in the criticality calculations).

The three fuel types, corresponding to each enrichment zone of Shippingport LWBR seed nuclear fuel were also added to the EQ6 thermodynamic database, each with a molecular weight of 100 and a large enough solubility product constant to ensure dissolution but prevent precipitation in the waste package. The pH and carbonate-dependent fuel degradation rates in Table 26 were derived from Östhols and Malmström 1995 (Figures 3 and 4, Equations 2 and 11) and normalized. For Cases 24 and 25 (Table 34), a temperature dependent fuel degradation rate constant was used (Th/U oxide ceramic release rate for 25°C; CRWMS M&O 2000i, Table 1) and normalized. When this rate was used, the three fuel types were entered in the EQ6 input files as “special reactants” (not minerals entered in the EQ6 database), and a different EQ6 database was used.

Table 26. Shippingport LWBR (Th/U Oxide) SNF Elemental Composition and Degradation Rates

	High-Fissile-U Binary Fuel (Mole Fraction)	Low-Fissile-U Binary Fuel (Mole Fraction)	Thoria Fuel (Mole Fraction)
<b>Element/Isotope</b>			
U-233	1.963E-02	1.637E-02	
U-234	2.567E-04	2.140E-04	
U-235	1.783E-05	1.487E-05	
U-236	3.947E-06	3.290E-06	
U-238	7.240E-05	6.035E-05	
Th	3.134E-01	3.167E-01	3.333E-01
O	6.667E-01	6.667E-01	6.667E-01
<b>Total</b>	1.000E+00	1.000E+00	1.000E+00
<b>Molecular Weight</b>	100	100	100
<b>Density (g/cm<sup>3</sup>)</b>	9.70155	9.63832	9.67752
<b>Total SNF Rate Constant = <math>K_1[H^+]^{0.93} + K_2[CO_3^{2-}]^{0.88}</math> (mol/cm<sup>2</sup>.s)</b>			
		<b>K<sub>1</sub></b>	<b>K<sub>2</sub></b>
<b>Low Rate Constant (liter/cm<sup>2</sup>.s)</b>		9.27603e-14	2.72497E-14
<b>Average Rate Constant (liter/cm<sup>2</sup>.s)</b>		9.27603e-13	2.72497E-13
<b>High Rate Constant (liter/cm<sup>2</sup>.s)</b>		9.27603e-12	2.72497E-12
<b>Special 25°C Rate Constant (mol/cm<sup>2</sup>.s)</b>			4.20033E-16

Source: CRWMS M&O 2000c, Table 4.

The web (consisting of divider plates, inner and outer brackets) of the waste package basket (see Appendix B) are composed of A 516 carbon steel and serve two purposes: they center and hold the DOE SNF canister in place and separate the glass pour containers and prevent them from transmitting excessive loads to the SNF canister in the event of a fall or tip over event. At the center of the webs is a thick (3.175 cm) cylindrical support tube, also fabricated of A 516. In a breach scenario, the webs are exposed to water and corrode before the rest of the package; they are expected to degrade within a few hundred to a few thousand years. The oxidation of steel forms hematite (Fe<sub>2</sub>O<sub>3</sub>), which decreases the void space in the package by ~13%, or it forms goethite (FeOOH), which can decrease the void space by ~22% (CRWMS M&O 2000c). The differences are due to the lower density of goethite compared to hematite (CRWMS M&O

2000c, Table 9). Thus, the void space can be significantly reduced after the breach of the package due to the formation of corrosion products from corrosion of the webs.

The DOE SNF canister fits inside the central support tube of the waste package basket. The canister is composed primarily of 316L, with two internal, thick impact plates of carbon steel (approximated as A516 in the calculations). A basket structure constructed of 316L stainless steel plates is located within the DOE SNF canister to maintain the position of the assembly in the center of the canister. For Shippingport LWBR SNF waste package degradation scenarios, void space within the DOE SNF canister surrounding the SNF seed assembly was filled with Al shot containing ~1 wt.% Gd (as GdPO<sub>4</sub>), added as neutron absorber. The composition, density, and degradation rates of the Al shot used in this technical report are in Table 27.

Table 27. Elemental Composition, Degradation Rate Constant, and Density of Aluminum Fill Material

Element	Weight %	Mole Fraction
Al	95.34	0.9673
Ti	0.15	0.0008
Cu	0.27	0.0012
Si	0.59	0.0058
Zn	0.25	0.0010
Mg	0.99	0.0111
Mn	0.15	0.0007
Fe	0.69	0.0034
Gd	0.98	0.0001
P	0.19	0.0017
O	0.40	0.0069
<b>Total</b>	100.00	1.0000
<b>Molecular Weight</b>		100
<b>Density (g/cm<sup>3</sup>)</b>		2.025
<b>Degradation Rate Constant (mol/cm<sup>2</sup>·s)</b>		2.53587E-13

Source: CRWMS M&O 2000c.

### 2.1.9.2 Chemical Composition of J-13 Well Water

The geochemistry calculations reported in this document have used the J-13 well water composition, which is shown in Table 28, for water dripping into the waste package. Since this water composition was determined from a well drilled into the saturated zone beneath the planned repository location, there is some question of the compositional deviations to be expected for water dripping into the repository drift, which is in the unsaturated zone. Several alternative versions of the J-13 well water composition have been proposed and used in other geochemistry calculations.

The rationale for the use of J-13 well water composition is that it is representative of the groundwater entering the drift because it was collected from the same stratigraphic unit that the repository will occupy. The fact that the J-13 well water samples were taken below the water table while the repository location is above the water table is not of concern for the following reasons. The groundwater composition is controlled largely by transport through the host rock, over pathways of hundreds of meters. The host rock composition is similar in both the

unsaturated and the saturated areas of this unit and is not expected to change substantially over time. Any groundwater chemistry alteration by the initial thermal perturbation from the waste package heat will have died out well before the initial waste package breach, which is estimated to extend beyond the regulatory time period (10,000 years) (CRWMS M&O 2000f, p. 5-2).

Silicate complexes with Gd were not included in this calculation because the available literature indicates that, if they exist, they are too unstable to permit measurement of their equilibrium constants. For example, the Gd silicates are not included in the classic study of rare-earth chemistry in the planned Swedish repository environment: *A Selected Thermodynamic Database for REE to be Used in HLNW Performance Assessment Exercises* (Spahiu and Bruno 1995, p. ii). This compilation is also suitable for use by the Yucca Mountain Project (YMP) because the chemical composition of granite (which is the host rock for the Swedish repository) is virtually identical to that of Yucca Mountain rhyolitic tuff. This document specifically states “In most natural waters, the carbonate complexes are accepted as the dominant soluble species of the rare earths” (Spahiu and Bruno 1995, p. 7). Additionally, some aspects of this issue have been more extensively discussed in a previous study of Gd loss from a waste package (CRWMS M&O 1997g, Section 5.3.2). The following two paragraphs address the sensitivity of geochemistry results to potential variations in the composition of the dripping water.

Table 28. Composition of J-13 Well Water

Component	mg/l
Na	45.8
K	5.04
Ca	13.0
Mg	2.01
NO <sub>3</sub> <sup>-</sup>	8.78
Cl <sup>-</sup>	7.14
F <sup>-</sup>	2.18
SO <sub>4</sub> <sup>2-</sup>	18.4
Si	28.5
Alkalinity (as HCO <sub>3</sub> <sup>-</sup> )	128.9
pH = 7.41	

DTN: MO0006J13WTRCM.000

Two major factors control how the J-13 well water chemistry might affect EQ6 calculations. The first factor is the presumed CO<sub>2</sub> pressure of equilibration, which is closely coupled to the pH of the J-13 well water; and the second is the content of dissolved species, which may react with package materials and fuel, and thus affect solubilities. An example of the second factor is the amount of available dissolved silica, which can precipitate uranium as insoluble minerals like soddyite and uranophane.

In other analyses of codisposal packages, order of magnitude variations in CO<sub>2</sub> pressure have not had significant effects on the calculated Gd loss (CRWMS M&O 1998f, Table 5.3-1). In codisposal packages, the chemistry of the package water is influenced, overwhelmingly, by the degradation of glass and other package materials. The alkali and alkaline earth content of the glass completely swamped the native J-13 well water composition in the bulk of the EQ6

scenarios run for the geochemical calculations (CRWMS M&O 2000c). The combination of steel and glass degradation drove the pH from ~3 to ~10, far greater than the range that exists in native J-13 well water (CRWMS M&O 1998j, Figures 5-2 through 5-20). The silica content of the glass is enormously greater than the amount of silica that can be contributed from J-13 water, even with long periods of flushing at relatively high rates. The calculations in CRWMS M&O 1998j showed that in cases of significant uranium solubility, the dominant aqueous species were carbonate and phosphate complexes. The phosphate was supplied overwhelmingly from the  $GdPO_4$  criticality control material and the glass, and the high aqueous carbonate concentration (resulted from glass dissolution and the fixed  $CO_2$  partial pressure).

### **2.1.9.3 Drip Rate of J-13 Well Water into a Waste Package**

The rates at which water drips onto a waste package and flows through it are represented as being equal. The drip rate is taken from a correlation between percolation rate and drip rate (CRWMS M&O 1998e, Tables 2.3-55 and 2.3-56, Figures 2.3-112 and 2.3-114). Specifically, percolation rates of 40 mm/yr and 8 mm/yr correlate with drip rates onto the waste package of  $0.15 \text{ m}^3/\text{yr}$  and  $0.015 \text{ m}^3/\text{yr}$ , respectively. The choice of these particular percolation and drip rates is discussed in detail in CRWMS M&O 1998g, p. 19.

For the present study, the range of allowed drip rates was extended to include an upper value of  $0.5 \text{ m}^3/\text{yr}$  and a lower value of  $0.0015 \text{ m}^3/\text{yr}$ . The upper value corresponds to the 95 percentile upper limit for a percolation rate of 40 mm/yr, and the lower value is simply 0.1 times the mean value for the percolation rate of 8 mm/yr (CRWMS M&O 1998e, pp. 2-110 through 2-113). These extreme values were used, because prior studies (CRWMS M&O 1998f, Table 5.3-1) suggested that when waste forms are codisposed with glass, the greatest chance of Gd removal occurs when: (1) initial high drip rates cause leaching of the glass and removal of alkali from the waste package due to overflow, and (2) subsequent low drip rates which allow acid to build from the degradation of stainless steel.

A correlation of percolation rate versus drip rate prepared for the Total System Performance Assessment (TSPA) for site recommendation (CRWMS M&O 2000g, Figure 3) indicates that the drip rates used in the present study correspond to percolation rates ranging from approximately 5 to 100 mm/yr.

## **2.2 FUNCTIONS AND DESIGN CRITERIA**

The design criteria are based on the *Defense High Level Waste Disposal Container System Description Document* (CRWMS M&O 2000j), hereafter referred to as the SDD. In this subsection, the key waste package design criteria from the SDD are identified for the following areas: structural, thermal, shielding, criticality within a breached but otherwise intact waste package, degradation and geochemistry, and criticality of a degraded waste package and waste form. SDD paragraph numbers are identified below as SDD X.X.X.X.

## 2.2.1 Structural

2.2.1.1 “The disposal container/waste package shall prevent the breach of the waste form canister during normal handling operations.”

(SDD 1.2.1.8)

2.2.1.2 “During the preclosure period, the disposal container/waste package, shall be designed to withstand (while in a vertical orientation) a drop from a height of 2 m (6.6 ft) (TBV-245) onto a flat, unyielding surface without breaching. (TBV-245)”

(SDD 1.2.2.1.3) (TBV-245)

2.2.1.3 “During the preclosure period, the disposal container/waste package, shall be designed to withstand (while in a horizontal orientation) a drop from a height of 2.4 m (7.9 ft) (TBV-245) onto a flat, unyielding surface without breaching. (TBV-245)”

(SDD 1.2.2.1.4) (TBV-245)

2.2.1.4 “During the preclosure period, the waste package shall be designed to withstand a tip over from a vertical position with slap down onto a flat, unyielding surface without breaching. (TBV-245)”

(SDD 1.2.2.1.6) (TBV-245)

Calculations of maximum potential energy for each handling accident scenario (horizontal drop, vertical drop, and tipover design-basis events [DBEs]) showed that the bounding dynamic load is obtained from a tipover case in which the rotating top end of the waste package experiences the highest impact load with maximum velocity of 9.62 m/sec (CRWMS M&O 1999a, p. 16). The maximum velocities of the waste package for 2.4 m horizontal and 2.0 m vertical drops are approximately 6.86 m/sec ( $v = \sqrt{2gh}$ , where  $g$  is the gravitational acceleration, and  $h$  is height) and 6.26 m/sec, respectively. Therefore, tipover structural evaluations are bounding for all waste package handling accident scenarios considered in the SDD. Section 3.3 addresses these requirements with respect to breach of the DOE SNF canister. This analysis assumes that MGR surface design will prevent events that exceed the bounding assumptions made in deriving the conclusions in this report.

The tipover DBE may only take place during a waste package transfer operation from vertical to horizontal position (just after waste package closure) or horizontal to vertical position (upon retrieval). Section 3, Structural Analysis, demonstrates that the waste package will not breach under such a handling-accident scenario.

## **2.2.2 Thermal**

**2.2.2.1** “The waste package shall maintain the temperature of HLW glass below 400 degrees C (752 degrees F) under normal conditions, and below 460 degrees C (860 degrees F) (TBV-245) for short-term exposure to fire, as specified by Criterion 1.2.2.1.11.”

(SDD 1.2.1.6) (TBD-245)

**2.2.2.2** “The waste package shall be designed to have a maximum thermal output of 11.8 kW.”

(SDD 1.2.4.2)

## **2.2.3 Shielding**

“Waste package design shall reduce the dose rate at all external surfaces of a waste package to 1,450 (TBV-248) rem/h or less. This criterion identifies a disposal container interface with the Disposal Container Handling System, the Waste Emplacement/Retrieval System, and the Performance Confirmation Emplacement Drift Monitoring System.”

(SDD 1.2.4.1)(TBV-248)

## **2.2.4 Degradation and Geochemistry**

There are no degradation and geochemistry criteria in the SDD to address.

## **2.2.5 Intact and Degraded Criticality**

“During the preclosure period, the disposal container/waste package shall be designed such that the effective multiplication factor ( $k_{\text{eff}}$ ) is less than or equal to 0.95 under assumed accident conditions considering allowance for the bias in the method of calculation and the uncertainty in the experiments used to validate the method of calculation. (TBV-245)”

(SDD 1.2.2.1.12)(TBV-245)

As stated in Section 8.5, the results from the intact waste-package criticality analysis show that the requirement of  $k_{\text{eff}}$  plus bias and uncertainty be less than or equal to 0.95 is satisfied. Criteria 1.2.2.1.13 and 1.2.2.1.14 are not considered because the frequency of criticality occurrence and the associated consequence are not within the scope of this report.

## **2.3 ASSUMPTIONS**

In the course of developing this document, assumptions are made regarding the waste package structural, thermal, shielding, intact criticality, degradation and geochemistry, and degraded component criticality analyses. The list of the major assumptions that are essential to this technical report are provided below.

### **2.3.1 Structural**

- 2.3.1.1** The waste package containment barriers are assumed to have solid connections at the adjacent surfaces. The rationale for this assumption is that the inner and outer barriers will be either shrunk fit or the inner barrier will be weld clad onto the outer barrier inner surface (CRWMS M&O 1997c). For each one of these fabrication processes, it is reasonable to assume solid contact between the barriers. Newer designs have a 0 to 4 mm gap between barriers. However, gaps within this range are negligible for the structural analysis, therefore the solid contact assumption between barriers is still applicable. This assumption is used in Section 3.
- 2.3.1.2** The target surface is conservatively assumed to be essentially unyielding by using a large elastic modulus for the target surface compared to the waste package. The rationale for this assumption is that a bounding set of results is required in terms of stresses and displacements and it is known that the use of an essentially unyielding surface results in slightly higher stresses in the waste package. This assumption is used in Section 3.

### **2.3.2 Thermal**

- 2.3.2.1** For Shippingport LWBR SNF, an axial power peaking factor (PPF) of 2.0 is assumed. The rationale for this assumption is that it allows for the inclusion of a radial uncertainty in the maximum axial peaking factor, reported as 1.79 (CRWMS M&O 2000b, Assumption 3.11), which is conservative. The HLW glass canisters are assumed to have an axial PPF of 1.00 (CRWMS M&O 1997f, p. 53). Heat generation in the HLW glass canisters does not exhibit a peaking behavior because the canister is geometrically wide. This assumption is used throughout Section 4.
- 2.3.2.2** Representing only conduction and radiant heat transfer inside the waste package is assumed to provide conservative results (higher temperature) for the calculations. The rationale for this assumption is the following: fill gas within the waste package will allow natural convective heat transfer to exist. However, since only a few small enclosed basket cavities exist and the temperature gradient in the enclosure is not significant, circulation of the fill gas is insignificant. Thus, the problem may be represented with only the dominant heat transfer modes, with a negligible or conservative impact upon the results. This assumption is used throughout Section 4.
- 2.3.2.3** It is assumed that a 2-D finite-element representation of a cross section at the midsection of the waste package will be the hottest portion of the waste package. Inherent to this assumption is that axial heat transfer does not significantly affect the solution. The rationale for this assumption is that the metal thermal conductivity and heat generation distributions are such that axial heat transfer is very small or negligible at the midsection. This assumption is used throughout Section 4.
- 2.3.2.4** It is assumed that the first arrival and emplacement of Shippingport LWBR SNF will occur in the year 2010. The rationale for this assumption is to assure correspondence

with CRWMS M&O 1997d, p. 7, and its evaluation of the throughput of waste forms. This assumption is used throughout Section 4.

- 2.3.2.5** The heat output of the Shippingport LWBR seed SNF is based on decay heats starting at 2010 and continuing until 2030, after which time the decay heat is held constant. The rationale for this assumption is that in reality the Shippingport LWBR seed SNF will continue to decay with time after 2030. Thus, this assumption is conservative, resulting in higher waste package temperatures. This assumption is used throughout Section 4.

### **2.3.3 Shielding**

- 2.3.3.1** The active fuel region of the Shippingport LWBR seed fuel assembly is homogenized inside its transverse dimensions. The rationale for this assumption is that the homogenization of the fuel rod inside the assembly gave the same waste package surface dose rate as the heterogeneous representation (CRWMS M&O 1998b, Section 6). This assumption is used to obtain the results provided in Section 5.

- 2.3.3.2** A PPF factor of 2.0 is used for the Shippingport LWBR fuel source terms for bounding the axial source distribution. This value is based on the rounded peaking factor for a seed assembly of 1.79 (DOE 1999b, Assumption 3.11), for conservative (higher) dose rate calculations. This assumption was used to obtain the results provided in Section 5.

- 2.3.3.3** It is assumed that the dose rates due to secondary gamma rays are negligible. The rationale for this assumption is that the neutron source intensities are about 6 and 7 orders of magnitude smaller than the gamma source intensity for the Shippingport LWBR SNF and HLW glass, respectively. Therefore, no coupled neutron-photon calculation is performed. This assumption is used to obtain the results provided in Section 5.

### **2.3.4 Degradation and Geochemistry**

- 2.3.4.1** It is assumed that water may circulate freely enough in the partially degraded waste package that all degraded solid products may react with one another in the aqueous solution. By facilitating contact of any acid that may result from the corrosion of steel with neutron absorbers in spent fuel, the code conservatively enhances potential preferential loss of neutron absorbers from the waste package. This assumption is used in Section 6.

- 2.3.4.2** It is assumed that precipitated solids remain in place and are not mechanically eroded or entrained as colloids in the advected water. The rationale for this assumption is that since dissolved fissile material (U, Th) may be adsorbed on colloids (clays, iron oxides) or may be precipitated as colloids during waste package degradation it is conservative, for internal criticality, to assume that all precipitated solids, including mobile colloids, will be deposited inside the waste package rather than transported out of the waste package. This assumption is used throughout Section 6.

- 2.3.4.3** It is assumed that sufficient decay heat is retained within the breached waste package over times of interest to cause convective circulation and mixing of the water inside the waste package. The analysis that serves as the rationale of this assumption is discussed in CRWMS M&O 1996, Attachment VI. This assumption is used throughout Section 6.
- 2.3.4.4** It is assumed that the corrosion resistant material (the outer shell) of the waste package will react so slowly with the infiltrating water (and water ponded in the waste package) that it will have a negligible effect on the solution's chemistry. The bases for this assumption consist of the facts that the corrosion resistant material is fabricated of Alloy 22, which corrodes very slowly compared (1) to other materials in the waste package and (2) to the rate at which soluble corrosion products will be flushed from the waste package. This assumption is used in Section 6.
- 2.3.4.5** For the purposes of calculating the disposition of degradation products (particularly the principal fissile element  $^{233}\text{U}$  and the principal neutron absorber Gd) it is assumed that the thermodynamic database used for EQ3/6 calculations is correct and sufficiently complete, with respect to the chemical reactions that could significantly effect the waste package chemistry. The rationale for this assumption is that previous results have been shown to be fairly insensitive to uncertainties in the thermodynamic constants of the relevant reactions (CRWMS M&O 1999e, Section 5.3.1). This assumption is used in Section 6.

### **2.3.5 Intact and Degraded Mode Criticality**

- 2.3.5.1** Beginning of life, pre-irradiation fuel compositions of Shippingport LWBR SNF were used for all calculations because it is conservative to assume fresh fuel as it is more neutronically reactive than spent fuel. This assumption is used throughout Section 7.
- 2.3.5.2** For the degraded configurations with intact fuel pins surrounded by degraded waste package internals, the placement and stacking of the pins is chosen to give a more reactive configuration rather than a more realistic stacking due to gravity. The rationale of this assumption is that it is more conservative since it gives a larger  $k_{\text{eff}}$  for the system. This assumption is used in Section 7.

### **2.3.6 General**

- 2.3.6.1** The technical information related to spent nuclear fuel (DOE 1999b), DOE SNF canister (DOE 1999a), glass pour canister (Taylor 1997), and source term of SRS HLW glass (CRWMS M&O 1997b) is only used to determine the bounding values and identify items that are important to criticality control for this fuel group by establishing the limits based on the representative fuel type (Shippingport LWBR) for this group (Th/U oxide fuel). The technical information used establishes the bounds for acceptance. The rationale for this assumption is that it was designated by the DOE SNF grouping in support of criticality and related calculations. The burden is placed on the custodian of the SNF to demonstrate, before acceptance of SNF by the CRWMS,

that SNF characteristics identified as important to criticality control or other analyses herein are not exceeded. This assumption is used in Sections 2 through 7.

- 2.3.6.2** It is assumed that the composition of Hanford HLW glass is identical with the composition of SRS HLW glass. The rationale for this assumption is that the Hanford HLW glass composition is not known at this time and the characteristics of the two types of glass are expected to be similar. This assumption is used in Sections 2 and 4 through 7.
- 2.3.6.3** Stainless steel type 316L (UNS S31603) is substituted for Type 315NG for the inner barrier of the waste package. The rationale for this is that the wt.% values used for Type 316L (see Table 23) fall within the composition ranges for Type 316NG (ASM International 1987, p. 931). The exception is the carbon content that is slightly higher for Type 316L, but this makes the composition used more conservative for the criticality analysis. For all the other analyses considered, the higher carbon content has a negligible influence on the results.

## **2.4 BIAS AND UNCERTAINTY IN CRITICALITY CALCULATIONS**

The purpose of this section is to document the MCNP (CRWMS M&O 1998c) (identified as Computer Software Configuration Item [CSCI] 30033 V4B2LV) evaluations of Laboratory Critical Experiments (LCEs) performed as part of the Disposal Criticality Analysis Methodology program. Only LCEs most relevant to Shippingport LWBR fuel are studied. LCE's results listed in this section are given in CRWMS M&O (1999f) for the thermal compound (heterogeneous) HEU systems and in CRWMS M&O (1999f) for the thermal solution U-233 systems. The objective of this analysis is to quantify the MCNP Version 4B2 code system's ability to accurately calculate the effective neutron multiplication factor ( $k_{\text{eff}}$ ) for various configurations. MCNP is set to use continuous-energy cross sections processed from the evaluated nuclear data files ENDF/B-V (Briesmeister 1997, App. G). These cross-section libraries are part of the MCNP code system that has been obtained from the Software Configuration Management (SCM) in accordance with appropriate procedures. Each of the critical core configurations is simulated, and the results reported from the MCNP calculations are the combined average values of  $k_{\text{eff}}$  from the three estimates (collision, absorption, and track length) and the standard deviation ( $\sigma$ ) of these results listed in the final generation summary in the MCNP output. When MCNP underpredicts the experimental  $k_{\text{eff}}$ , the experimental uncertainty is added to the uncertainty at 95% confidence from the MCNP calculation to obtain the bias. This bias along with the 5% margin (see Section 2.2.5) is used to determine the interim critical limit for all MCNP calculations of the waste package with Shippingport LWBR DOE SNF canister.

### **2.4.1 Benchmarks Related to Intact Waste Package Configurations**

Several surrogate critical experiments with highly enriched fuel rods are used for the Shippingport LWBR fuel with respect to intact criticality analyses: HEU-COMP-THERM-003, HEU-COMP-THERM-005, HEU-COMP-THERM-006, and HEU-COMP-THERM-007 (NEA 1998). Critical experiments that used Shippingport LWBR rods are being evaluated by the NSNFP and will be used to calculate the final critical limit for licensing.

A series of critical experiments with water-moderated hexagonally-pitched lattices of highly enriched fuel rods of cross-shaped cross section was performed over several years in the Russian Research Center "Kurchatov Institute." The 22 experiments analyzed under this category in this report consist of the following:

1. Fifteen critical two-zone lattice experiments corresponding to different combinations of inner and peripheral zones of cross-shaped fuel rods at two pitches. For detailed descriptions of these experimental configurations see pages 2, and 7 through 14 of NEA (1998), HEU-COMP-THERM-003 (HCT-003).
2. One critical configuration of hexagonal pitched clusters of lattices of fuel rods with copper (Cu) rods. Detailed experimental configuration descriptions are available on pages 2 through 8 of NEA (1998), HEU-COMP-THERM-005 (HCT-005).
3. Three critical configurations with uniform hexagonal lattices with pitch values of 5.6, 10.0, and 21.13 mm. Detailed experimental configuration descriptions are available on pages 2, 5, and 6 of NEA (1998), HEU-COMP-THERM-006 (HCT-006).
4. Three critical configurations with double hexagonal lattices of fuel rods and zirconium (Zr) hydride rods. Detailed experimental configuration descriptions are available on pages 2 through 8 of NEA (1998), HEU-COMP-THERM-007 (HCT-007).

The pitch, number of rods, and number of fuel rods were the parameters that were varied. The maximum bias for this set of calculations is 0.019 (CRWMS M&O 1999c, pp. 16 through 19, and 76).

#### **2.4.2 Benchmarks Related to Degraded Waste Package Configurations**

Critical experiments with highly enriched U-233 (approximately 97.7 wt.%) nitrate solution are described in detail in NEA (1998) (U233-SOL-THERM-001, U233-SOL-THERM-008). The concentration of fissile element and of neutron absorber (boron) in the solution, and tank diameter were among the parameters that were varied. The maximum bias for this set of experiments is 0.018 (CRWMS M&O 1999f, pp. 23 and 24).

#### **2.4.3 Critical Limit**

The worst-case bias, calculated from the MCNP simulations of the experiments described in Sections 2.4.1 and 2.4.2, is increased to 0.03 to cover all intact and degraded rod cases. This bias includes the bias in the method of calculation and the uncertainty in the experiments. Based on this bias, the interim critical limit is determined to be 0.92 after allowance for a five-percent margin, for the bias in the method of calculation and the uncertainty in the experiments used to validate the method of calculation. This interim critical limit will be used until an addendum to the topical report is prepared to establish the final critical limit based on critical experiments that used Shippingport LWBR fuel.

### 3. STRUCTURAL ANALYSIS

#### 3.1 USE OF COMPUTER SOFTWARE

The finite-element analysis (FEA) computer code used for this evaluation is ANSYS Version (V) 5.4. The information regarding the code and its use for the structural analysis is documented in CRWMS M&O 1999a.

#### 3.2 DESIGN ANALYSIS

Finite-element structural analyses for the components of the 5-DHLW/DOE SNF-long waste package are summarized in this section. A detailed description of the finite-element representations, the method of solution, and the results are provided in CRWMS M&O (1999a). The results of these analyses are compared to the design criteria in the 1995 American Society of Mechanical Engineers (ASME) Boiler and Pressure Vessel Code (BPVC), Section III, Subsection NB (ASME 1995), so that conclusions can be drawn regarding the structural performance of the 5-DHLW/DOE SNF-long waste package design.

The design approach for determining the adequacy of a structural component is based on the stress limits given in the 1995 ASME BPVC.  $S_u$  is defined as the ultimate tensile strength of the materials, and  $S_m$  is defined as the design stress intensity of the materials. Table 29 summarizes the design criteria as obtained from appropriate sections of the 1995 ASME BPVC.

Table 29. Containment Structure Allowable Stress-limit Criteria

Category	Containment Structure Allowable Stresses	
	Normal Conditions - Elastic Analysis (ASME 1995, Division 1, Subsection NB, Articles NB-3221.1 and NB-3221.3)	Accident Conditions - Plastic Analysis (ASME 1995, Division 1, Appendix F, Article F-1341.2)
Primary membrane stress intensity	$S_m$	$0.7S_u$
Primary membrane plus primary bending stress intensity	$1.5S_m$	$0.9S_u$

This analysis is within the bounds of the structural design criteria in Section 2.2.1; however, it does not consider incredible DBEs (e.g., crane two-block events).

#### 3.3 CALCULATIONS AND RESULTS

##### 3.3.1 Description of the Finite-Element Representation

A two-dimensional (2-D) transient dynamic calculation has been performed for the structural analysis of the Shippingport LWBR SNF canister within the 5-DHLW DOE SNF-long waste package. This analysis, performed with ANSYS V5.4, considers a bounding dynamic load from a tip-over design basis event on the cross section of the waste package at its rotating end. Since the potential energy of the rotating end is larger than the potential energy of any other DBEs, the tipover DBE is considered both bounding and appropriately conservative for structural design purposes. The Shippingport LWBR seed fuel assembly is represented as a single lumped mass,

since the worst-case loading is a point loading in the middle of the canister assembly plates. Aluminum shot is to be placed within the 18-inch-diameter DOE SNF canister, and is represented in the calculation as individual lumped masses.

The 2-D finite-element representation is developed using the dimensions provided in Appendices A and B. A one-half-symmetry finite-element representation is developed for the waste package (see Figure 8). The finite-element representation includes the outer and inner barriers, basket assembly, support tube, uppermost HLW pour canister, DOE SNF canister shell and basket (Appendices A and B). The finite-element representation also includes masses of the other four pour canisters and the fuel assembly. The barriers are assumed to have solid connections at the adjacent surfaces (Assumption 2.3.1.1) and are constrained in a direction perpendicular to the symmetry plane. The one HLW pour canister that is located above the DOE SNF canister is created using 2-D elements. The remaining pour canisters are included in the representation as point mass elements at the points of contact of the pour canisters with the inner barrier and the divider plates. These locations are approximately at the mid-point of each component or segment at which the pour canisters would be in contact. This approach is a realistic way to simulate the effect of each pour canister in contact with the waste-package internals. This approach reduces the computer execution time needed for this analysis. The finite-element representation is used to determine the maximum closure of the clearance space inside the DOE SNF canister basket plates so that they can be compared to the Shippingport LWBR seed fuel assembly dimensions to determine whether there is contact between the basket plates and the fuel assembly.

First, the impact velocity of the outer surface of the inner lid is calculated for a waste package tipover DBE. Then, this velocity is conservatively used in the 2-D finite-element analysis. Since the 2-D representation does not model the lids, the calculations will indicate that the waste package components undergo more deflection and stress than would actually occur if the lids were included. The target surface is conservatively assumed to be essentially unyielding because the elastic modulus used for the target surface is large compared to the elastic modulus used for the waste package (Assumption 2.3.1.2). The target surface is constrained at the bottom to prevent its horizontal and vertical motion. Contact elements are defined between the top pour canister and the inner brackets, and between the outer barrier and the target surface. Initial configuration of the finite-element representation includes a negligibly small gap for each contact element. This approach allows enough time and displacement for the waste package and its internals to ramp up to the specified initial velocity before the impact. With this initial velocity, the simulation is then continued throughout the impact until the waste package begins to rebound; at that time, the stress peaks, and the maximum displacements are obtained.

The HLW glass material properties are represented by ambient material properties of general borosilicate glass. This document does not specifically report any results for the individual HLW glass canisters.

ANSYS 5.4

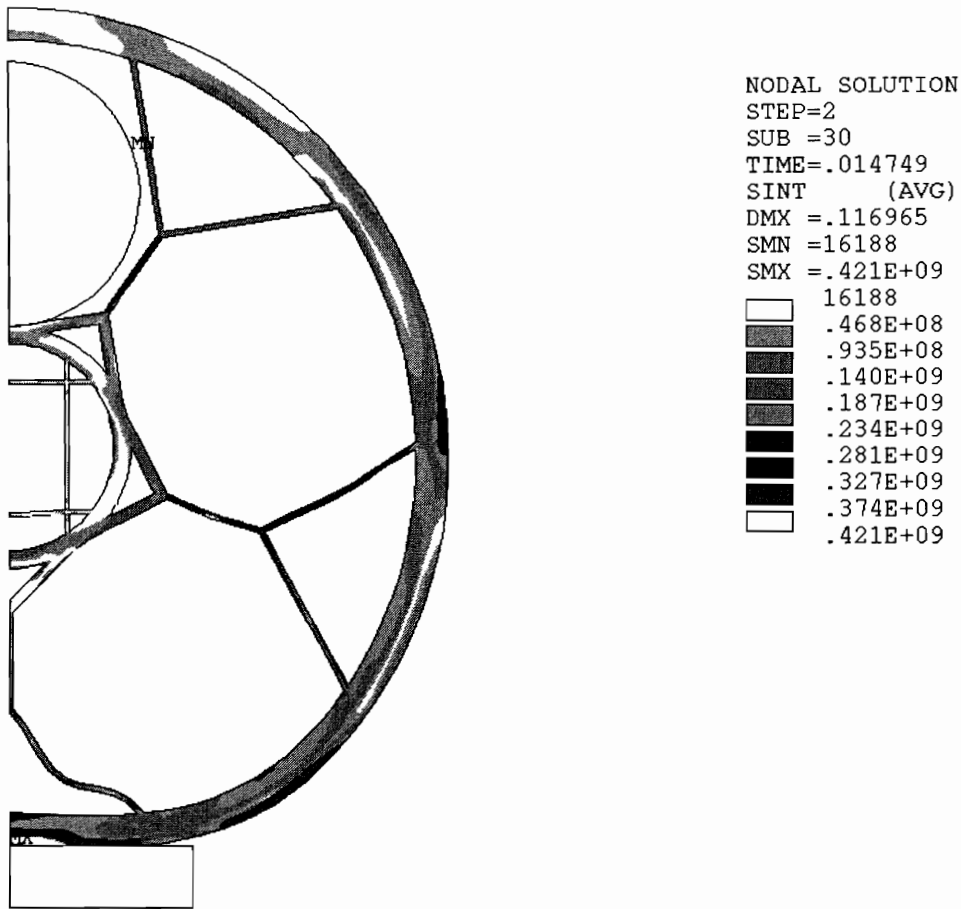


Figure 8. Stresses in the 5-DHLW/DOE SNF-Long Waste Package

### 3.3.2 Results

The structural response of the waste package to tipover accident loads is reported using maximum stress values and displacements obtained from the finite-element solution to the problem. The results show that the cavity between the Shippingport LWBR seed fuel assembly and the basket plates does not close, but on the contrary, becomes larger because of the dynamic load applied on the bottom plate by the fuel assembly as shown in Figure 9. Hence, there will be no interference between the fuel assembly and the basket plates because of a tipover DBE. The maximum stress in the DOE SNF canister structural components and internals is 243.6 MPa (CRWMS M&O 1999a, p. 21), which is less than 0.9 or 0.7 of the ultimate tensile strength of 316L stainless steel, 483 MPa (CRWMS M&O 1999a, p. 21), therefore the allowable stress-limit criteria presented in Table 29 are met.

The calculations in CRWMS M&O (1999a) also show that the maximum bending stress on the base plate due to the weight of the structural components and the fuel is 16.6 MPa which is less than the 172 MPa yield strength of 316L stainless steel (CRWMS M&O 1999a, p. 21).

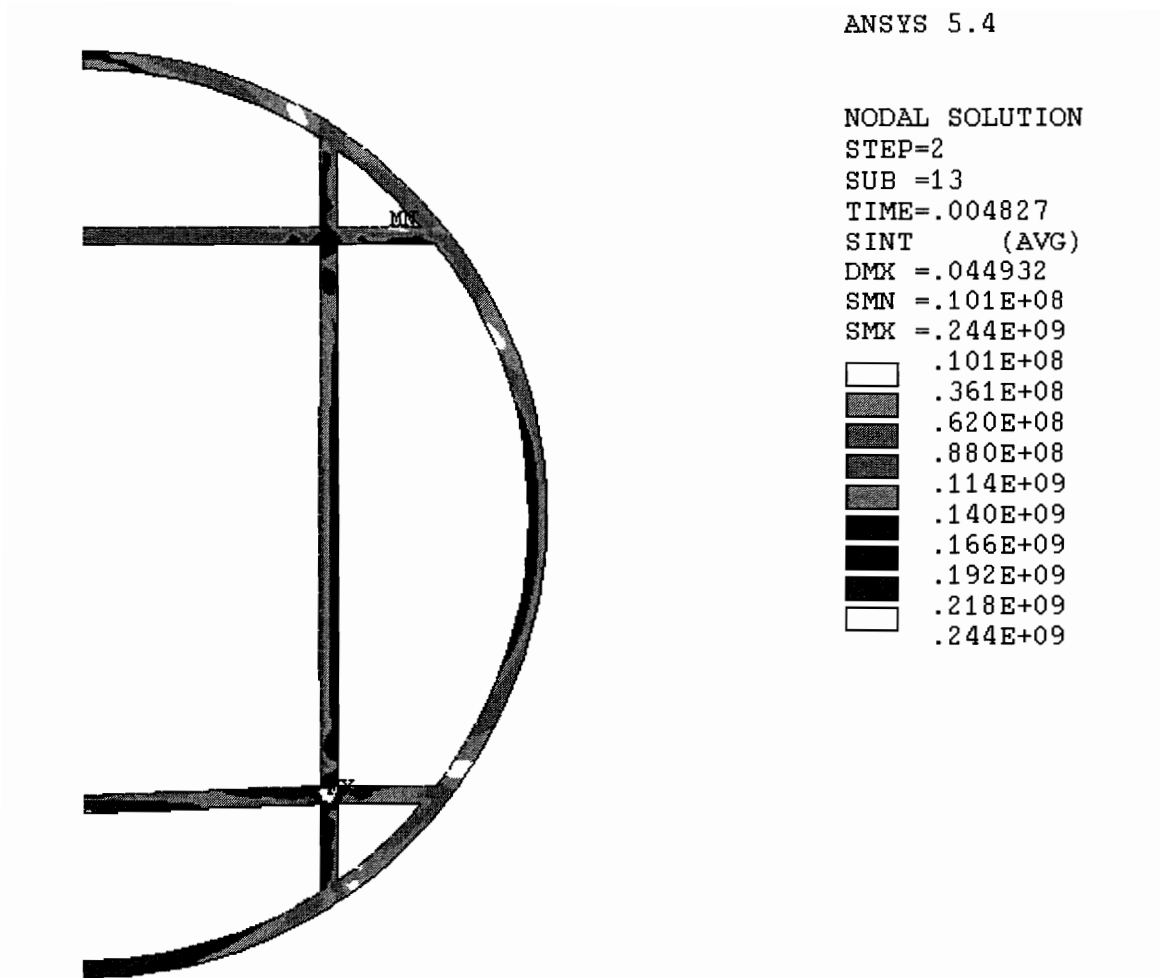


Figure 9. Stresses in the DOE SNF Canister

Finally, the critical stress for buckling to take place on the spacer tube (see Figure 5) is 1.43 GPa, whereas the compressive stress is only 2.06 MPa (CRWMS M&O 1999a, p. 21). Therefore, the Shippingport LWBR fuel assembly will not be crushed within the basket structure.

The calculations given in CRWMS M&O (1999a), Sections 5.7 and 5.8 utilize the maximum DOE SNF canister mass, 2721 kg, and the maximum HLW glass canister mass, 4200 kg; therefore, the results of the bending and buckling calculations given in this section are bounding for all design concepts.

### 3.4 SUMMARY

The results given in Section 3.3 show that there is sufficient clearance between the inner diameter of the support tube and the outer diameter of the DOE SNF canister in the case of a tipover DBE. Hence, there will be no interference between the two components, and the DOE SNF canister can be removed from the support tube if necessary to set it inside another waste package. Additionally, there will be no breach of the DOE SNF canister.

## 4. THERMAL ANALYSIS

### 4.1 USE OF COMPUTER SOFTWARE

The FEA computer code used for this evaluation is ANSYS Version (V) 5.4. The information regarding the code and its use for the thermal analysis is documented in CRWMS M&O 2000b.

### 4.2 THERMAL DESIGN ANALYSIS

A detailed description of the finite-element representations, the method of solution, and the temperature history results are provided in CRWMS M&O (2000b). This waste package is loaded with five Hanford 15-foot HLW glass canisters (Figure 2) and one DOE SNF canister (Figures 3, 4 and 5). The DOE SNF canister holds one Shippingport LWBR seed assembly. Two different fill gases are considered for the Shippingport LWBR DOE SNF canister: helium and argon. The waste package is filled with helium. These calculations evaluate heat conduction and thermal radiation within the waste package. Heat transfer by means of natural convection is assumed to be insignificant and is not considered (see Assumption 2.3.2.2).

Figure 10 presents a finite-element representation of the 5-DHLW/DOE SNF-long waste package with the DOE SNF canister containing Shippingport LWBR SNF. Figure 11 presents a finite-element representation of one-sixth section of the Shippingport LWBR SNF seed assembly.

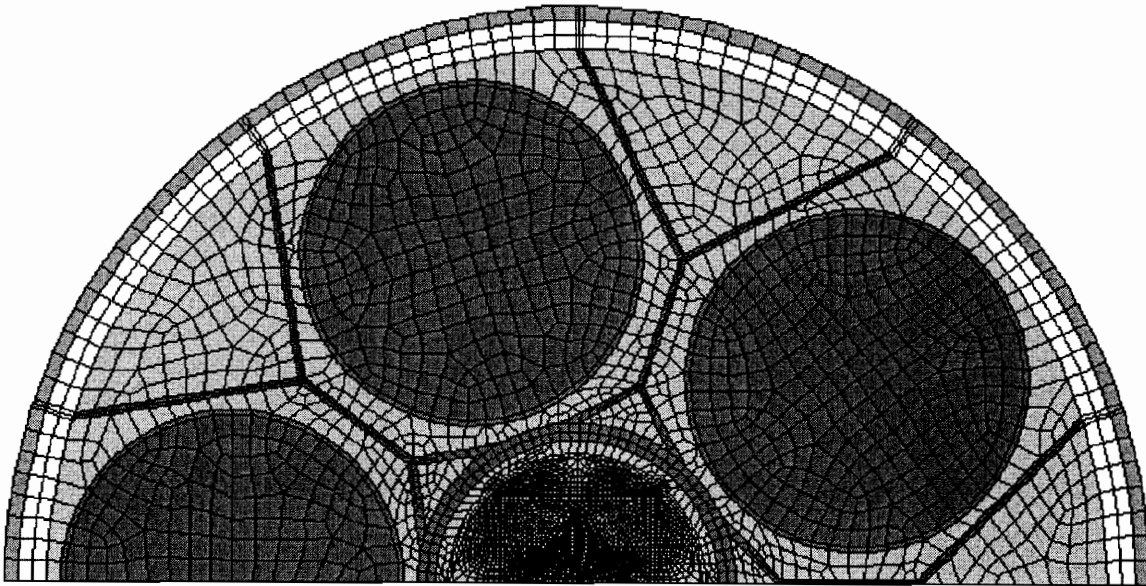


Figure 10. Finite-Element Representation of the 5-DHLW/DOE SNF-Long Waste Package

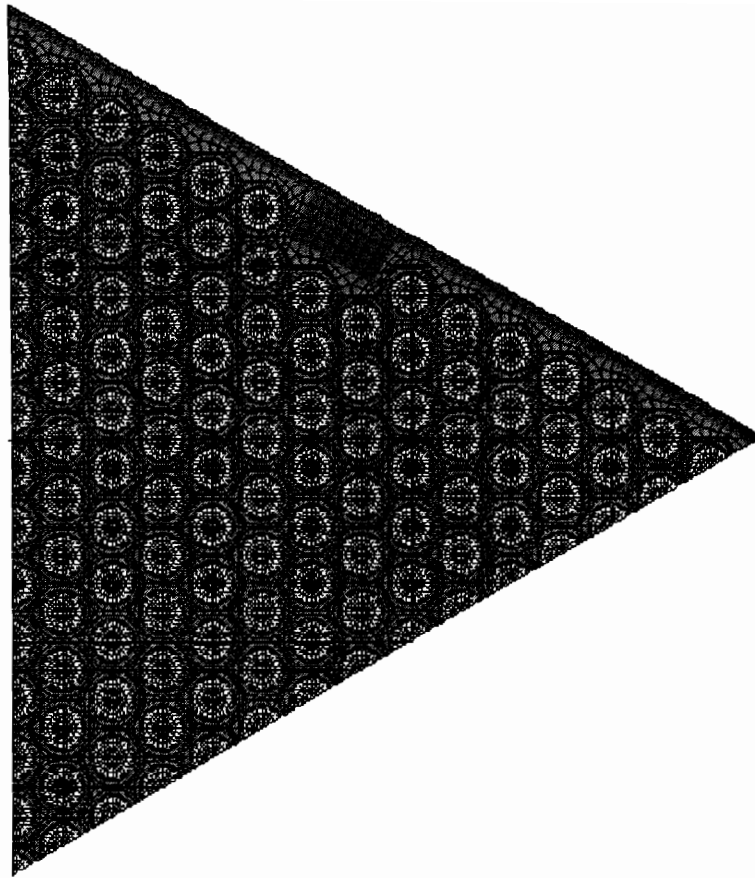


Figure 11. Finite-Element Representation of the Shippingport LWBR Seed Assembly Fuel (one-sixth section)

As shown in these figures, symmetry is across the center of the waste package. Therefore, this representation includes half of the 5-DHLW/DOE SNF-long waste package, half of the DOE SNF canister, two-and-a-half Hanford long HLW glass canisters, and half of the Shippingport LWBR seed assembly. In addition, the HLW glass canisters and the Shippingport LWBR seed assembly are positioned in the center of their compartments to maximize radiation heat transfer to waste package surfaces.

#### 4.3 CALCULATIONS AND RESULTS

Table 30 summarizes the peak temperatures for components of interest and time of occurrence for each DOE SNF canister fill gas (CRWMS M&O 2000b). For the EDA II waste package designs and emplacement parameters, the results indicate that argon fill gas in the DOE SNF canister causes the peak Shippingport LWBR fuel temperature, which occurs after nine years, to be approximately 7% higher than for helium fill gas. The peak DHLW glass and waste package surface temperatures are not affected by the choice of the fill gas in the Shippingport LWBR DOE SNF canister (see also Figure 12). Figure 13 plots WP peak temperatures versus radial location from the center of the waste package with the Shippingport LWBR DOE SNF canister filled with argon or helium gas for both VA and EDA II designs.

Table 30. Peak Temperature versus Time for Various Components

<b>VA Waste Package Design and Emplacement Parameters</b>					
<b>Component and Location</b>	<b>Location from Center of Waste Package (m)</b>	<b>Helium Fill Gas</b>		<b>Argon Fill Gas</b>	
		<b>Peak Temperature (°C)</b>	<b>Time of Peak Temperature (years)</b>	<b>Peak Temperature (°C)</b>	<b>Time of Peak Temperature (years)</b>
Inside the DOE Shippingport LWBR SNF Canister (Figures 4 and 5 show components )					
Center of Shippingport LWBR Seed SNF Assembly	0.000	249.46	20.0	285.57	9.0
Center of A-Plate	0.133	231.46	20.0	234.41	234.41
Center of SNF Canister Outer Shell	0.224	223.63	20.0	225.66	20.0
Outside the DOE Shippingport LWBR SNF Canister but Inside the Waste Package (Figure 1 shows components)					
Center of Support Tube	0.267	220.43	20.0	220.44	20.0
Center of Divider Plate	0.484	214.54	20.0	214.55	20.0
Inside of Waste Package Corrosion Resistant Shell	0.940	193.78	30.0	193.78	30.0
Waste Package Corrosion Resistant and Corrosion Allowance Shells Interface	0.960	193.68	30.0	193.68	30.0
Outside of Waste Package Corrosion Allowance Shell	1.060	193.61	30.0	193.61	30.0

<b>EDA II Waste Package Design and Emplacement Parameters</b>					
<b>Component and Location</b>	<b>Location from Center of Waste Package (m)</b>	<b>Helium Fill Gas</b>		<b>Argon Fill Gas</b>	
		<b>Peak Temperature (°C)</b>	<b>Time of Peak Temperature (years)<sup>a</sup></b>	<b>Peak Temperature (°C)</b>	<b>Time of Peak Temperature (years)</b>
Inside the DOE Shippingport LWBR SNF Canister (Figures 4 and 5 show components)					
Center of Shippingport LWBR Seed SNF Assembly	0.000	325.55	9.0	347.46	9.0
Center of A-Plate	0.133	310.85	9.0	312.50	9.0
Center of SNF Canister Outer Shell	0.224	304.91	9.0	305.97	9.0
Outside the DOE Shippingport LWBR SNF Canister but Inside the Waste Package (Figure 1 shows components)					
Center of Support Tube	0.267	302.55	9.0	302.54	9.0
Center of Divider Plate	0.484	298.68	9.0	298.68	9.0
Inside of Waste Package Inner Shell	0.940	287.97	9.0	287.98	9.0
Waste Package Inner and Outer Shell Interface	0.990	287.33	9.0	287.84	9.0
Outside of Waste Package Outer Shell	1.015	287.77	9.0	287.77	9.0

Source: CRWMS M&amp;O 2000b, Table 6-3.

NOTE: <sup>a</sup> Time after 50 years ventilation period.

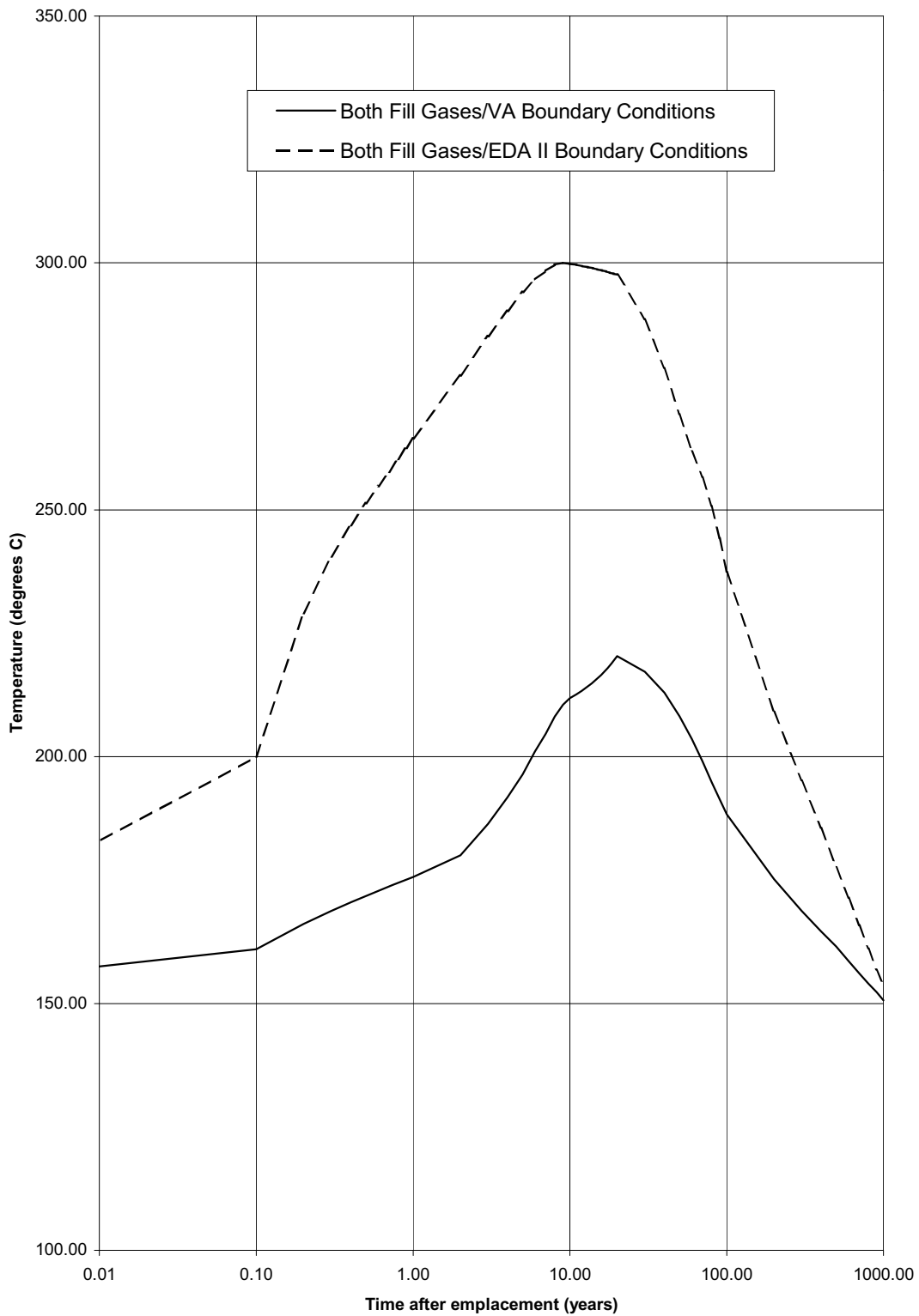


Figure 12. DHLW Peak Temperature versus Time

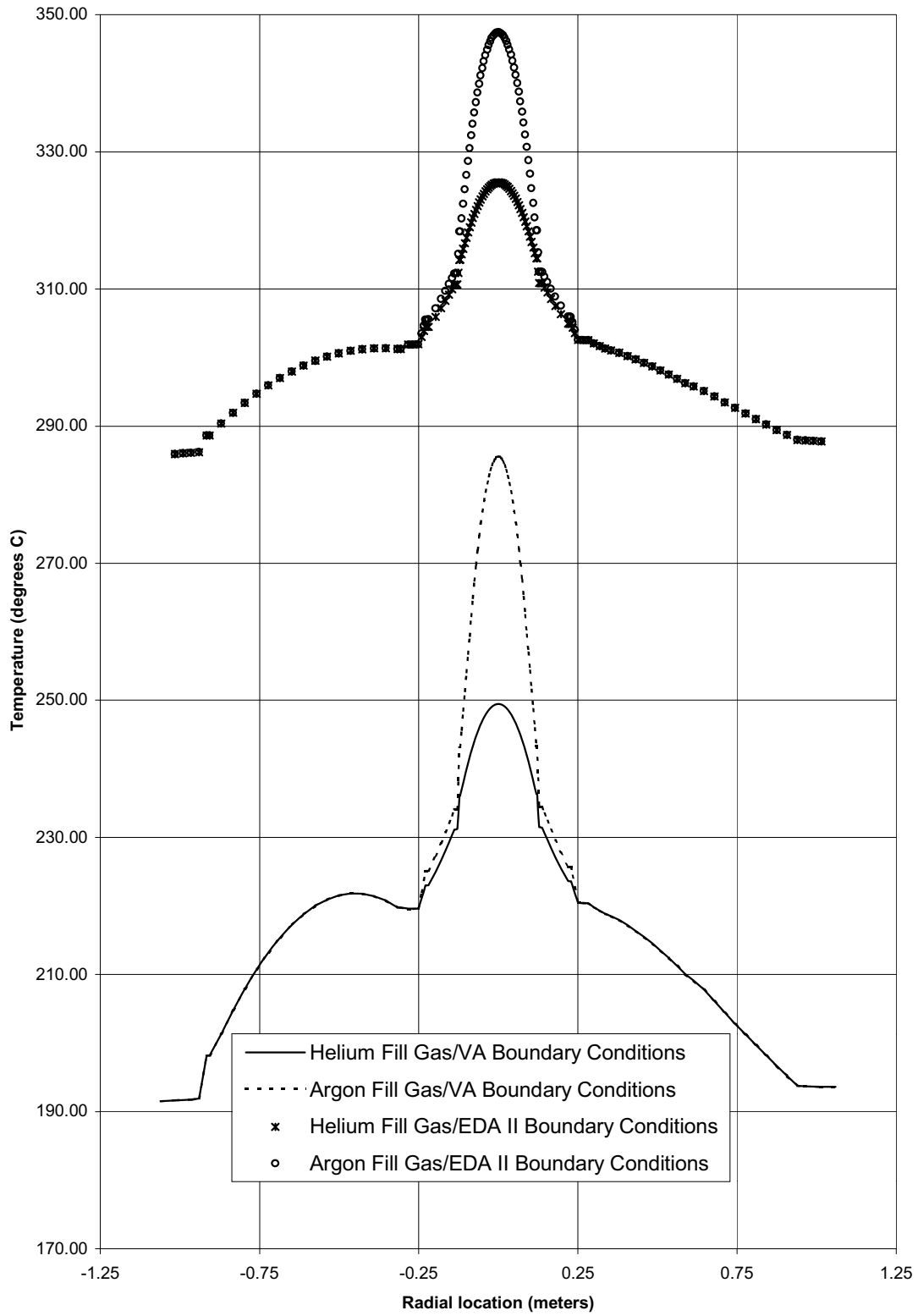


Figure 13. Radial Temperature Profile of the Waste Package

#### **4.4 SUMMARY**

The results indicate that the maximum DHLW glass temperature for the EDA II design is 300.04 °C (Argon) (CRWMS M&O 2000b, Table 6-2), which is less than SDD criterion (Section 2.2.2.1) of 400 °C. The waste package thermal output at emplacement is 8007.1 W for both VA and EDA II design and emplacement parameters. Both are less than the 11.8 kW criterion set in the SDD (Section 2.2.2.2).

## 5. SHIELDING ANALYSIS

### 5.1 USE OF COMPUTER SOFTWARE

The Monte Carlo particle transport code, MCNP, Version 4B2, is used to calculate average dose rates on the surface of waste package. The information regarding the code and its use for the shielding analysis is documented in CRWMS M&O 1999b.

### 5.2 SHIELDING DESIGN ANALYSIS

The Monte Carlo method of solving the integral Boltzmann transport equation, which is implemented in the MCNP computer program, is used to calculate radiation dose rate for the waste package. MCNP uses continuous-energy neutron and photon cross-sections processed from the evaluated-nuclear-data files, ENDF (Briesmeister 1997, pp. 2-17 through 2-22 and App. G). The flux averaged over a surface is tallied, and the flux-to-dose rate conversion factors (Briesmeister 1997, App. H) are applied to obtain surface dose rates for gamma and neutron radiation.

### 5.3 CALCULATIONS AND RESULTS

CRWMS M&O 1999b gives the details of the calculations and the results. The geometric representation of the waste package used in MCNP calculations is shown in Figure 14. Previous dose-rate calculations for the 5-HLW/DOE SNF waste package have shown that the angular dose rate over waste package radial surfaces is uniform (CRWMS M&O 1998h, p. 33). Therefore, only axial variation of the dose rates on the waste-package radial surfaces and the radial variation of the dose rates on the waste-package top and bottom axial surfaces are studied. Figure 15 shows the surfaces and segments that are used in the dose-rate calculations. The radial surface, between the bottom and top planes of HLW glass, are equally divided into five segments, each of which is 67.108-cm high. The first radial segment (segment 1), 125.11-cm high, corresponds to the empty portion of the HLW canister, which is between the top of the waste package cavity and the top of the HLW glass.

Tables 31 and 32 list the MCNP estimates of the radial and axial dose rates on the outer surface of the waste package containing five 4.5-m-long HLW glass canisters and the Shippingport LWBR DOE SNF canister. The estimated relative error, which is the ratio of the estimated standard deviation and the estimated tally, is also provided for each segment dose rate in Tables 31 and 32. The dose rates in rem/h and rad/h are practically the same due to the insignificant contribution of the neutron dose rate to the total dose rate (CRWMS M&O 1999b, pp. 19-21, and Attachment VI).

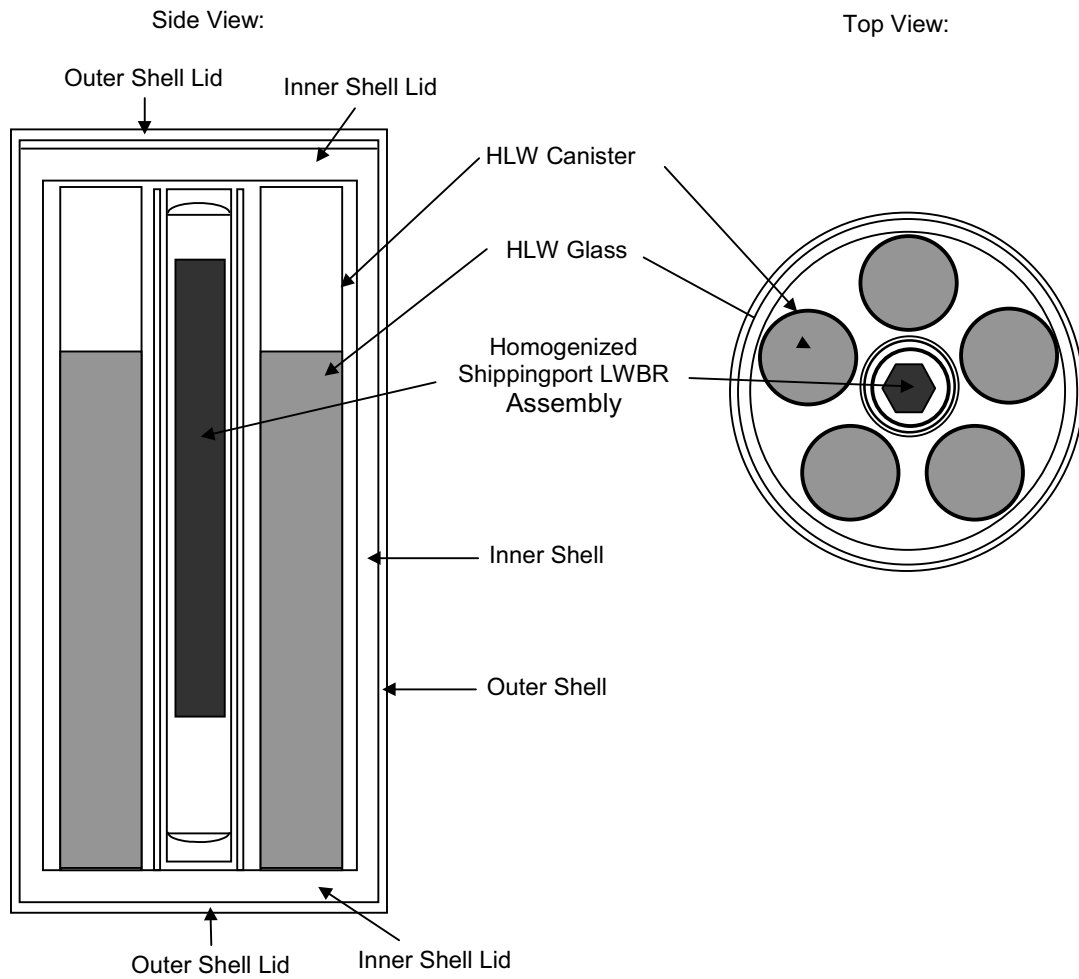


Figure 14. Vertical and Horizontal Cross Sections of the MCNP Geometry Representation

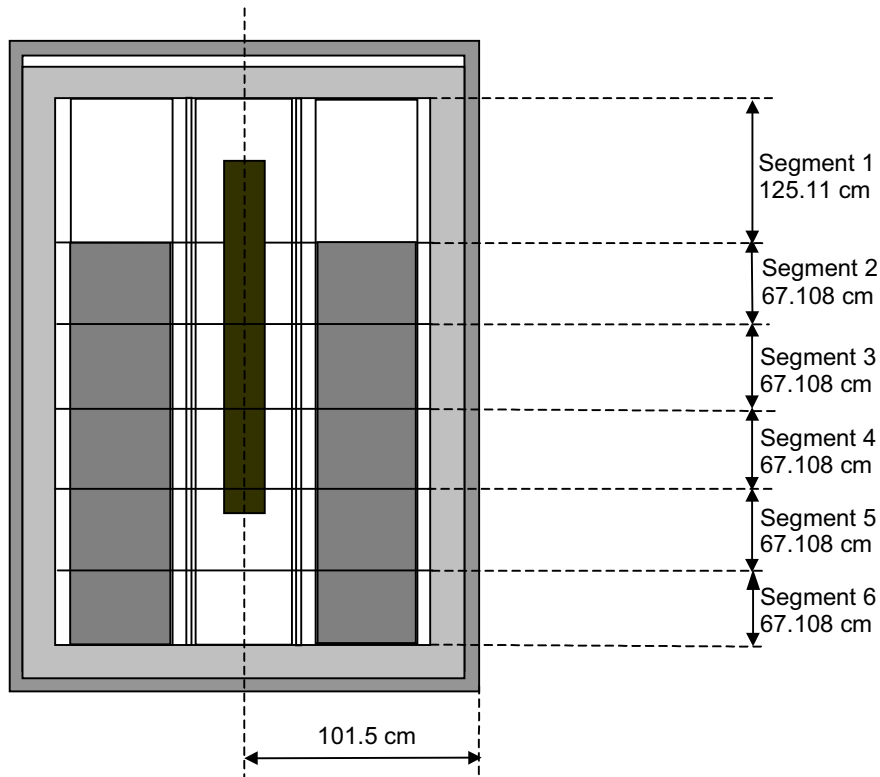


Figure 15. Surfaces and Segments Used for Dose-Rate Calculations

Table 31. Dose Rates on the Waste Package Outer Radial Surface

Axial Location (Figure 15)	Gamma		Neutron		Total	
	Dose Rate (rem/h)	Relative Error	Dose Rate (rem/h)	Relative Error	Dose Rate (rem/h)	Relative Error
Segment 1	9.6170E+00	0.0191	2.5418E-01	0.0038	9.8712E+00	0.0186
Segment 2	7.2129E+01	0.0109	2.5634E-01	0.0050	7.2385E+01	0.0109
Segment 3	8.0643E+01	0.0104	2.5985E-01	0.0050	8.0902E+01	0.0104
Segment 4	8.0426E+01	0.0104	2.3333E-01	0.0053	8.0660E+01	0.0104
Segment 5	8.1163E+01	0.0106	1.7181E-01	0.0062	8.1334E+01	0.0106
Segment 6	7.4584E+01	0.0109	1.1881E-01	0.0076	7.4703E+01	0.0109

Table 32. Dose Rates on the Waste Package Axial Surfaces

Axial Location (Figure 15)	Gamma		Neutron		Total	
	Dose Rate (rem/h)	Relative Error	Dose Rate (rem/h)	Relative Error	Dose Rate (rem/h)	Relative Error
Bottom surface of waste package	3.0317E+00	0.0379	6.3251E-02	0.0113	3.0950E+00	0.0371
Top surface of waste package	6.0081E-01	0.0802	9.0493E-02	0.0088	6.9130E-01	0.0697

The maximum dose rate at the external surfaces of a waste package that contains only the five 4.5-m-long HLW glass canisters is 83.05 rem/h (dose rate + 2 $\sigma$ ) (CRWMS M&O 1999b, p. 20).

#### **5.4 SUMMARY**

The maximum dose rate on the external surfaces of the waste package is 83.05 rem/h. It occurs on segment 5 of the outer radial surface of the waste package. The dose rates on the bottom and top surfaces of the waste package are one and two orders of magnitude, respectively, smaller than the maximum dose rate on the outer radial surface. The design criterion specifies a maximum dose rate of 1450 rem/h (TBV-248, Section 2.2.3) at all external surfaces of the waste package. Therefore the maximum dose rate at the external surfaces of the waste package is about than eighteen times smaller than the value specified in the design performance criterion.

## 6. DEGRADATION AND GEOCHEMISTRY ANALYSIS

### 6.1 USE OF COMPUTER SOFTWARE

The EQ3/6 geochemistry software package, Version 7.2B, is used for this evaluation. The information regarding the code and its use for the degradation and geochemistry analysis is documented in CRWMS M&O 2000c.

### 6.2 DESIGN ANALYSIS

#### 6.2.1 Systematic Investigation of Degradation Scenarios and Configurations

Degradation scenarios comprise a combination of features, events, and processes that result in degraded configurations to be evaluated for criticality. A configuration is defined by a set of parameters characterizing the amount and physical arrangement, at a specific location, of the materials that can significantly affect criticality (e.g., fissile materials, neutron-absorbing materials, reflecting materials, and moderators). The variety of possible configurations is best understood by grouping them into classes. A configuration class is a set of similar configurations whose composition and geometry is defined by specific parameters that distinguish one class from another. Within a configuration class the values of configuration parameters may vary over a given range.

A master scenario list and set of configuration classes relating to internal criticality is given in the *Disposal Criticality Analysis Methodology Topical Report* (YMP 1998, pp. 3-1 through 3-13) and also shown in Figures 16 and 17. This list was developed by a process that involved workshops and peer review. The comprehensive evaluation of disposal criticality for any waste form must include variations of the standard scenarios and configurations to ensure that no credible degradation scenario is neglected. All of the scenarios that can lead to criticality begin with the breaching of the waste package, followed by entry of the water, which eventually leads to degradation of the SNF and/or other internal components of the waste package. This degradation may permit neutron absorber material to be mobilized (made soluble) and either be flushed out of the waste package or separated from the fissile material, thereby increasing the probability of criticality.

The standard scenarios for internal criticality divide into two groups:

1. When the waste package is breached only on the top, water flowing into the waste package collects and fills the waste package. This ponding provides water for moderation to potentially increase the probability of criticality. Further, after a few hundred years of steady dripping, the water can overflow through the hole on the top of the waste package and flush out any dissolved degradation products.
2. When the waste package breach occurs on the bottom as well as the top, the water can flow through the waste package. This group of scenarios allows the soluble degradation products to be removed more quickly, but does not directly provide water for moderation. Criticality is possible, however, if the waste package fills with corrosion

products that can add water of hydration and/or plug any holes in the bottom of the waste package while fissile material is retained and absorbers are removed or separated. Silica released by the degrading HLW glass may form clay with enough water of hydration to support criticality.

The standard scenarios for the first group shown in Figure 16, which have the waste package breached only at the top, are designated IP-1, -2, and -3 (IP stands for internal to the package) according to whether the waste form degrades before the other waste package internal components, at approximately the same time (but not necessarily at the same rate), or later than the waste package internal components. The standard scenarios for the second group shown in Figure 17, which have the waste package breached at both the top and the bottom, are designated IP-4, -5, or -6 based on the same criteria. The internal criticality configurations resulting from these scenarios fall into six configuration classes described below (YMP 1998, pp. 3-10 through 3-12):

1. Basket is degraded but waste form is relatively intact and sits on the bottom of the waste package (or the DOE SNF canister), surrounded by, and/or beneath, the basket corrosion products (see Figure 18). This configuration class is reached from scenario IP-3.
2. Both basket and waste form are degraded (see Figure 19). The composition of the corrosion product is a mixture of fissile material and iron oxides, and may contain clay. It is more complex than for configuration class 1, and is determined by geochemical calculations as described in Section 6.3. This configuration class is most directly reached from standard scenario IP-2, in which all the waste package components degrade at the same time. However, after many tens of thousands of years the scenarios IP-1 and IP-3, in which the waste form degrades before or after the other components, also lead to this configuration.
3. Fissile material is moved some distance from the neutron absorber, but both remain in the waste package (see Figure 20). This configuration class can be reached from IP-1.
4. Fissile material accumulates at the bottom of the waste package, together with moderator provided by water trapped in clay (see Figure 21). The clay composition is determined by geochemical calculation, as described in Section 6.3. This configuration class can be reached by any of the scenarios, although IP-2 and IP-5 lead to this configuration by the most direct path; the only requirement is that there be a large amount of glass in the waste package (as in the codisposal waste package) to form the clay.
5. Fissile material is incorporated into the clay, similar to configuration class 4, but with the fissile material not at the bottom of the waste package (see Figure 22). Generally the mixture is spread throughout most of the waste package volume, but could vary in composition so that the fissile material is confined to one or more layers within the clay. Generally, the variations of this configuration are less reactive than for configuration class 4, therefore, they are grouped together, rather than separated according to where

the fissile layer occurs or whether the mixture is entirely homogeneous. This configuration class can be reached by either standard scenario IP-1 or IP-4.

6. Fissile material is degraded and spread into a more reactive configuration but not necessarily moved away from the neutron absorber, as in configuration class 3 (see Figure 23). This configuration class can be reached by scenario IP-1.

The configuration classes 1, 2, 4, and 5 require that most of the neutron absorber be removed from the waste package. However, in configuration classes 3 and 6, the fissile material is simply moved away from the absorber or into a more reactive geometry.

Note that most of these configurations or configuration pairs (Figures 18 through 23) look quite different even though both pair members belong to the same configuration class. This apparent dissimilarity arises from the configuration class definition strategy, which classifies critical configurations according to the geometry and composition of the materials, irrespective of the container (either the DOE SNF canister, or the entire waste package).

In Sections 6.2.1.1 through 6.2.1.6, the scenarios and the resulting configuration classes that are applicable to the 5-DHLW/DOE SNF-long waste package with Shippingport LWBR fuel in the DOE SNF canister are discussed. The naming convention used for the standard scenarios in Sections 6.2.1.1 through 6.2.1.6 is slightly different from the convention used in the topical report (YMP 1998), which is shown in Figures 16 and 17. The naming convention used in these sections contains refinements to the configurations described in the topical report based on CRWMS M&O 1999g.

The report titled *Generic Degradation Scenario and Configuration Analysis for the DOE Codisposal Waste Package* (CRWMS M&O 1999g) serves as the basis for the specific degraded waste package criticality analysis to be performed for any type of DOE spent nuclear fuel that will be codisposed with the HLW in a codisposal waste package. Starting from these guidelines, a set of degradation scenarios and resultant configurations has been developed for the codisposal waste package containing Shippingport LWBR SNF. The following brief description focuses on the correspondence between both different classes of configurations and their refinements. This approach allows a systematic treatment of the degraded internal criticality analysis, taking into account all possible configurations with potential for internal criticality.

The characteristics of both the Shippingport SNF and the DOE SNF canister are conservatively taken into account in the present analysis. The analysis provides the basis for evaluating the required amount of neutron absorber (Gd) that has to be distributed inside the DOE canister to keep the system's effective neutron multiplication factor ( $k_{\text{eff}}$ ) below the critical limit. This approach considers bounding arrangements and compositions of the configurations resulting from the internal degradation of the waste package. Parametric studies are subsequently performed for identifying the most reactive configurations. The ability to specify the most reactive credible configuration allows evaluation of the neutron absorber concentration that would bring  $k_{\text{eff}}$  below the critical limit. Supplementary calculations are performed to verify the effectiveness of the neutron absorber under different moderation regimes.

NOTE: WP = waste package  
 WF = waste form  
 FM = fissile material

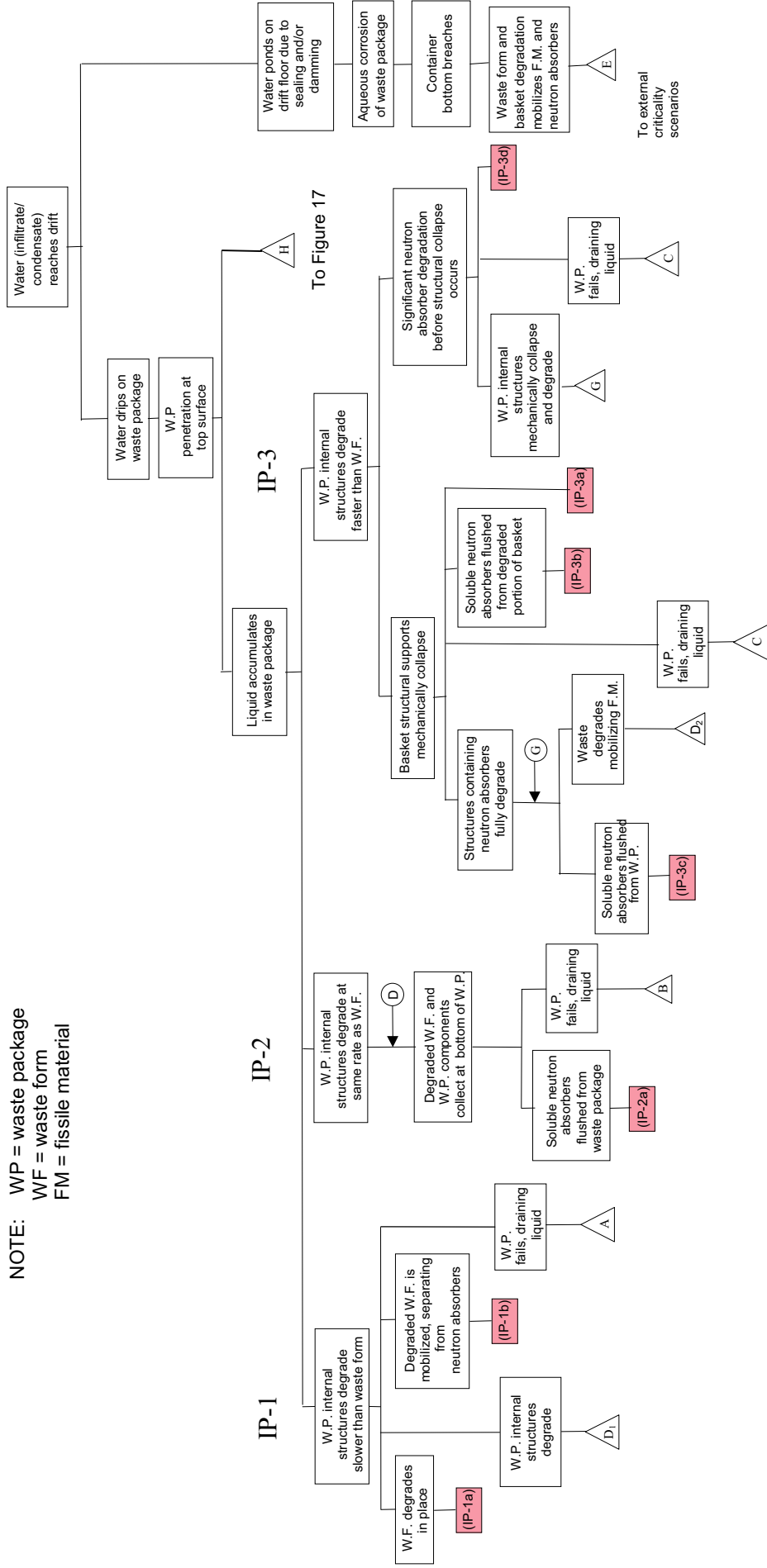
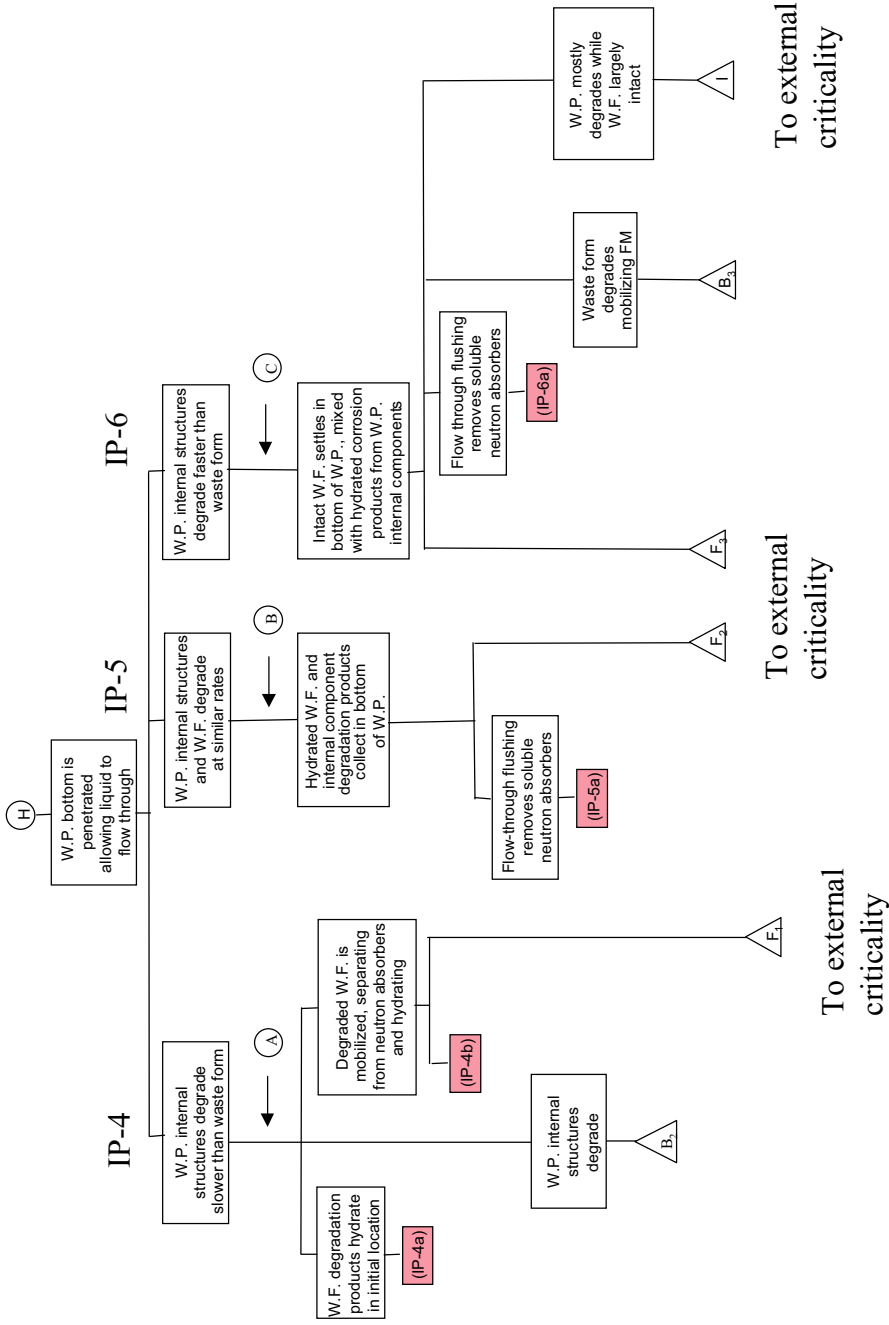


Figure 16. Internal Criticality Master Scenarios, Part 1 (YMP 1998)

From Figure 16



Note: hydrated degradation products may include hydrated metal oxides, metal hydroxides, and clayey materials

Figure 17. Internal Criticality Master Scenarios, Part 2 (YMP 1998)

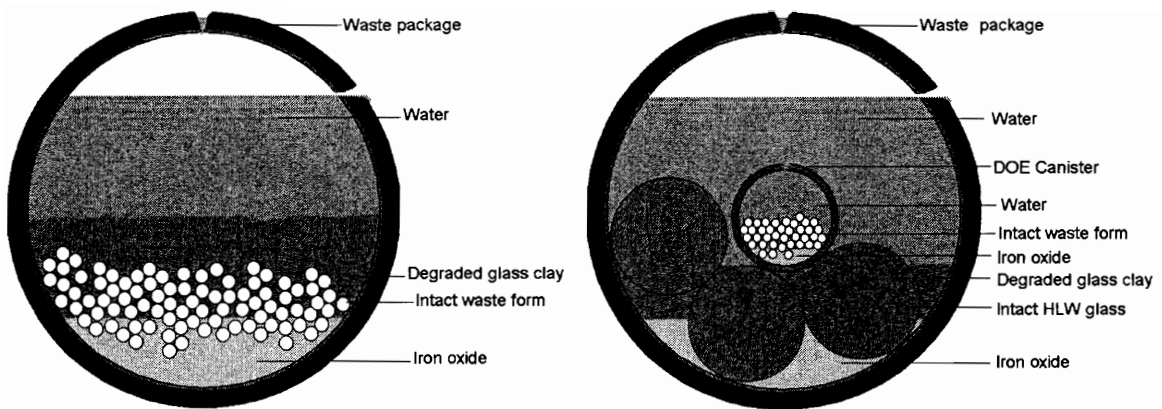


Figure 18. Examples of Degraded Configurations from Class 1

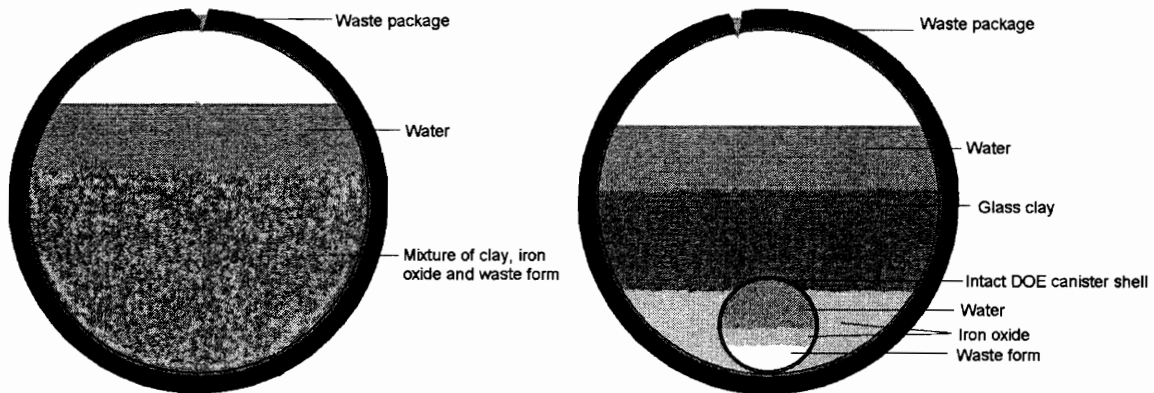


Figure 19. Examples of Degraded Configurations from Class 2

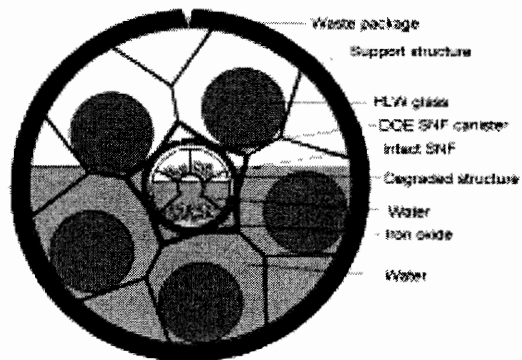


Figure 20. Example of Degraded Configuration from Class 3

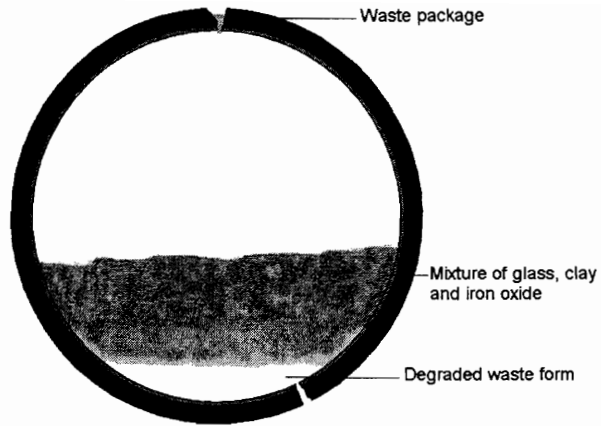


Figure 21. Example of Degraded Configuration from Class 4

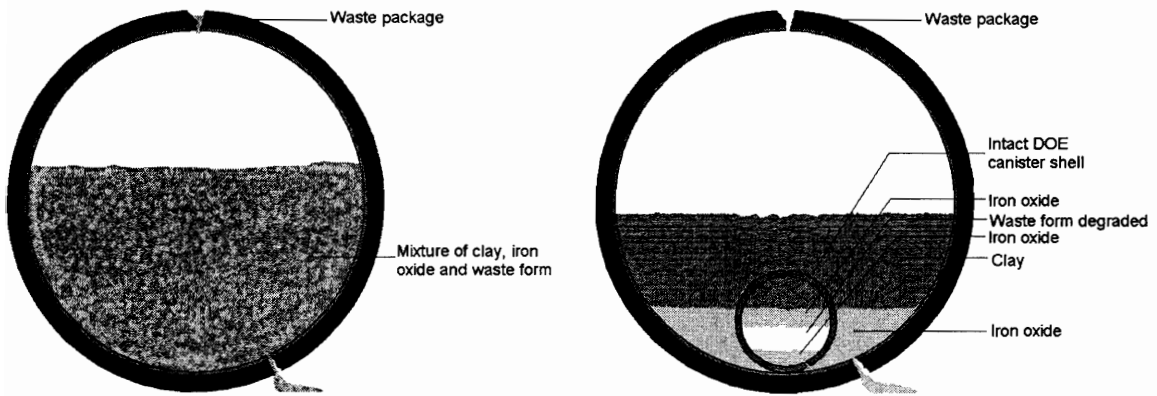


Figure 22. Examples of Degraded Configurations from Class 5

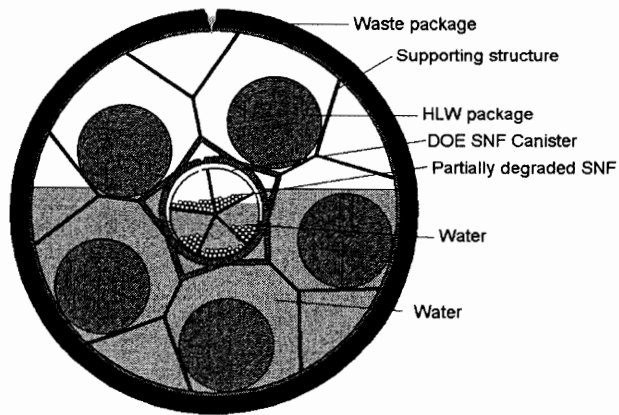


Figure 23. Example of Degraded Configuration from Class 6

### 6.2.1.1 Most Likely Scenario for Shippingport LWBR SNF

The parameters that need to be considered to develop the most likely or probable degradation scenario/configuration for the Shippingport LWBR SNF are: the materials of the components associated with the waste package; the DOE SNF canister and the SNF; thickness of the materials and the associated corrosion rates. The sequence of degradation can be developed, and the most probable degradation scenario/configuration can be identified by using these parameters, which are discussed below.

**Corrosion Rates**—The material corrosion rates are presented in Section 2.1.9 of this report. Stainless steels, Type 316L and Type AM-350 degrade at approximately the same rate. The carbon steel (Type A 516) degrades more rapidly than the stainless steels (Type 304L, Type 316L or Type AM350). The corrosion rate of Zircaloy-4 is conservatively selected as 0.0079  $\mu\text{m}/\text{yr}$  (3.1 mils in 10,000 years) (Hillner et al. 1998, Table 1). When compared to the corrosion rates of stainless steel, Zircaloy-4 can be considered inert. Also, for the same reason the Inconel X-750 and Inconel 600 in the fuel rods and assemblies are considered inert. The corrosion rate of the SNF (Th/U oxide mixture) is represented by the corrosion rate of thorium oxide (Zimmer 1984). This is reasonable because 94.8 % or more in the fuel is  $\text{ThO}_2$ . When compared to the corrosion rates of stainless steel,  $\text{ThO}_2$  can be considered inert.

**Most Probable Degradation Path**—Based on the corrosion rates and the material thickness given in Table 33, the most probable degradation path for the waste package, the DOE SNF canister, and the Shippingport LWBR SNF follows the following sequence:

1. Waste package is penetrated and flooded internally. The waste package basket, (outer and inner brackets and support tube) degrades first because of the high corrosion rate for A 516 carbon steel.
2. HLW glass canister's stainless steel shell and glass begin to degrade. After this, there are two degradation paths:
  - 2a. DOE SNF canister stays intact. Intact DOE SNF canister and intact SNF assembly fall on top of degraded products near the bottom of the waste package. The neutron absorber stays together with the fuel rods.
  - 2b. DOE SNF canister starts to degrade.
3. DOE SNF canister is penetrated and flooded.
4. Components internal to the DOE canister are in contact with water. These components include the SNF basket structure, the fuel assembly, and filler material (aluminum shot).
5. The aluminum shot will degrade first. There is a possibility of a partial separation between the neutron absorber and the fuel rods.
6. SNF cladding gets in contact with water.

7. DOE SNF canister basket degrades. After this, there are two paths:
  - 7a. SNF assembly and rods stay intact and fall on top of degraded DOE SNF canister basket and settle on the bottom of the DOE SNF canister.
  - 7b. DOE SNF canister degrades. Intact SNF assembly and rods fall on top of all degradation products near the bottom of the waste package. Given time, the SNF assembly shell might be degraded enough that the rods scatter on top of all degradation products.
8. Given a very long period of time, it is postulated that everything will degrade including cladding and fuel. This corresponds to degradation scenario group IP-2. This is not likely because of very long lifetime of Zircaloy-4, which will most likely outlast the waste package. To bound the potential degraded cases, degradation of the SNF can be considered. The degraded SNF and other degradation products could mix and pile up near the bottom of waste package. However, there is no mechanism to cause complete and uniform mixing of all the degradation products inside the waste package.

Table 33. Materials and Thicknesses

Components	Material	Thickness (mm)
Waste package basket	A516 Carbon Steel	12.7
Waste package inner bracket	A516 Carbon Steel	25.4
Waste package support tube	A516 Carbon Steel	31.75
HLW glass shell	304L Stainless Steel	10.5
HLW glass	Glass	N/A
DOE SNF canister	316L Stainless Steel	9.525
DOE SNF canister basket	316L Stainless Steel	9.5
Neutron absorber (Al shot with 1 wt.% Gd)	Al/GdPO <sub>4</sub>	3.0 <sup>a</sup> (nominal diameter)
Seed assembly hexagonal shell	Zircaloy-4	2.032
SNF cladding	Zircaloy-4	0.563118
SNF pellets in seed assembly	ThO <sub>2</sub> and UO <sub>2</sub> mixture	6.4008 (nominal diameter)
	ThO <sub>2</sub> only	6.49224 (nominal diameter)

Source: Section 2.

NOTE: <sup>a</sup> CRWMS M&O 1999m, Section 3.1.

**Most Probable Degradation Scenario/Configuration**– Based on *Generic Degradation Scenario and Configuration Analysis for DOE Codisposal Waste Package* (CRWMS M&O 1999g), the above degradation sequences match with the degradation scenario/configurations of IP-3-A to IP-3-C (equivalent to IP-2). The details of these degradation scenario/configurations are discussed in Section 7.4.1 and 7.4.2. The most probable degradation configuration is the one with the degradation of all components inside the waste package and the DOE SNF canister. The SNF assembly remains intact and positioned on the bottom of the waste package (Section 7.5.1). The degradation scenario of IP-1, i.e., SNF degrades faster than the other materials, is not probable, since the SNF is clad with Zircaloy-4 that practically do not degrade as compared to stainless steel. If the Zircaloy-4 clad is breached, thus allowing water to come in contact with

the fuel, due to the very low degradation rate for thorium dioxide, the fuel degradation will be negligible within the time range studied.

The configurations described in Sections 6.2.1.2 through 6.2.1.4 are the most probable configurations.

#### **6.2.1.2 Degraded DOE SNF Canister Basket and Intact SNF**

For these cases of intact fuel assembly within degraded basket, the scenarios and configuration classes are applied to the DOE SNF canister and its contents. This configuration is a variation of configuration class 1 and can be reached from standard scenario IP-3. The results of the criticality calculations for this configuration are given in Section 7.4.1.

#### **6.2.1.3 Intact DOE SNF Canister and Degraded Waste Package Internals**

In this case, the concepts of scenario and configuration are applied to the entire waste package. The fuel assembly and the DOE SNF canister shell are intact. This configuration is a variation of configuration class 1 and can be reached from standard scenario IP-3. The results of the criticality calculations for this configuration are given in Section 7.4.3.

#### **6.2.1.4 Degraded DOE SNF Canister and Waste Package Internals, Intact SNF**

In this case, the concepts of scenario and configuration are applied to the entire waste package. The DOE SNF canister, waste package internals, and HLW glass canisters are degraded. The fuel assembly is intact. This configuration is achievable because of very low degradation rate of Zircaloy-4, which envelops and protects the fuel. This configuration is a variation of configuration class 1 and can be reached from standard scenario IP-3. The results of the criticality calculations for this configuration are given in Sections 7.5.1 and 7.5.2.

#### **6.2.1.5 Degraded SNF with Intact DOE Canister or Waste Package**

In this case, the SNF could be partially or fully degraded. As a variation, the internal components of DOE SNF canister could be also degraded. This configuration is a variation of configuration class 6 and can be reached from standard scenario IP-1. The results of criticality calculations for this configuration are given in Section 7.4.2.

#### **6.2.1.6 Partially or Completely Degraded DOE SNF Canister and Waste Package Internals**

In this case, the concepts of scenario and configuration are applied to the entire waste package. Degradation products from the DOE SNF canister and contents form a layer on the bottom of the waste package. The degradation products (clay) from waste package internals and HLW glass canisters form a layer above. This configuration is a variation of configuration class 2 and can be reached from standard scenario IP-1, IP-2, or IP-3. The results of the criticality calculations for this configuration are given in Sections 7.4.4 and 7.5.3.

### 6.2.2 Basic Design Approach for Geochemistry Analysis

The method used for this analysis involves eight steps as described below:

1. Use the basic EQ3/6 capability to trace the progress of reactions as the chemistry evolves, including estimating the concentrations of material remaining in solution as well as the composition of precipitated solids. EQ3 is used to determine a starting fluid composition for EQ6 calculations; it does not simulate reaction progress.
2. Evaluate available data on the range of dissolution rates for the materials involved, to be used as material/species input for each time step.
3. Use the “solid-centered flow-through” mode in EQ6. In this mode, an increment of aqueous “feed” solution is added continuously to the waste-package system, and a like volume of the existing solution is removed. This mode simulates a continuously stirred tank reactor.
4. Determine the fissile concentrations of fissile materials in solution as a function of time (from the output of EQ6-simulated reaction times up to  $3.17 \cdot 10^5$  years).
5. Calculate the amount of fissile material released from the waste package as a function of time (which thereby reduces the chance of criticality within the waste package).
6. Determine the concentrations of neutron absorber material, such as gadolinium (Gd), in solution as a function of time (from the output of EQ6 over time up to  $3.17 \cdot 10^5$  years).
7. Calculate the amount of neutron absorber material retained within the waste package as a function of time.
8. Calculate the composition and amounts of solids (precipitated minerals or corrosion products and unreacted package materials).

### 6.3 CALCULATIONS AND RESULTS

The calculations begin using selected representative values from known ranges for composition, amounts, and reaction rates of the various components of the waste package. Surface areas are calculated based on the initial package geometry. The input to EQ6 consists of the composition of J-13 well water, together with a rate of influx to the waste package (Section 2.1.9.3). In some cases, the degradation of the waste package is divided into stages (e.g., degradation of HLW glass before breach of the SNF canister and exposure of the fuel and its basket material to the water). The EQ6 outputs include the compositions and amounts of solid products and the solution composition. Summary of the results are presented in Section 6.3.1 below. The calculation process is described in more detail in CRWMS M&O 2000c.

### 6.3.1 Results of EQ6 Runs

Table 34 summarizes the conditions used for the EQ6 runs and the total percentage of Gd, U and Th remaining at the end of runs. If fissile material remains behind in the waste package while the Gd and other neutron absorbers are flushed from the system, an internal criticality could be possible. A solubility scoping calculation revealed that total concentration of dissolved Gd phosphate complexes as a function of pH and total dissolved phosphate never exceeds concentrations much greater than  $10^{-9}$  molal for pH values between 4 and 9, and thus would not result in significant Gd loss from the system (CRWMS M&O 1998j).

Twenty-six EQ6 reaction path calculations were carried out to span the range of possible system behavior and to assess the specific and coupled effects of SNF degradation, steel corrosion, HLW glass degradation, and fluid influx rate on U, Gd and Th mobilization. Fluids having a composition of J-13 well water were represented as steady-state reactants with waste package components over time spans of up to 317,000 years. Corrosion product accumulation (primarily of iron oxide and smectite) and U, Gd, and Th mobilization were examined as well.

High predicted losses of U (94-95%), mostly from HLW glass degradation, occurred for conditions of low steel degradation rate, high HLW glass degradation rate, and low J-13 water flushing rate (Cases 2, 12, 19 and 20). Total predicted loss of U (from fuel and glass, 6% and 94% of the total moles of U in the waste package, respectively) from the waste package occurred if a high SNF degradation rate was also used in the run (Cases 3 and 13).

Cases 15 through 17 and Case 25 were run to examine the effects of different run conditions combined with breached cladding on U losses from the SNF only. Table 34 shows that only ~2% of the U in the SNF would be lost from the waste package with conditions of low steel, high HLW glass (VA), and low fuel degradation rates plus a low J-13 water flushing rate (Case 16). If a high SNF degradation rate is used with these run conditions, then 100% loss of the U from SNF degradation was predicted (Case 17). If average steel, high (Ebert; see Table 24) HLW glass, and the 25°C special fuel degradation rates are combined with the low J-13 well water flushing rate, a loss of one-third of the U from SNF is predicted.

Low, but significant, predicted U losses (5-17%) occurred for conditions of moderate steel degradation rate, and high J-13 well water flushing rate (Cases 4, 5, 6a, 7, 14 and 21). These conditions would tend to decrease pH (increase acidity) until the waste package steel degrades. Then, the high J-13 well water flushing rate would prevent build up of alkalinity as HLW glass degradation continued, thus decreasing solubility of U in the waste package solution compared with the conditions mentioned above.

Very low predicted U losses (0-4%) occurred for conditions of low steel, low (VA) glass, and low fuel degradation rates, with a high J-13 water flushing rate (Cases 1, 11, 15, and 18). Under these conditions, very little SNF degradation occurred while the EDA II liner and HLW glass also persisted to the end of the runs (~317,000 years), buffering pH to values around 8.1. Uranium mobility was controlled largely by formation of soddyite  $[(\text{UO}_2)_2(\text{SiO}_4) \cdot 2\text{H}_2\text{O}]$ . For these cases, an internal criticality would be possible if the  $\text{GdPO}_4 \cdot \text{H}_2\text{O}$ , formed by degradation of the Al fill material, was not well distributed around the remaining SNF and within the waste package corrosion products.

Table 34. Summary of Geochemistry Results

Case	% Fuel Exposure	% Th Loss <sup>a</sup>	% Gd Loss	% U Loss <sup>a</sup>	Degradation/Drip Rates <sup>l</sup>				Fe Oxide
					Steel	Glass	Fuel	J-13 Well Water	
1 <sup>f</sup>	100	0.00	2.18	2.46	1	1	1	3	Hematite
2 <sup>f</sup>	100	0.29	0.03	94.25	1	2	1	1	Hematite
3 <sup>f</sup>	100	0.69	0.03	100.0	1	2	3	1	Hematite
4 <sup>f</sup>	100	0.00	1.56	5.11	2	1	3	3	Hematite
5 <sup>f</sup>	0	0.00	0.00	13.99	2	2	0	4	Hematite
	100	0.00	0.14	0.19	2	0	2	2	
6a	0 <sup>f</sup>	0.00	0.00	13.99	2	2	0	4	Hematite
	100/10 <sup>d</sup>	0.00	0.14	0.18	2	0	2	2	
6b <sup>i</sup>	0 <sup>f</sup>	0.00	0.00	2.66	2	2	0	4	Hematite
	100/10 <sup>d</sup>	0.00	0.16	0.16	2	0	2	2	
7 <sup>e</sup>	0	0.00	0.00	17.19	2	2	0	4	Goethite
	100	0.00	0.14	0.28	2	0	2	2	
8 <sup>b</sup>	0	0.00	0.00	84.74	2	2	0	4	Hematite
	100	0.00	0.32	0.22	2	0	2	2	
9 <sup>g</sup>	0	0.00	0.00	94.04	2	2	0	4	Hematite
	100	0.00	0.06	0.04	2	0	2	2	
10 <sup>f</sup>	0	0.00	0.00	94.15	1	2	0	3	Hematite
	100	0.00	0.00	0.02	1	0	2	1	
11 <sup>e</sup>	100	0.00	2.36	3.44	1	1	1	3	Goethite
12 <sup>e</sup>	100	0.26	0.01	94.24	1	2	1	1	Goethite
13 <sup>e</sup>	100	0.55	0.01	100.0	1	2	3	1	Goethite
14 <sup>e</sup>	100	0.00	2.85	8.71	2	1	3	3	Goethite
15 <sup>c,f</sup>	100	0.00	2.18	0.09 <sup>j</sup>	1	1	1	3	Hematite
16 <sup>c,f</sup>	100	0.33	0.03	1.93 <sup>j</sup>	1	2	1	1	Hematite
17 <sup>c,f</sup>	100	1.38	0.03	100 <sup>j</sup>	1	2	3	1	Hematite
18 <sup>f,h</sup>	1	0.00	2.18	2.46	1	1	1	3	Hematite
19 <sup>f,h</sup>	1	0.01	0.03	94.15	1	2	1	1	Hematite
20 <sup>f,h</sup>	1	0.29	0.03	94.21	1	2	3	1	Hematite
21 <sup>f,h</sup>	1	0.00	1.56	5.11	2	1	3	3	Hematite
22 <sup>k</sup>	0 <sup>f</sup>	0.00	0.00	94.15	4	4	0	4	Hematite
	100/10 <sup>d</sup>	0.00	0.25	0.00	4	0	2	2	
23 <sup>e,k</sup>	100	0.00	3.63	84.36	4	3	3	3	Goethite
24 <sup>f,k</sup>	100	0.10	0.04	96.09	3	4	4	1	Hematite
25 <sup>c,f,k</sup>	100	0.06	0.05	33.15 <sup>j</sup>	3	4	4	1	Hematite

NOTES: <sup>a</sup> U and Th losses are a percentage of total moles of U and Th in fuel and HLW glass.

<sup>b</sup> No EDA II liner.

<sup>c</sup> U in HLW glass replaced by Np.

<sup>d</sup> 100% fuel moles and 10% fuel surface area exposed to corrosion.

<sup>e</sup> These cases were run with hematite suppressed.

<sup>f</sup> Hematite not suppressed for these runs.

<sup>g</sup> Used a different HLW glass composition and degradation rate (CRWMS M&O 1999j, Table 5-3).

<sup>h</sup> Only 1% of fuel moles and surface area exposed to corrosion.

<sup>i</sup> Case 6b was run with the degradation rates in Table 16.

<sup>j</sup> U loss is a percentage of total moles of U in the fuel only.

<sup>k</sup> These cases used a different EQ6 database ("data0.ymp" in Attachment 1of CRWMS M&O 2000c).

<sup>l</sup> Rates encoding-

Steels: 1=low rate; 2=moderate rate; 3=average rate; 4=high rate (CRWMS M&O 2000c, Table 2),

Glass: 0=no glass present; 1=moderate VA rate; 2=high VA rate; 3=moderate Ebert HLW; 4=high Ebert HLW (CRWMS M&O 2000c, Table 3),

Fuel: 0=no fuel present; 1=low rate; 2=average rate; 3=high rate; 4=25°C temperature dependent rate (CRWMS M&O 2000c, Table 4),

J-13 Well Water: 1=0.0015 m<sup>3</sup>/year; 2=0.015 m<sup>3</sup>/year; 3=0.15 m<sup>3</sup>/year; 4=0.5 m<sup>3</sup>/year (CRWMS M&O 2000c, Section 5.3.1).

Predicted loss of Th from the waste package was less than 2% for all the cases run. The predicted amount of Th in solution was controlled to very low levels by formation of the extremely insoluble mineral thorianite ( $\text{ThO}_2$ ). Therefore, this calculation predicts that in times through ~317,000 years most of the Th will remain in the SNF or the waste package corrosion products.

Since Gd loss was low (0-4%) for all of the EQ3/6 cases run in this calculation, the risk of a criticality occurring inside the waste package seems unlikely if the precipitated  $\text{GdPO}_4 \cdot \text{H}_2\text{O}$  is well distributed in the waste package corrosion products.

#### **6.4 SUMMARY**

A principal objective of these calculations is to assess the chemical circumstances that could lead to removal of neutron absorbers (Gd) from the waste package, while fissile materials (U) remain behind. Such circumstances could increase the probability of a nuclear criticality occurrence within the waste package. Gadolinium is assumed to be present as  $\text{GdPO}_4$  that is combined with aluminum shot, which is distributed in the void space inside the DOE SNF canister. Water with the composition of J-13 well water is assumed to drip in through an opening at the top of the waste package, pooling inside and eventually overflowing, allowing removal of soluble components through continual dilution. This calculation selected 25 EQ6 cases and examined the results to identify the reasons for the chemical changes during degradation of waste package materials and flushing by J-13 well water. It appeared that, even in unusual conditions, loss of Gd was insignificant, when the element is present in the package as solid  $\text{GdPO}_4$ . The scenarios and conditions of EQ6 cases are chosen to emphasize the conditions that could create either acid or alkaline environments and to determine if these conditions are of sufficient duration to induce Gd loss. In all cases, the differences in the results were all very small.

These geochemistry results are valid within the scope of the criticality calculations for which they are intended, particularly as specified in Assumption 2.3.4.5. These results are not intended for input into TSPA, or to serve as a model for additional geochemistry calculations involving other configurations of waste package degradation. However, it should be noted that the results are consistent with the waste package geochemistry analysis model report (CRWMS M&O 2000h), which used the EQ3/6 geochemistry code in the same manner as was used for the present analysis, and with similar material parameters. The principal difference is that the present analysis focuses on the loss of Gd, while CRWMS M&O 2000h does not. In this regard, the validation in CRWMS M&O 2000h can be viewed as supporting this document.

## 7. INTACT- AND DEGRADED-MODE CRITICALITY ANALYSIS

### 7.1 USE OF COMPUTER SOFTWARE

The Monte Carlo particle transport code, MCNP, Version 4B2, is used to estimate the effective neutron-multiplication factor ( $k_{\text{eff}}$ ) of the codisposal waste package. The information regarding the code and its use for the criticality analysis is documented in CRWMS M&O 2000d.

### 7.2 DESIGN ANALYSIS

The MCNP Version 4B2 is used to estimate the  $k_{\text{eff}}$  values for various geometrical configurations of the Shippingport LWBR SNF in the 5-DHLW/DOE SNF-long waste package. The  $k_{\text{eff}}$  results represent the average combined collision, absorption, and track-length estimator from the MCNP calculations. The standard deviation ( $\sigma$ ) represents the standard deviation of  $k_{\text{eff}}$  related to the average combined collision, absorption, and track-length estimate due to the Monte Carlo calculation statistics. The calculations are performed using continuous energy cross-section libraries that are part of the qualified MCNP code system (CSCI: 30033 V4B2LV). All calculations are performed with fresh-fuel isotopics (Assumption 2.3.5.1).

CRWMS M&O 2000d describes the Monte Carlo representations, the method of solution, and the results for nuclear criticality evaluations that were performed for intact, partially degraded and degraded modes of the DOE SNF canister contained in the waste package. The intact mode is defined as that mode in which no component of the DOE SNF canister is dislocated due to degradation of structural members within the canister (see Figure 24). These intact cases are described in Section 7.3.1. The partially degraded mode is treating the configurations obtained as a result of partial degradation of the DOE canister internal supporting structure (see Figures 25 and 27). These partially degraded cases are described in Section 7.4.1. The criticality analysis for the degraded-mode configurations obtained in the subsequent stages of internal degradation of the DOE canister components and waste package internal constituents are summarized in Sections 7.4 and 7.5.

The MCNP results are presented in the following section in order to demonstrate that all foreseeable intact and degraded configurations inside the codisposal waste package (see Section 6) have been investigated and the values of  $k_{\text{eff}}$  are below the interim criticality limit of 0.92. The minimum necessary amount of neutron absorber to fulfill the above requirement on  $k_{\text{eff}}$  for all investigated configurations is 10.12 kg of GdPO<sub>4</sub>. This amount of GdPO<sub>4</sub> is equivalent to 1.0 wt.% Gd content in the initial mass of aluminum shot-GdPO<sub>4</sub> mixture placed within the DOE canister. Each of the configurations presented in Section 6 are addressed, but many are bound by results in subsequent configurations, and are not, therefore, fully parameterized. The limiting case for  $k_{\text{eff}}$  was obtained for DOE SNF canister contents fully degraded and it bounds all intermediate stages of degradation of the contents of the DOE SNF canister.

## 7.3 CALCULATIONS AND RESULTS—PART I: INTACT-MODE CRITICALITY ANALYSIS

### 7.3.1 Intact Mode

This section presents the results of the intact-mode criticality analysis. Although the components (fuel assembly, cladding, supporting structures, and canisters) are considered structurally intact, water intrusion into the components is assumed in order to determine the highest  $k_{\text{eff}}$  resulting from optimum moderation. The contents of the waste package outside the DOE SNF canister are intact in all cases considered in this section except as noted.

For the intact mode, the contents of the DOE SNF canister are in an “as-welded/loaded position and condition,” as depicted in Figure 24 showing a fuel assembly. The void space outside the fuel assembly and inside the SNF canister is filled with aluminum (Al) shot containing gadolinium phosphate ( $\text{GdPO}_4$ ). Different weight percentages of Gd in the Al- $\text{GdPO}_4$  mixture (including zero) are investigated, with a baseline of 1 wt.% Gd in the mixture (10.12 kg  $\text{GdPO}_4$ ).

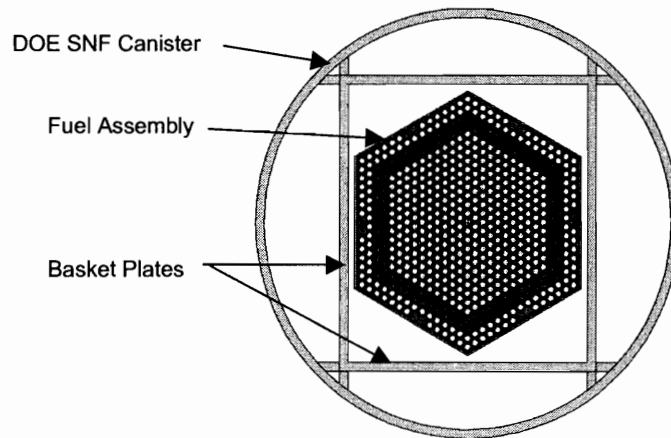


Figure 24. Cross-Sectional View of the Waste Package Showing the Contents of the DOE SNF Canister for the Intact-Mode Analysis

The aluminum shot is used as a means of uniformly distributing the gadolinium phosphate throughout the SNF canister, and the gadolinium phosphate is used as an insoluble neutron absorber. However, since the waste package is to be emplaced horizontally in the MGR, the various components inside the waste package are considered to be settled for most cases of interest.

The configurations investigated for intact-mode analysis and the representative results obtained are given in Table 35 (CRWMS M&O 2000d, Section 6.1). The base intact configuration from Table 35 is similar to the one shown in Figure 24, but the DOE SNF canister contains water saturated aluminum fill material and no gadolinium phosphate. Vacant spaces in the waste package outside the SNF canister are treated as voids while the waste package is reflected by full density water. Void spaces in the fuel pins and fuel pellets are saturated with water.

Cases with water replacing the filler and with no GdPO<sub>4</sub> are also studied to determine how  $k_{\text{eff}}$  of the intact mode is affected by these conditions. Water density variations are investigated for these cases to evaluate their impact on the value of  $k_{\text{eff}}$ . The water density is varied inside the DOE SNF canister and also inside the waste package but outside the DOE SNF canister. Effects of partially filling the voids in the fuel pellets with water for the base intact configuration are also investigated. It should be noted that while some cases do not seem to be realistic (i.e., physically possible), they are considered in order to obtain more conservative (higher) estimates for  $k_{\text{eff}}$ . The results of some of the representative cases are given in Table 35.

Table 35. Results of the Intact-Mode Criticality Analysis

Case Description	Filler (Aluminum Shot)	Gd Content in the Al-GdPO <sub>4</sub> mix (wt.%)	$k_{\text{eff}} + 2\sigma$
Base intact case: fuel pellets saturated with water and contents settled due to gravity; no neutron absorber added to the filler	Yes	0	0.9140
Similar to above case but the contents of the waste package are centered neglecting gravity and filler replaced with water	No, replaced with full density water	0	0.9001
Similar to base case, but fill material contains gadolinium	Yes	0.1	0.8659
Like above, but contents of waste package are centered and glass canisters positioned at closest possible position to the center of the waste package	Yes	0.1	0.8657
Similar to base case, but no water is in the fuel pellets	Yes	0	0.8993
Like previous case, but fill material contains gadolinium	Yes	0.1	0.8537
Like base case, but no water is in the fuel pellets and filler replaced with water	No, replaced with full density water	0	0.8905
Like base case, but no water is in the fuel pellets and reduced water density	No, replaced with water of density 0.6 g/cm <sup>3</sup>	0	0.6925
Like base case, but no water is in the fuel pellets and reduced water density	No, replaced with water of density 0.2 g/cm <sup>3</sup>	0	0.4374
Like base case, but no water is in the fuel pellets and water fills the waste package outside the SNF canister	No, replaced with full density water	0	0.8865
Similar to base case, but fill material contains gadolinium, waste package is reflected by dry tuff and SNF canister is at bottom of waste package surrounded by prebreach clay	Yes	0.1	0.8660

As can be seen from the above results, the largest variation in  $k_{\text{eff}}$  for the base intact mode configuration results when the filler material is replaced with reduced density water. If the water density is increased to full density (1.0 g/cm<sup>3</sup>) the value of  $k_{\text{eff}}$  is still slightly smaller than for the base intact configuration. Repositioning the components in the waste package to account for gravity or any other centering have essentially a negligible effect on the results. The  $k_{\text{eff}} + 2\sigma$  of 0.9140 for the base intact configuration is reduced to 0.8659 by the addition of 0.1 wt.% Gd to the filler. The final baseline design is based on 1.0 wt.% Gd in the filler, which provides a large margin for all these cases. The results also show that reducing the water density in the DOE SNF canister produces a significant decrease of  $k_{\text{eff}}$ . This demonstrates that the system is not over-moderated.

The last case in Table 35 represents a configuration where the waste package components are degraded and the DOE SNF canister is breached but with contents intact. By comparing this case with the third case from Table 35, it can be seen that the conditions outside DOE SNF canister have a negligible impact on the  $k_{\text{eff}}$  of the system. Replacing the water reflector that

surrounds the waste package and degrading the contents of the waste package outside the SNF canister have a minor effect on the results.

Occurrence of design basis events, including those with the potential for flooding the disposal container prior to its sealing, is considered and bounded by the analysis results presented in Table 35 for many different intact configurations.

## 7.4 CALCULATIONS AND RESULTS–PART II: SCENARIOS WITH FISSILE MATERIAL RETAINED IN THE DOE SNF CANISTER

### 7.4.1 Intact Fuel Assembly in Partially Degraded DOE SNF Canister

The partially degraded mode refers to the cases where the basket plates of the DOE SNF canister have fully degraded to goethite. Cases where the aluminum has degraded to diaspore are also considered. The assembly is intact and water fills the voids between fuel pins (coolant channels) in the assembly. This mode has been analyzed in detail in CRWMS M&O 2000d (Section 6.1.3) and a typical representation is shown in Figure 25. The waste package contents outside the DOE SNF canister are considered intact in all cases unless otherwise noted. The degradation configurations and their refinements belong to the standard configuration Class 1 that is obtained via standard group scenario IP-3 (YMP 1998, p. 3-8).

Cases are presented with different layers of goethite, diaspore or aluminum fill and varying volume fractions of water in these materials. As mentioned in CRWMS M&O 2000d, there is no mechanism to cause significant segregation/stratification of the layers containing degradation products. These cases are overly conservative and unlikely, and are presented for completeness. Additional cases are presented where the diaspore, goethite and water are mixed together. These cases bound all possible compositions with higher hydrated products of Al (e.g., gibbsite). The representative cases and their results are presented in Table 36. The waste package is reflected by full density water, and vacant spaces are treated as voids for cases where the contents of the waste package are intact. Voids in the fuel pins and pellets are filled with water. The coolant passages inside the assembly are filled with full density water. The gadolinium content in the aluminum fill is also given in the table for each case investigated.

Table 36. Results of the Intact Assembly with Degraded Basket Plates

Case Description	Gd Content in the Al-GdPO <sub>4</sub> Mix (%)	k <sub>eff</sub> + 2σ
Assembly surrounded by dry goethite and covered by wet Al fill	1.0	0.9028
Assembly surrounded by dry goethite and covered by dry diaspore	0.1	0.9215
Similar to previous case, but with higher Gd content	1.0	0.9146
Assembly surrounded by goethite mixed with 40 vol.% water and covered by dry diaspore	1.0	0.9166
Assembly surrounded by dry diaspore and covered by dry goethite	0.1	0.8985
Assembly surrounded by dry diaspore and covered by dry goethite	1.0	0.8734
Assembly surrounded by a mixture of goethite, diaspore and water (38 vol.%) and covered by dry diaspore; the Gd amount in the bottom layer represents approximately 3% of the total Gd content in the DOE SNF canister	1.0	0.8935
Similar to previous case, but the DOE SNF canister is centered in dry prebreach clay in the waste package	1.0	0.8950

The results listed in Table 36 (CRWMS M&O 2000d, Section 6.1.3) show that  $k_{\text{eff}}$  remains below the interim critical limit of 0.92, as long as the aluminum or diaspore (if the aluminum has degraded) remains in contact with the fuel assembly. Diaspore gives slightly higher values of  $k_{\text{eff}}$  than aluminum fill material for equivalent configurations. If the assembly is surrounded by goethite and the gadolinium containing material is above the assembly (which is a very unlikely configuration), then increasing the amount of gadolinium has only a limited effect on decreasing  $k_{\text{eff}}$ . Complete separation of the layers of the degradation products inside the DOE SNF canister is impossible for the present design, where the fill material is distributed on both sides of the basket. The  $k_{\text{eff}}$  remains below the interim critical limit if more than 3% of the total Gd is distributed in the mixture that surrounds the fuel assembly. The remaining diaspore and Gd is positioned above the assembly. As mentioned above, the initial Al-GdPO<sub>4</sub> mixture is uniformly distributed around the fuel assembly, therefore a separation in a layer is extremely unlikely. The cases analyzed in Table 36 are very conservative and bound all possible configurations with an intact fuel assembly in the DOE SNF canister.

Last two cases in Table 36 show again that the conditions outside the DOE SNF canister have a minor influence on the  $k_{\text{eff}}$  of the system.

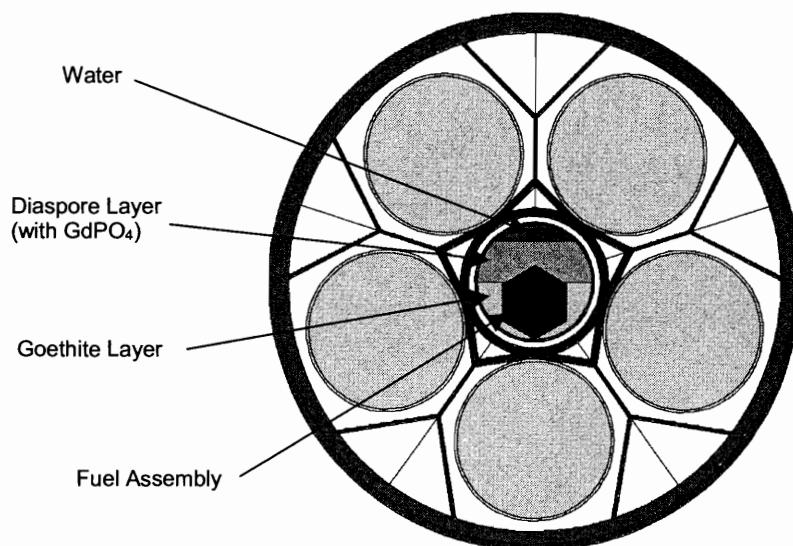


Figure 25. Intact Assembly Surrounded by Degraded Contents of the DOE SNF Canister in an Intact Waste Package

#### 7.4.2 Partially Degraded Fuel Assembly in Intact DOE SNF Canister

In these configurations the DOE SNF canister and its internal components are intact while the assembly is partially degraded. The degradation of the assembly is partial since only the pitch of the fuel pins or the axial spacing between fuel pellets in the fuel pins are affected. These cases are described in CRWMS M&O (1999g, p. 27) under refinement IP-1-A belonging to configuration class 6. For these cases the pitch is expressed as a “pitch fraction” that is defined as  $(p - p_{\text{min}})/(p_{\text{org}} - p_{\text{min}})$ , where  $p$  is the pitch,  $p_{\text{org}}$  is the original pitch of the intact assembly, 0.9398 cm, and  $p_{\text{min}}$  is the minimum pitch, which occurs when the pins are touching, and is

simply the pin diameter, 0.778002 cm. When the fuel pellets become axially separated water fills the space and the cladding is assumed to surround the pellets. This makes the fuel pins fictitiously long, but gives more conservative results (larger values of  $k_{eff}$ ) since it allows the pellets to become more optimally moderated. These results are given in Table 37, and the configuration is depicted by the first representation in Figure 26. Aluminum-fill material surrounds the assembly inside the DOE SNF canister for all cases.

Table 37. Results of the Degraded Assembly with the Components in the DOE SNF Canister Intact

Case Description	Gd Content in the Al-GdPO <sub>4</sub> mix (wt.%)	Pitch Fraction	Axial Separation (cm)	$k_{eff} + 2\sigma$
Pitch changes to minimum and is uniform in the assembly	0	0	0	0.6445
Similar to previous case, but higher pitch	0	0.5	0	0.7936
Similar to previous case, but higher pitch	0	0.978	0	0.9095
Pellets become axially separated in the fuel pin	1.0	1.0	0	0.8424
Similar to previous case, but higher axial spacing	1.0	1.0	0.8	0.9019
Similar to previous case, but higher axial spacing	1.0	1.0	1.0	0.9040
Similar to previous case, but higher axial spacing	1.0	1.0	1.2	0.9018

As the pitch decreases the configurations become less reactive, which is consistent with the assembly being undermoderated. Increases in pitch are not considered since as long as the pins remain inside the assembly shroud it is highly improbable, if not impossible, for the pitch to increase due to degradation.

Increases in the axially separation between fuel pellets initially increases the reactivity of the systems, but reaches a maximum value of  $k_{eff}$  that corresponds to a separation of 1.0 cm between pellets. Values in the Table 37 are for the fuel pins having the initial pitch. Any decrease in pitch would correspondingly decrease the reactivity. Changing the boundary conditions outside DOE SNF canister (e.g., prebreach clay) has a minor influence on  $k_{eff}$  of the system (CRWMS M&O 2000d, Section 6.2.1 and 6.2.2). The results show a large margin even for an optimally moderated condition, which is extremely unlikely.

### 7.4.3 Partially to Totally Degraded Internal Structures of DOE SNF Canister with Intact Fuel Pins

These configurations comprise the intact fuel pins distributed inside the DOE SNF canister at various stages of degradation of the internal supporting structure. Two variations are shown in Figure 26. By applying the IP-1 scenario to DOE SNF canister (YMP 1998) the fuel pins will end up stacked in a different configuration in the DOE SNF canister (collapsed assembly). The configuration is a variation of refinement IP-1-A mentioned in Section 7.4.2 above. Configurations with fuel pins completely separated from the neutron absorber are not possible with the present configuration because a uniform mixture of aluminum shot and neutron absorber initially surrounds the assembly and there is no identified mechanism to cause significant segregation/stratification of the layers.

The assembly is assumed to have degraded to the point that only individual fuel pins remain and the degradation products (other than the fuel pins) are conservatively neglected. For the DOE

SNF canister partially degraded, the basket plates are assumed to be intact and cases with the aluminum fill material intact and degraded are considered. The pins are assumed to remain in a triangular lattice array for all cases. The intact pitch is assumed for most cases, but variations in pitch are also investigated. Since the assembly contains four different types of fuel pins with different fissile loadings, once the pins become loose there is a very large number of configurations possible due to the many different ways of positioning the four pin types. To minimize the number of possible configurations and to still obtain conservative results all pins are replaced by each of the four different types of pins. Representative results are presented in Table 38, and the second arrangement in Figure 26 shows a typical configuration of this type where the pins fill the basket.

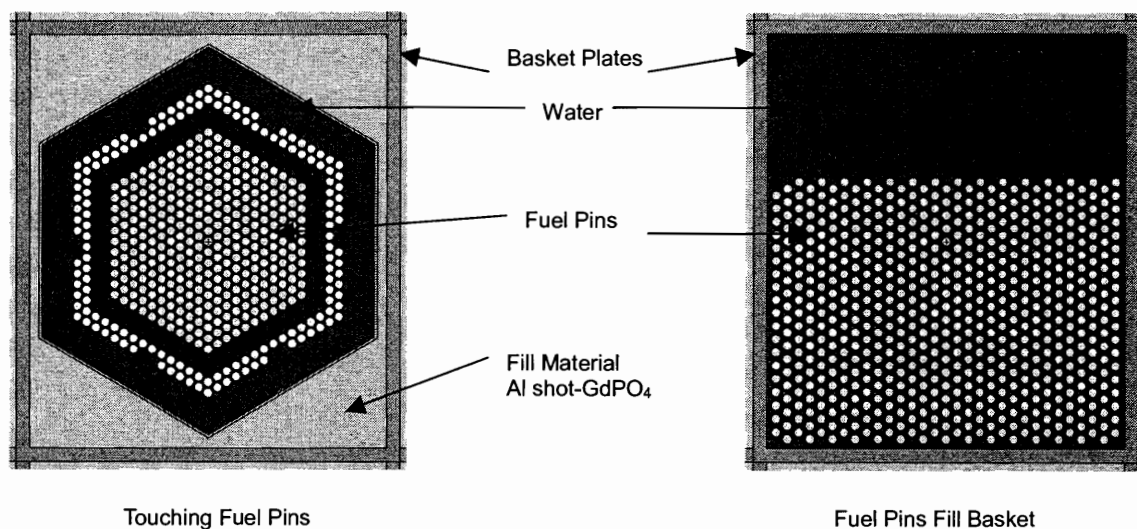


Figure 26. Different Arrangements of Fuel Pins Inside DOE SNF Canister

Table 38. Results for Loose Fuel Pins with Intact Basket Plates in the DOE SNF Canister

Case Description	Gd Content in the Al-GdPO <sub>4</sub> mix (wt.%)	Pitch Fraction	k <sub>eff</sub> + 2σ
Assembly duct is neglected, pins (fictitiously) maintain their intact configuration, water is inside the basket structure and Al fill material is outside basket	0.1	1.0	0.9079
Similar to previous case, but higher Gd content	1.0	1.0	0.9039
Pins fill basket, water is inside the basket and Al fill material is outside basket	0.1	1.0	0.8830
Similar to previous case, but uses only Type 5 fuel pins (most reactive type)	0.1	1.0	0.9135
Similar to previous case, but with a smaller pitch	0.1	0.8	0.8651
Similar to previous case, but uses only Type 4 fuel pins (next most reactive type) and greater pitch	0.1	1.0	0.8713
Type 5 pins touching, water is inside the basket and Al fill material is outside basket	0	0	0.6263
Pins surrounded by Al fill mixture with a layer of water above, Al fill mixture outside basket and Type 5 pins	0.1	1.0	0.6232
Diaspore mixed with 62.5 vol.% water fills basket, Al fill mixture outside basket and Type 5 pins	0.1	1.0	0.8025
Type 5 pins fill basket, water is inside the basket, Al fill material is outside basket and canister is surrounded by dry prebreach clay in the waste package	0.1	1.0	0.9126

These results show that the values of  $k_{eff}$  are significantly reduced if the spaces between fuel pins are filled with the gadolinium-containing material. Also noted is that if the gadolinium containing material is placed only outside the basket plates, then increasing the amount of gadolinium in the fill material does not significantly affect  $k_{eff}$ . This shows the necessity of having the filler with  $GdPO_4$  placed in close contact with the fuel assembly. Any reduction in the pitch of the fuel pins significantly reduces the configuration's  $k_{eff}$  value. Changing the boundary outside DOE SNF canister with dried prebreach clay slightly increases the  $k_{eff}$  of the system.

By assuming a further degradation of the basket plates, the loose pins will spread in the DOE SNF canister in a mass of degraded products. The configuration is represented by refinement IP-3-A in CRWMS M&O (1999g, p. 31). For the totally degraded supporting structure and contents of the DOE SNF canister, the canister shell is assumed to be breached but structurally intact. The degradation products resulting from degradation of the canister internals (mainly  $FeOOH$  [goethite] and  $AlOOH$  [diaspore]) are distributed among the fuel pins. All fuel pins from the assembly are modelled as being from the zone with the highest fissile concentration, therefore the most reactive. The placement of pins in the canister is irregular. The effect of pitch variations for the array of intact pins on  $k_{eff}$  of the system is investigated. The minimum necessary amount of neutron absorber to bring  $k_{eff}$  below the interim critical limit of 0.92 is determined. The layout of this type of configuration is presented in Figure 27.

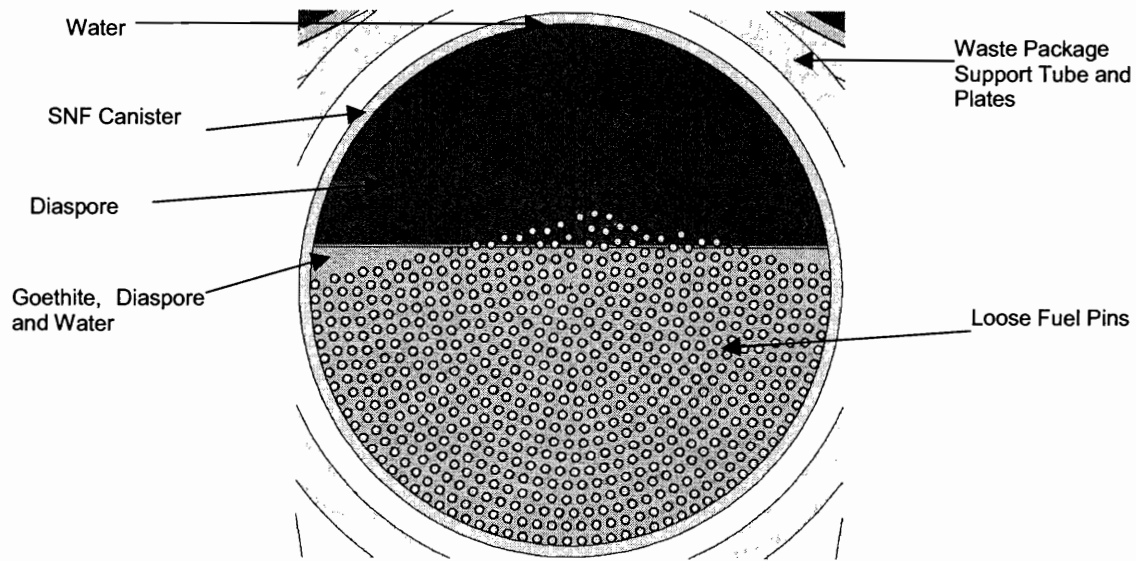


Figure 27. Cross-Sectional View of the Degraded Configuration with Intact Fuel Pins Dispersed within the DOE Canister Shell

Results for these cases are presented in Table 39. In all of these cases, the waste package is water-reflected and the contents of the waste package are intact unless noted otherwise. Empty spaces in the waste package are conservatively treated as voids.

Table 39. Results for Loose Fuel Pins with Degraded Internal Structures of the DOE SNF Canister

Case Description	Gd Content in the Al-GdPO <sub>4</sub> mix (%)	Pitch (cm)	k <sub>eff</sub> + 2σ
Water fills canister (fill material is neglected)	0	0.9398	0.9958
Pins surrounded by goethite and 60 vol.% water below a layer of dry diaspore	1.0	0.9398	0.8951
Same as previous case, but less Gd	0.1	0.9398	0.8956
Similar to previous case but pins touching	1.0	0.7782	0.6473
Similar to previous case but pitch is increased	1.0	0.8590	0.7927
Similar to previous case but pitch is further increased	1.0	1.25	1.0529
Similar to previous case but pitch is further increased	1.0	1.5	0.9497
Similar to previous case but pitch is further increased	1.0	1.62	0.8991
Pins surrounded by goethite, 60 vol.% water and diaspore below a layer of dry diaspore; the Gd amount in the layer is approximately 3% of the total Gd present in the DOE SNF canister	1.0	1.25	0.8849
Similar to previous case, but DOE SNF canister top is aligned with the top of the dry prebreach clay in the waste package (highest reflection)	1.0	1.25	0.8978
Similar to previous case but prebreach clay mixed with 20% water	1.0	1.25	0.8746

These results show that the greatest effect on k<sub>eff</sub> of the system results from changes in the fuel pin pitch. The pitch producing the largest value of k<sub>eff</sub> occurs at about 1.25 cm. The results presented in Table 39 for this pitch are above the interim criticality limit but they assume a complete separation of the neutron absorber above the fuel. As discussed in Section 7.4.1, there is no known mechanism to cause significant segregation/stratification of the layers containing degradation products. For this case, at least 0.18 kg of Gd (approximately 3% of the total Gd mass in the DOE SNF canister) mixed with the goethite and water is sufficient to reduce k<sub>eff</sub> well below the interim critical limit of 0.92. Given the relatively uniform initial configuration of the GdPO<sub>4</sub> in the DOE SNF canister the degraded configuration should also be relatively uniform, providing a large margin. If the pitch is no greater than the intact value and material is mixed between the fuel pins, then values of k<sub>eff</sub> are well below the interim criticality limit. The credibility of scenarios with separated pins (large pitch) must be demonstrated to insure that they do not defy gravity. Also, there is no identified mechanism to cause significant segregation/separation of the neutron absorber above the fuel. Since the expected values for the mixing fractions of diaspore (containing Gd) with goethite are much higher than the investigated values, there is a large margin to prevent criticality.

#### 7.4.4 Degraded Waste Package and DOE SNF Canister Internal Structures with Intact DOE SNF Canister Shell

The configurations analyzed in this section are refinements of the configuration Class 2 discussed in Section 6 (CRWMS M&O 1999g) and can be obtained via any of the standard scenarios. The configurations include an intact (but breached) DOE SNF canister outer shell that contains the mixture of degraded fissile material and other degradation products from the DOE SNF canister. All other internal structures inside waste package but external to the DOE SNF canister are degraded. The general configuration is shown in Figure 28. This is a very unlikely configuration given the corrosion resistance of the fuel pin cladding, but is analyzed for completeness (see also Section 6.2.1.1).

Various compositions and densities of the degraded mixture inside the DOE SNF canister have been evaluated (CRWMS M&O 2000d, Table 6-17). The initial footprint lengths of the four axial fuel regions are preserved. The thoria content from the fuel pins is conservatively neglected for all cases unless noted otherwise. The initial gadolinium content of the filler material is 1.0 wt.%. Any vacant spaces in the DOE SNF canister are filled with water (typically above the highest layer of degradation material). A typical configuration is shown in Figure 28 and selected representative results are given in Table 40. The table lists the contents of the bottom, middle and top (if present) layers by volume percent.

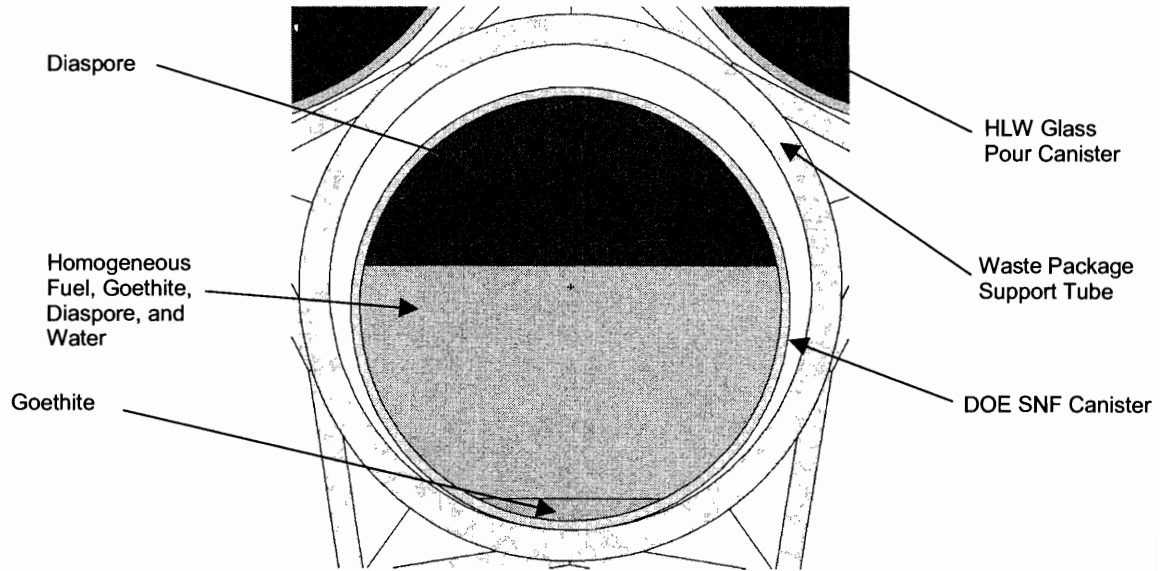


Figure 28. Cross-Sectional View of the Breached Intact DOE SNF Canister Containing Fully Degraded Fuel

Table 40. Results for Fully Degraded Waste Package Internals and Degraded SNF Contents in the Intact DOE SNF Canister

Case Description	Bottom Layer Contents by Volume (%)	Next Layer Contents by Volume (%)	Top Material Layer Contents by Volume (%)	$k_{eff} + 2\sigma$
Separated layers of fuel, goethite and diaspore in DOE SNF canister	Fuel 12.5 Water 87.5	Goethite 100	Diaspore 100	0.8753
Similar to previous case, but fuel is mixed with some goethite	Fuel 5.0 Goethite 95.0	Goethite 100	Diaspore 100	0.8021
All goethite is mixed in fuel layer	Fuel 3.0 Goethite 97.0	Diaspore 100	—	0.8357
Water added in bottom layer; all fuel levels set equal to highest axial fuel level; more fuel modeled than actually present	Fuel and Goethite 80.0 Water 20.0	Diaspore 100	—	0.9856
Some diaspore containing Gd mixed in the fuel layer; Gd content in the fuel layer represents 3.25% of the total Gd present in the DOE SNF canister	Fuel and Goethite 26.0 Water 69.0 Diaspore 5.0	Diaspore 100	—	0.9231
Similar to previous case, but more diaspore mixed in the fuel layer; Gd amount represents approximately 4% of the total Gd present in the DOE SNF canister	Fuel and Goethite 26.0 Water 68.0 Diaspore 6.0	Diaspore 100	—	0.8750

Table 40. Results for Fully Degraded Waste Package Internals and Degraded SNF Contents in the Intact DOE SNF Canister (Continued)

Case Description	Bottom Layer Contents by Volume (%)	Next Layer Contents by Volume (%)	Top Material Layer Contents by Volume (%)	$k_{eff} + 2\sigma$
All fuel levels set equal to highest axial fuel level (more fuel modeled than actually present; the Gd amount mixed in the layer represents approximately 4% of the total Gd present in the DOE SNF canister)	Fuel and Goethite 36.55 Water 55.0 Diaspore 8.45	Diaspore 100	—	0.8894
100% of goethite is in layer below fuel	Goethite 100	Fuel 1.3 Water 90.7 Diaspore 8.0	Diaspore 100	0.8846
All fuel levels set equal to highest fuel level; the DOE SNF canister is full of fuel mixture and diaspore and it is nearly centered in dry prebreach clay in waste package; the Gd amount mixed in the layer represents approximately 4% of the total Gd present in the DOE SNF canister	Fuel and Goethite 26.0 Water 68.0 Diaspore 6.0	Diaspore 100	—	0.8861

The highest values of  $k_{eff}$  for the system occur when the fuel without thoria is mixed with goethite and water and rests at the bottom of the SNF canister. The values of  $k_{eff}$  for the system increase with increasing water volume fraction, though increasing the amount of water in the mixture also increases the probability that these configurations will attempt to float a higher density layer over a lower density layer thus defy gravity. If at least 4% of the Gd present in the DOE SNF canister is distributed in the layer containing degraded fuel, the  $k_{eff}$  for the system will be below the interim critical limit of 0.92. Given the relatively uniform distribution of Gd in the initial configuration, the degraded configuration should have also a relatively uniform distribution of Gd, providing a large margin. If the thoria is included in the fuel, goethite and water mixture,  $k_{eff}$  for the system decreases but neutron absorber is still required to be mixed with the fuel to keep  $k_{eff}$  below interim criticality limit (CRWMS M&O 2000d, Table 6-17). The contents of the waste package outside the DOE SNF canister play an absorbing role for neutrons. Based on the position of the aluminum shot and neutron absorber in the intact configuration, the neutron absorber will always be mixed with degradation products and fuel. The cases presented above represent overly conservative configurations that will bound any configurations with intact fuel.

## 7.5 CALCULATIONS AND RESULTS—PART III: SCENARIOS WITH FISSILE MATERIAL DISTRIBUTED IN WASTE PACKAGE

### 7.5.1 Degraded Waste Package Internal Structures with Intact Fuel Assembly

This group of configurations, characterized by an intact fuel assembly immersed in the degradation materials resulting from the degradation of the HLW glass and other internal components of the waste package and the DOE SNF canister, represents a refinement of the configuration Class 1 (see also Section 6.2.1.4). It should be noted that spacer grids are made of stainless steel, therefore the preservation of the fuel assembly in the initial configuration is highly improbable. These cases are divided into 3 separate sets (CRWMS M&O 2000d, Tables 6-7 through 6-9). The first treats the degraded contents from the DOE SNF canister mixing the prebreach clay but water fills the voids between fuel pins inside the assembly. This configuration is unlikely given the initial distribution of the filler material. The second set deals

with the same degradation products but in these cases some of the degradation products fill the voids between fuel pins inside the assembly. Finally, the last set deals with post-breach clay in the waste package. For all cases the initial Gd content of the filler material is 1.0 wt.%. A representative configuration for these cases is depicted in Figure 29.

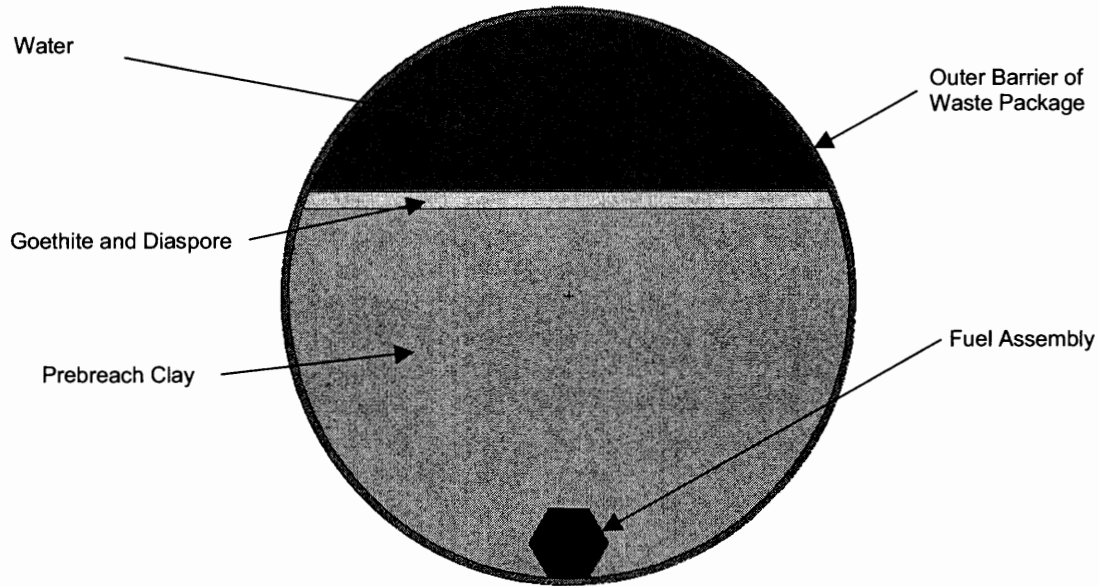


Figure 29. Cross-Sectional View of the Intact Fuel Assembly with Degraded DOE SNF Canister and Degraded Contents of the Waste Package

The most likely set of cases is with voids inside the assembly filled with a mixture of prebreach clay and water. The prebreach clay is formed from the complete degradation of components outside the DOE SNF canister: HLW glass canisters, and waste package internal web-like structure and tube. Table 41 lists some of the most representative cases (see CRWMS M&O 2000d, Table 6-8).

Table 41. Results for Intact Fuel Assembly with Degraded DOE SNF Canister and Degraded Contents of the Waste Package (Prebreach Clay)<sup>a</sup>

Case Description	$k_{eff} + 2\sigma$
Assembly sets on bottom of the waste package and is filled and covered by prebreach clay with a water volume content of 31.2%; goethite and diaspore are neglected	0.6495
Assembly sets on bottom of the waste package, is covered by prebreach clay with a water volume content of 31.2% and contains clay with a water volume content of 60%; goethite and diaspore are neglected	0.7925
Like previous case, but water volume content of prebreach clay in assembly is 90%	0.8977
Assembly sets on bottom of waste package and is filled and covered by a dry mixture of prebreach clay, goethite and diaspore	0.5180
Assembly sets on bottom of waste package and is covered by a dry mixture of prebreach clay, goethite and diaspore; this mixture with a water volume content of 80% fills the assembly	0.9063
Like previous case but waste package is surrounded by dry tuff	0.9063
Assembly sets on bottom of waste package and is covered by dry prebreach clay below a dry layer of goethite and diaspore; the assembly is filled with water mixed with a 10 vol.% of diaspore that contains approximately 2% of the initial Gd mass	0.8808

NOTE: <sup>a</sup> Degradation products fill assembly voids.

The results show that the presence of absorbing impurities inside the assembly has a major role in reducing the reactivity of the system. Increasing the water content in the post-breach clay results in an increase of the  $k_{\text{eff}} + 2\sigma$ . If at least 10.0 % of the mixture filling the voids inside the assembly is prebreach clay the  $k_{\text{eff}}$  of the system is below the interim criticality limit, even by neglecting the presence of Gd in the system. The waste package outer boundary conditions have a negligible effect on the reactivity of the system for these configurations. The presence of a very small amount of Gd distributed inside the fuel assembly is also very effective in reducing  $k_{\text{eff}}$  of the system. These results recommend having some of the neutron absorber distributed from the beginning inside the void spaces of the fuel assembly. This will assure a considerable higher margin for criticality.

The final set of results using the post-breach clay in the waste package and also filling the voids inside the assembly are given in Table 42. The post-breach clay is formed through the mixing of the prebreach clay with the completely degraded components of the DOE SNF canister. For these cases water fills any voids in the waste package not filled by the post-breach clay.

Table 42. Results for Intact Fuel Assembly with Degraded SNF Canister and Degraded Contents of the Waste Package (Post-Breach Clay)

Case Description	$k_{\text{eff}} + 2\sigma$
Assembly positioned at a distance about equal to 1/2 the thickness of the clay layer below top of post-breach clay	0.5164
Assembly positioned near center of waste package, surrounded and filled with post-breach clay containing a water volume content of 20%	0.5946
Previous case, but water volume content is 25%; waste package is completely filled by wet clay mixture	0.6117
Previous case, but assembly filled with water containing only 5% post-breach clay by volume	0.8954

The results show that the presence of post-breach clay results in much lower  $k_{\text{eff}} + 2\sigma$  values than in the previous cases (Table 41).

### 7.5.2 Degraded Waste Package Internal Structures with Intact Fuel Pins

This group of configurations, characterized by intact fuel pins immersed in the clayey material resulting from the degradation of the HLW glass and other internal components of the waste package and the DOE SNF canister, represents a further refinement of the configuration Class 1. It can be reached by applying the standard scenario group IP-3 to both the DOE SNF canister and waste package and results as a subsequent stage of degradation of the configuration presented in Section 7.5.1 (see also Section 6.2.1.4). The configurations are considered likely due to the high corrosion resistance of the zirconium fuel cladding.

The intact fuel pins are assumed dispersed in the degradation products in a lattice with constant pitch. Two distinct sets of configurations are analyzed. The first one assumes that the prebreach clay from the waste package either mixes or forms separate layers with the degradation products from the DOE SNF canister internals and shell. The main constituents of the DOE SNF canister degradation products considered are diaspore and goethite.

The second set of configurations assumes that the degradation products from the DOE SNF canister and waste package have formed a (post-breach) clay in the waste package. The results

of the criticality analysis (CRWMS M&O 2000d, Section 6.2.5) are summarized in this section. Representative configurations are presented in Figures 30 and 31.

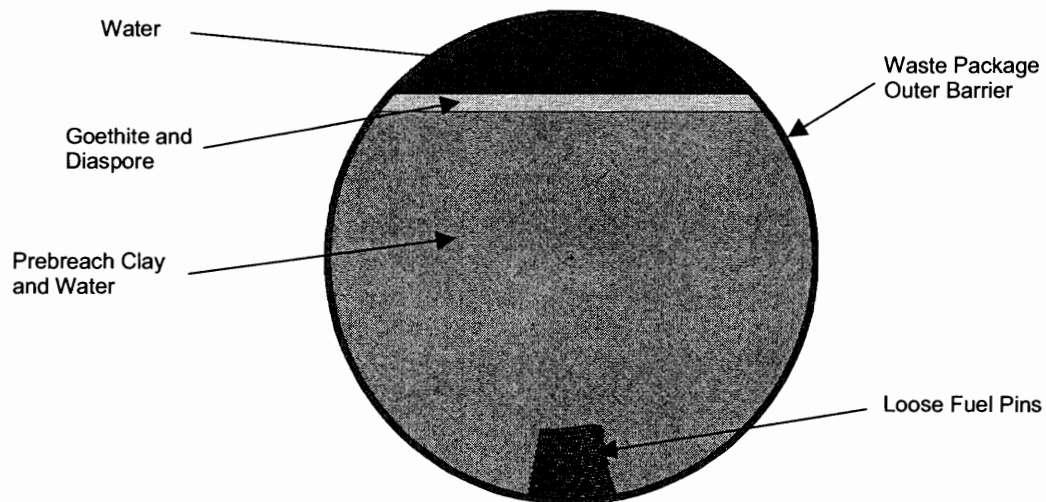


Figure 30. Cross-Sectional View of Loose Fuel Pins (compact arrangement) in the Waste Package

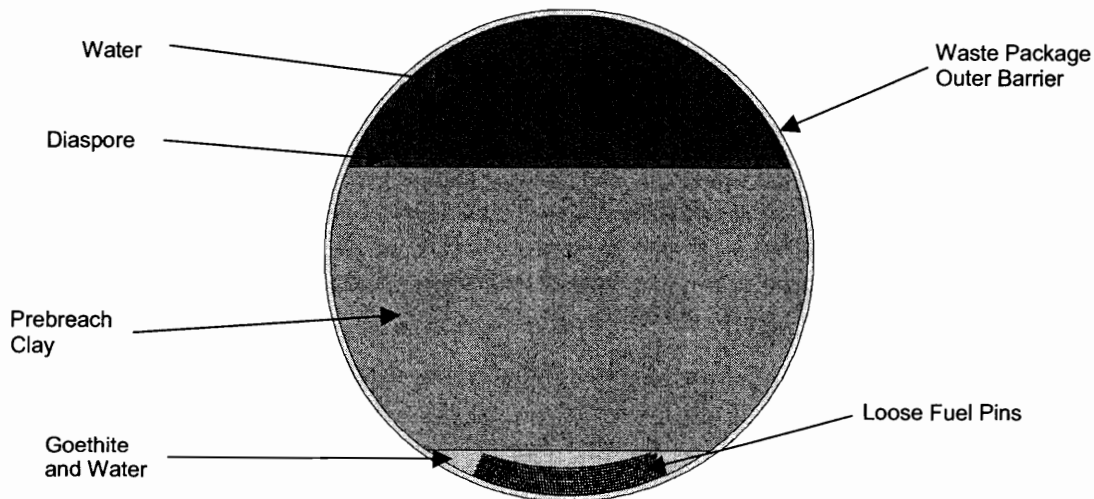


Figure 31. Cross-Sectional View of Loose, Spread Out Fuel Pins in the Waste Package

The initial Gd content of the fill material is 1.0 wt.%. Water fills any vacant spaces in the waste package.

Fuel pins surrounded only by a mixture of clay and water result in a configuration with  $k_{eff}$  below 0.85 for pitch values varying from 0.77 to 3 cm.

The results show that the larger values of  $k_{eff} + 2\sigma$  occur for cases with a pitch larger than the pitch of the intact assembly. The largest value (for a pitch of 1.25 cm) occurs for the pins

surrounded by a layer of goethite and 60% water by volume below a separated layer of clay and diasporite. Significantly smaller values of  $k_{\text{eff}}$  can be obtained if the pins are in a more spread out configuration (Figure 31) or if a small amount of diasporite is mixed in the layer surrounding the pins ( $k_{\text{eff}} + 2\sigma = 0.8824$ ). It is improbable that the fuel pins can be stacked into configurations without the pins touching hence reducing the pitch. Also complete separation of a layer containing  $\text{GdPO}_4$  is very unlikely, as mentioned in previous sections.

For the case mentioned above, if only 5.5% of the total amount of Gd in the waste package is mixed in the layer with fuel, the maximum  $k_{\text{eff}} + 2\sigma$  is 0.8824. The boundary conditions outside the waste package have a greater effect on the  $k_{\text{eff}}$  than most other configurations. For example, replacing the water reflector with dry tuff increases  $k_{\text{eff}}$  with approximately 3% (from 0.8824 to 0.9115).

Results for the fuel pins surrounded by post-breach clay show that  $k_{\text{eff}} + 2\sigma$  are much smaller than in previous cases. The pins are arranged into a relatively tight configuration similar to that shown in Figure 30 with a pitch of 1.25 cm. The initial Gd content of the filler is 1.0 wt.%. Water fills any vacant spaces in the waste package. The range of the results for  $k_{\text{eff}} + 2\sigma$  is between 0.5623 and 0.7475.

There are no criticality concerns for these cases, since these results are well below the limit of 0.92. Any increase or reduction in the pitch or spreading out of the fuel pins would only further reduce these values of  $k_{\text{eff}}$ .

### **7.5.3 Degraded DOE SNF Canister Mixture Settled at the Bottom of the Waste Package**

After the complete degradation of all waste package internal constituents, including the DOE SNF canister, the resultant configurations can include the degradation products as layers or complex mixtures settled within the waste package. These configurations belong to Class 2 (CRWMS M&O 1999g). It comprises a large number of refinements and variations, and it can be reached by any of the standard top-breach scenarios (IP-1, IP-2, or IP-3). A bounding approach was also adopted for this analysis, investigating various possible combinations of the fissile material with different degradation constituents. A typical geometry for this group of configurations is shown in Figure 32.

Two different sets of configurations are treated. The first set considers the degradation products from the degraded DOE SNF canister mixed with prebreach clay from the contents of the waste package. The second set considers post-breach clay. These cases neglect the thoria content of the fuel unless noted otherwise. The Gd initial content in the filler material is 1.0 wt.%. The initial footprint lengths of the four axial fuel regions are preserved for all cases.

A first set of cases investigated the effect of the complete separation of the layers containing degraded fuel, goethite, prebreach clay and diasporite mixed with the gadolinium phosphate. As expected, these extremely unlikely configurations are very reactive. Varying, for example, the water content in the bottom fuel layer between 0 and 95 % increases  $k_{\text{eff}} + 2\sigma$  from 0.6497 to 1.0392 (CRWMS M&O 2000d, Table 6-18). Mixing degraded fuel with goethite and water in the bottom layer and keeping the upper layers of prebreach clay and diasporite dry, also results in

very high values of  $k_{\text{eff}} + 2\sigma$ , well above the interim criticality limit. If the thoria is not neglected in the fuel mixture the reactivity of the system is slightly reduced. In all above configurations the neutron absorber ( $\text{GdPO}_4$ ) is completely separated from the degraded fuel in an upper layer, which is very unlikely. As already mentioned there is no physical mechanism to separate/segregate the neutron absorber above the fuel.

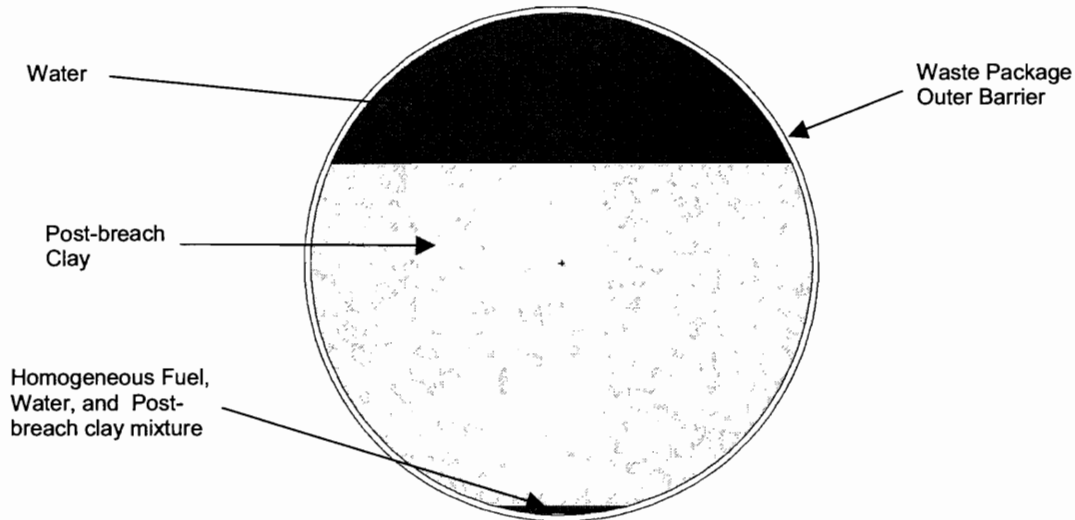


Figure 32. Fully Degraded DOE SNF Canister Settled at the Bottom of Waste Package

Subsequent calculations investigate the minimum amount of diasporite containing  $\text{GdPO}_4$  that needs to be mixed in the layer containing fuel in order to bring the  $k_{\text{eff}} + 2\sigma$  below the interim criticality limit.

If at least 5 vol.% of the mixture containing degraded fuel is diasporite (containing  $\text{GdPO}_4$ ), the  $k_{\text{eff}} + 2\sigma$  is below 0.92 even considering the most conservative reflective boundary conditions. This corresponds to 0.316 kg of Gd being distributed uniformly in the layer containing degraded fuel (5% of the total amount). It can be noted the large margin present, since the expected values of mixing fractions will be much higher for the initially uniform distribution of Gd around the fuel.

The inclusion of the prebreach clay in the fuel mixture further reduces the  $k_{\text{eff}}$  of the system, but only for volumes significantly greater than the volume of diasporite.

If at least 5 vol.% of the fuel mixture is prebreach clay, the presence of 1.75 vol.% of diasporite +  $\text{GdPO}_4$  in the layer, which represents only 1.85% of the total Gd in the waste package, will bring the  $k_{\text{eff}} + 2\sigma$  to 0.8785, well below the interim criticality limit. Since these kinds of final mixtures are the most probable due to the evolution of the system, there are no criticality concerns for the fully degraded configurations. Changing the waste package boundary conditions from water reflector to dry tuff produces an increase in  $k_{\text{eff}} + 2\sigma$  from 0.8785 to 0.9123.

Results for the degraded fuel mixed with the post-breach clay in the waste package are given in Table 43.

Table 43. Results for Fully Degraded Fuel with Degraded SNF Canister and Degraded Contents in the Waste Package with Post-Breach Clay

Bottom Layer Contents by Volume (%)	Next Layer Contents by Volume (%)	$k_{\text{eff}} + 2\sigma$
Fuel 100	Clay 100	0.3813
Fuel 12.5 Water 87.5	Clay 100	0.6901
Fuel 5.0 Water 85.0 Clay 10.0	Clay 100	0.8941
Fuel 0.25 Water 40.0 Clay 59.75	Clay 100	0.5219

Results for the cases with post-breach clay show that if at least 10% by volume of the fuel mixture (fuel, water and clay) is clay then there are no criticality concerns. If only water is mixed with the fuel then the large amount necessary to raise  $k_{\text{eff}}$  above the limit of 0.92 would result in the density of the mixture being such that it would not be capable of supporting the clay above it.

## 7.6 CALCULATIONS AND RESULTS—PART IV: Additional Topics of Interest

### 7.6.1 Axial Redistribution of Degraded DOE SNF in the Canister and in the Waste Package

Results are presented in CRWMS M&O 2000d for cases where the fully degraded fuel in the bottom of either the SNF canister or the waste package is axially redistributed, i.e., its length becomes shorter or longer than its intact footprint length. These results show that as the length becomes greater the  $k_{\text{eff}}$  of the system becomes smaller. Likewise, any decrease in the length of the fuel region leads to an increase in the system  $k_{\text{eff}}$ . As an example for the cases presented, a 10.0 % increase in length leads to at least a 1.5% decrease in  $k_{\text{eff}}$ , while the largest increase in  $k_{\text{eff}}$  is 5.2% for a 10% decrease in length. These results suggest the necessity of imposing a limit on the linear loading for the fissile material in the DOE SNF canister. A homogeneous model of the fuel was developed to demonstrate that similar fuels (U/Th oxide), containing the same amount (or less) of fissile material, are bound by the results for Shippingport LWBR SNF. The results (CRWMS M&O 2000d, Table 6-22) show that for the various homogeneous configurations considered (with different degrees of simplification), the  $k_{\text{eff}}$  of the system is lower or within the uncertainty band of the maximum heterogeneous case.

### 7.6.2 Results for Uranium Decay Effects

The half-life of U-233 is several orders of magnitude smaller than that of U-235, 159200 years and 704000000 years, respectively (Parrington 1996, p.49). The shorter of these times is certainly of the order of what is of immediate concern for the life of the repository. Therefore, results for selected cases are given in CRWMS M&O 2000d for the system  $k_{\text{eff}}$  after a passage of 50000, 100000 and 150000 years. For the cases examined the minimum decrease in  $k_{\text{eff}}$  after a passage of 50000 years is about 5.3 % whereas, the minimum decrease after 150000 years is

17.5 %. These results show that uranium decay has a very important effect in reducing the  $k_{\text{eff}}$  of the system. The highly degraded configurations (that require long times) have a drastically reduced potential for criticality.

## 7.7 SUMMARY

The results of three-dimensional (3-D) Monte Carlo criticality calculations for all anticipated intact and degraded configurations show that the requirement of  $k_{\text{eff}}+2\sigma$  less than or equal to the interim critical limit of 0.92 is satisfied for the Shippingport LWBR codisposal waste package with at least 1.0% by mass of gadolinium in the aluminum shot-GdPO<sub>4</sub> filler (10.12 kg GdPO<sub>4</sub>). The gadolinium must be uniformly distributed in the initial aluminum shot-GdPO<sub>4</sub> filler, and there must be some reasonable degree of mixing of the gadolinium containing filler (or degraded filler) with the fuel mixture layer for many degraded cases. The results show that a uniform distribution of filler material in all available void spaces inside the DOE SNF canister (including void spaces in the fuel assembly) is highly desirable and further increases the margin for criticality.

Most cases analyzed require only a fraction of the indicated insoluble neutron absorber in order to be below the interim criticality limit. The representative intact configurations that were investigated are very near the interim criticality limit without neutron absorber and at best would require only a tenth of the amount of neutron absorber that is listed above. The limiting case for the configurations with the fuel inside DOE SNF canister was obtained for a homogeneous mixture of fuel and hydrated products inside DOE SNF canister, which require 10.12 kg of GdPO<sub>4</sub> in the canister. At least 4% of the Gd must be mixed uniformly with the layer containing the degraded fuel. The overall limiting case was obtained for an extremely conservative configuration comprising a pile of fuel pins stacked at the bottom of the waste package. This configuration required the same amount of insoluble neutron absorber (10.12 kg of GdPO<sub>4</sub>) present in the waste package with at least 5.5% of it distributed uniformly in the layer that covers the fuel.

## 8. CONCLUSIONS

This document may be affected by technical product input information that requires confirmation. Any changes to this document that may occur as a result of completing the confirmation activities will be reflected in subsequent revisions. The status of the input information quality may be confirmed by review of the Document Input Reference System database.

All of the analyses presented in this report are based on the Enhanced Design Alternative (EDA) II. The thermal analysis is performed also for the Viability Assessment (VA) (DOE 1998a) design of the 5-DHLW/DOE SNF waste package. An impact evaluation of the results presented in this report should be performed for future waste package designs.

### 8.1 STRUCTURAL ANALYSIS

The results from the 2-D FEA calculations given in Section 3.3 show that there is sufficient clearance between the inner diameter of the basket support tube and the outer diameter of the DOE SNF canister for the canister to be removed from the waste package after a tipover DBE, which is the limiting DBE within the criteria specified in the SDD (CRWMS M&O 2000j).

The maximum deformations in each component of the waste package are acceptable. The outer barrier is directly exposed to a dynamic impact with an essentially unyielding surface. Therefore, local plastic deformations are unavoidable on the outer surface. Similarly, the basket support structure receives the direct impacts of pour canisters, which results in limited permanent deformations of the basket plates.

The maximum stress in the DOE SNF canister structural components, including internals is determined to be 243.6 MPa. This magnitude of stress is less than 0.9 or 0.7 of the ultimate tensile strength of 316L stainless steel, 483 MPa, therefore the allowable stress-limit criteria presented in Section 3.2 are met. It is concluded that the performance of the 5-DHLW/DOE SNF waste package internal design is structurally acceptable when exposed to a tipover event, as long as the DOE SNF canister loaded mass limit of 2721 kg is not exceeded, and the HLW glass canister loaded mass limit of 4200 kg is not exceeded for each of the five canisters.

### 8.2 THERMAL ANALYSIS

The HLW glass dominates the thermal heat output of the waste package. The maximum temperatures for both VA and EDA II designs are shown in Table 44.

Table 44. Shippingport LWBR Codisposal Waste Package Thermal Results and Governing Criteria

Waste Package Metric	SDD Criterion	Shippingport LWBR Codisposal Waste Package Value	
		VA Design	EDA II Design
Maximum Waste Package heat output (W)	< 11,800	8007.1	8007.1
Maximum HLW temperature (°C)	< 400	220.34	300.04

The SDD criterion for thermal calculations, SDD 1.2.1.6 cited in Section 2.2.2, contains TBV-245. TBV-245 restricts the HLW glass temperature to less than 400°C, under normal operation conditions. The results indicate that the maximum HLW glass temperature for the EDA II design is 300.04 °C (Argon), which is less than the temperature specified in SDD 1.2.1.6 criterion.

The waste package thermal output at emplacement is 8007.1 W for both the VA and EDA II designs and emplacement parameters. Both designs satisfy the 11.8 kW criterion set in the SDD 1.2.4.2. (cited in Section 2.2.2).

### **8.3 SHIELDING ANALYSIS**

The maximum dose rate at the external surfaces of the waste package is 83.05 rem/h (dose rate +  $2\sigma$ ). This value occurs on the radial outer surface of the waste package (segment 5 in Figure 14). The maximum dose rates on the bottom and top surfaces of the waste package are about two-tenth and one-hundredth, respectively, of the maximum dose rate. The neutron dose rates represent less than two percent of the primary gamma dose rates. Therefore, the gamma dose rates dominate the total dose rates.

Although the gamma spectra and intensities of each 4.5-m-long HLW glass canister and the Shippingport LWBR SNF assembly are similar, the dose generated by the HLW glass dominates the dose at the external surfaces of the waste package. The Shippingport LWBR assembly makes a rather insignificant contribution to the dose rate at the external surfaces of the waste package because of the fuel self-shielding and the shielding effect of the internal structural materials and the HLW glass canisters.

The SDD criterion for waste package design (SDD 1.2.4.1), cited in Section 2.2.3, specifies a maximum dose rate of 1450 rem/h (TBV-248) at the external surface of the waste package. This analysis shows that the maximum dose rate at the external surfaces of the waste package is 81.33 rem/h, which is about 18 times lower than the criterion value. This demonstrates that waste package design complies with SDD 1.2.4.1 criterion and that there is a large margin to the maximum allowable dose rate specified in SDD 1.2.4.1 criterion.

### **8.4 GEOCHEMISTRY ANALYSIS**

The geochemistry analyses that evaluate potential critical configurations from intact through degraded follow the general methodology developed for application to all waste forms containing fissile material. Sequences of the events and/or processes of component degradation are developed. Standard scenarios listed in the topical report are refined using the unique fuel characteristics of the Shippingport LWBR SNF. Potentially critical configurations were identified and analyzed.

The greatest Gd losses are in the EQ6 runs that maximize exposure of Gd to the high pH caused by the degradation of the HLW glass. Nonetheless, the maximum Gd loss is never greater than 3.6 % over 300000 years for any of the scenarios.

## 8.5 INTACT- AND DEGRADED-MODE CRITICALITY ANALYSIS

The criticality analyses considered all aspects of intact and degraded configuration of the codisposal waste package containing Shippingport LWBR SNF, including optimum moderation condition, rearrangements of the fuel pins and fissile material, and neutron absorber distribution. The results of 3-D Monte Carlo calculations from both the intact and the degraded component criticality analyses show that the interim critical limit requirement of  $k_{\text{eff}}+2\sigma$  be less than or equal to 0.92 is satisfied for the proposed design. The amount of neutron absorber (gadolinium phosphate) required to satisfy the above criterion is 10.12 kg of  $\text{GdPO}_4$  in or on the initial aluminum shot- $\text{GdPO}_4$  filler, which must be placed in void spaces of the DOE SNF canister loaded with the Shippingport LWBR seed fuel assembly. This amount is equivalent to 1 wt.% of Gd in the aluminum shot- $\text{GdPO}_4$  filler. With this design, there will be approximately twelve DOE SNF canisters with Shippingport LWBR SNF, which correspond to twelve waste packages.

A number of parametric analyses were run to address or bound the configuration classes discussed in Sections 6.2, 7.4 and 7.5. These parametric analyses identified conditions of optimum moderation, optimum spacing between fuel pins, optimum fissile concentration, and minimum neutron absorber requirements. The results from the degraded criticality analyses show that the most reactive configurations are the configurations with fully degraded components inside DOE SNF canister and the configurations with intact fuel pins dispersed in the waste package. These configurations result in  $k_{\text{eff}}+2\sigma$  less than or equal to 0.92 with at least 10.12 kg  $\text{GdPO}_4$  distributed in the initial aluminum- $\text{GdPO}_4$  filler. 10 kg or more of  $\text{GdPO}_4$  should be loaded to provide extra margin (defense in depth).

Due to the basket design and the aluminum shot- $\text{GdPO}_4$  filler, the codisposal waste package containing a DOE SNF canister of spent Shippingport LWBR fuel will not form critical configurations for any credible degradation scenarios. The uranium decay has a beneficial effect on further reducing the  $k_{\text{eff}}$  of the system containing Shippingport LWBR SNF. The effect is very significant after 50000 years (at least 5% reduction in  $k_{\text{eff}}$ ) and should completely diminish the potential for criticality for postulated waste package breach times of the same order of magnitude.

The SDD criterion for criticality calculations (SDD 1.2.2.1.12), cited in Section 2.2.5, has TBV-245 relating to values of the interim critical limit. Intact and degraded component criticality calculations include variations on moderators and moderator densities, which encompass flooding the waste package. Occurrence of design basis events, including those with the potential for flooding the disposal container prior to disposal container sealing, is considered and analyzed using very conservative assumptions for many different intact configurations. All these configurations were below the interim critical limit of 0.92; therefore, the TBV-245 is non-critical and is not carried through the conclusions in this section.

## 8.6 ITEMS IMPORTANT TO CRITICALITY CONTROL

As part of the criticality licensing strategy, items that are important to criticality control will be identified during evaluation of the representative fuel types designated by the National Spent Nuclear Fuel Program. As a result of the analyses performed for the evaluation of the codisposal viability of U/Th Oxide DOE-owned fuel, several items are identified as important to criticality

control. The DOE SNF canister shell is naturally an item that is important to criticality control since it initially confines the fissile elements to a specific geometry and location within the waste package. The internal structure that was designed for the DOE SNF canister containing the Shippingport LWBR fuel is also an important item for criticality control since it confines the fissile elements to a specific geometry and location within the DOE SNF canister. The use and distribution of the aluminum shot-GdPO<sub>4</sub> filler with at least 10.12 kg GdPO<sub>4</sub> is also important to criticality control. A factor of two or more is suggested on GdPO<sub>4</sub> mass initially placed into the canister for margin.

Based on the conclusions derived in Section 7.7, the specified amount of gadolinium phosphate neutron absorber will have to be added with the aluminum shot used to fill all void space inside the DOE SNF canister to the height of the fuel assembly. The calculations show that a relatively uniform mixture of the neutron absorber in the DOE SNF canister is highly desirable, and must include the void spaces inside the intact fuel assemblies. Therefore, the amount of gadolinium phosphate absorber material that will be placed inside the DOE SNF canister is also an item important to criticality control.

All calculations are based on a maximum of 16.6 kg U-233 per DOE SNF canister. The analyses are based on the fuel type that has the highest U-233 concentration. The degraded configurations of the Shippingport LWBR SNF bound the other types of U-Th DOE-owned SNF, as long as the limits on mass of uranium and its enrichment, and the linear density, are not exceeded.

Hence, the total mass of fissile element (U-233) should not exceed the mass used in deriving the conclusions of this report, which is 16.6 kg of U-233 per DOE SNF canister. The maximum fissile concentration in the fuel is 5.2 % in U-233. The linear density of the U-233 should not exceed 92.5 g/cm in the canister. This value is calculated for the axial zone with maximum fissile loading by summing the initial linear fissile density per rod for all the rods in the seed assembly.

## 9. REFERENCES

### 9.1 DOCUMENTS CITED

ASM International 1987. *Corrosion*. Volume 13 of *Metals Handbook*. 9th Edition. Metals Park, Ohio: American Society for Metals. TIC: 209807.

ASM International 1990. *Properties and Selection: Nonferrous Alloys and Special-Purpose Materials, Specific Metals and Alloys*. Volume 2 of *Metals Handbook*. 10th Edition. Metals Park, Ohio: American Society for Metals. TIC: 239807.

Briesmeister, J.F., ed. 1997. *MCNP-A General Monte Carlo N-Particle Transport Code*. LA-12625-M, Version 4B. Los Alamos, New Mexico: Los Alamos National Laboratory. ACC: MOL.19980624.0328.

CRWMS M&O 1996. *Second Waste Package Probabilistic Criticality Analysis: Generation and Evaluation of Internal Criticality Configurations*. BBA000000-01717-2200-00005 REV 00. Las Vegas, Nevada: CRWMS M&O. ACC: MOL.19960924.0193.

CRWMS M&O 1997a. *Waste Package Design Basis Events*. BBA000000-01717-0200-00037 REV 00. Las Vegas, Nevada: CRWMS M&O. ACC: MOL.19971006.0075.

CRWMS M&O 1997b. *DHLW Canister Source Terms for Waste Package Design*. BBA000000-01717-0200-00025 REV 00. Las Vegas, Nevada: CRWMS M&O. ACC: MOL.19970711.0019.

CRWMS M&O 1997c. *Waste Package Fabrication Process Report*. BBA000000-01717-2500-00010 REV 02. Las Vegas, Nevada: CRWMS M&O. ACC: MOL.19971218.0275.

CRWMS M&O 1997d. *Waste Quantity, Mix and Throughput Study Report*. B00000000-01717-5705-00059 REV 01. Las Vegas, Nevada: CRWMS M&O. ACC: MOL.19971210.0628.

CRWMS M&O 1997e. Not used.

CRWMS M&O 1997f. *Preliminary Design Basis for WP Thermal Analysis*. BBAA00000-01717-0200-00019 REV 00. Las Vegas, Nevada: CRWMS M&O. ACC: MOL.19980203.0529.

CRWMS M&O 1997g. *Degraded Mode Criticality Analysis of Immobilized Plutonium Waste Forms in a Geologic Repository*. Predecisional Document. A00000000-01717-5705-00014 REV 01. Las Vegas, Nevada: CRWMS M&O. ACC: MOL.19980422.0911.

CRWMS M&O 1998a. Not used.

CRWMS M&O 1998b. *Calculation of the Effect of Source Geometry on the 21-PWR WP Dose Rates*. BBAC00000-01717-0210-00004 REV 00. Las Vegas, Nevada: CRWMS M&O. ACC: MOL.19990222.0059.

CRWMS M&O 1998c. *Software Qualification Report for MCNP Version 4B2, A General Monte Carlo N-Particle Transport Code*. CSCI: 30033 V4B2LV. DI: 30033-2003, Rev. 01. Las Vegas, Nevada: CRWMS M&O. ACC: MOL.19980622.0637.

CRWMS M&O 1998d. Not used.

CRWMS M&O 1998e. "Unsaturated Zone Hydrology Model." Chapter 2 of *Total System Performance Assessment-Viability Assessment (TSPA-VA) Analyses Technical Basis Document*. B00000000-01717-4301-00002 REV 01. Las Vegas, Nevada: CRWMS M&O. ACC: MOL.19981008.0002.

CRWMS M&O 1998f. *EQ6 Calculations for Chemical Degradation of Pu-Ceramic Waste Packages*. BBA000000-01717-0210-00018 REV 00. Las Vegas, Nevada: CRWMS M&O. ACC: MOL.19980918.0004.

CRWMS M&O 1998g. *EQ6 Calculations for Chemical Degradation of PWR LEU and PWR MOX Spent Fuel Waste Packages*. BBA000000-01717-0210-00009 REV 00. Las Vegas, Nevada: CRWMS M&O. ACC: MOL.19980701.0483.

CRWMS M&O 1998h. *Dose Calculations for the Co-Disposal WP of HLW Canisters and the Fast Flux Test Facility (FFTF) Fuel*. BBA000000-01717-0210-00019 REV 00. Las Vegas, Nevada: CRWMS M&O. ACC: MOL.19990129.0075.

CRWMS M&O 1998i. Not used.

CRWMS M&O 1998j. *EQ6 Calculations for Chemical Degradation of Fast Flux Test Facility (FFTF) Waste Packages*. BBA000000-01717-0210-00028 REV 00. Las Vegas, Nevada: CRWMS M&O. ACC: MOL.19981229.0081.

CRWMS M&O 1998k. Not used.

CRWMS M&O 1998l. "Waste Form Degradation, Radionuclide Mobilization, and Transport Through the Engineered Barrier System." Chapter 6 of *Total System Performance Assessment - Viability Assessment (TSPA-VA) Analyses Technical Basis Document*. B00000000-01717-4301-00006 REV 01. Las Vegas, Nevada: CRWMS M&O. ACC: MOL.19981008.0006.

CRWMS M&O 1999a. *Structural Calculations for the Codisposal of Shippingport LWBR Spent Nuclear Fuel in a Waste Package*. BBA000000-01717-0210-00057 REV 00. Las Vegas, Nevada: CRWMS M&O. ACC: MOL.20000224.0398.

CRWMS M&O 1999b. *Dose Calculations for the Codisposal WP of HLW Glass and the Shippingport LWBR SNF*. BBAC00000-01717-0210-00016 REV 00. Las Vegas, Nevada: CRWMS M&O. ACC: MOL.19991117.0141.

CRWMS M&O 1999c. *LCE for Research Reactor Benchmark Calculations*. B00000000-01717-0210-00034 REV 00. Las Vegas, Nevada: CRWMS M&O. ACC: MOL.19990329.0394.

CRWMS M&O 1999d. *DOE SRS HLW Glass Chemical Composition*. BBA000000-01717-0210-00038 REV 00. Las Vegas, Nevada: CRWMS M&O. ACC: MOL.19990215.0397.

CRWMS M&O 1999e. *EQ6 Calculation for Chemical Degradation of Pu-Ceramic Waste Packages: Effects of Updated Materials Composition and Rates*. CAL-EDC-MD-000003 REV 00. Las Vegas, Nevada: CRWMS M&O. ACC: MOL.19990928.0235.

CRWMS M&O 1999f. *Laboratory Critical Experiment Reactivity Calculations*. B00000000-01717-0210-00018 REV 01. Las Vegas, Nevada: CRWMS M&O. ACC: MOL.19990526.0294.

CRWMS M&O 1999g. *Generic Degradation Scenario and Configuration Analysis for DOE Codisposal Waste Package*. BBA000000-01717-0200-00071 REV 00. Las Vegas, Nevada: CRWMS M&O. ACC: MOL.19991118.0180.

CRWMS M&O 1999h. *FY99 Criticality DOE SNF, 2101 9076 M3*. Activity Evaluation, March 5, 1999. Las Vegas, Nevada: CRWMS M&O. ACC: MOL.19990330.0477.

CRWMS M&O 1999i. *DOE Spent Nuclear Fuel (SNF) - 2101 2310 M1-M8*. Activity Evaluation, October 1, 1999. Las Vegas, Nevada: CRWMS M&O. ACC: MOL.19991001.0154.

CRWMS M&O 1999j. *EQ6 Calculations for Chemical Degradation of Shippingport PWR (HEU Oxide) Spent Nuclear Fuel Waste Packages*. CAL-EDC-MD-000002 REV 00. Las Vegas, Nevada: CRWMS M&O. ACC: MOL.19991220.0322.

CRWMS M&O 1999k. Not used.

CRWMS M&O 1999l. Not used.

CRWMS M&O 1999m. *Volumes, Masses, and Surface Areas for Shippingport LWBR Spent Nuclear Fuel in a DOE SNF Canister*. BBA000000-01717-0210-00056 REV 00. Las Vegas, Nevada: CRWMS M&O. ACC: MOL.19991027.0143.

CRWMS M&O 2000a. *DOE SNF Analysis Plan for FY 2000*. Development Plan TDP-EDC-MD-000003 REV 01. Las Vegas, Nevada: CRWMS M&O. ACC: MOL.20000510.0169.

CRWMS M&O 2000b. *Thermal Evaluation of the Shippingport LWBR SNF Codisposal Waste Package*. CAL-EDC-ME-000001 REV 00. Las Vegas, Nevada: CRWMS M&O. ACC: MOL.20000307.0808.

CRWMS M&O 2000c. *EQ6 Calculation for Chemical Degradation of Shippingport LWBR (Th/U Oxide) Spent Nuclear Fuel Waste Package*. CAL-EDC-MD-000008 REV 00. Las Vegas, Nevada: CRWMS M&O. URN-0551

CRWMS M&O 2000d. *Intact and Degraded Criticality Calculations for the Codisposal of Shippingport LWBR Spent Nuclear Fuel in a Waste Package*. CAL-EDC-NU-000004 REV 00. Las Vegas, Nevada: CRWMS M&O. URN-0582

CRWMS M&O 2000e. *Defense High Level Waste Glass Degradation*. ANL-EBS-MD-000016 REV 00. Las Vegas, Nevada: CRWMS M&O. ACC: MOL.20000329.1183.

CRWMS M&O 2000f. *Waste Package Degradation Process Model Report*. TDR-WIS-MD-000002 REV 00 ICN 01. Las Vegas, Nevada: CRWMS M&O. ACC: MOL.20000717.0005.

CRWMS M&O 2000g. *Abstraction of Drift Seepage*. ANL-NBS-MD-000005 REV 00. Las Vegas, Nevada: CRWMS M&O. ACC: MOL.20000322.0671.

CRWMS M&O 2000h. *Summary of In-Package Chemistry for Waste Forms*. ANL-EBS-MD-000050 REV 00. Las Vegas, Nevada: CRWMS M&O. ACC: MOL.20000217.0217.

CRWMS M&O 2000i. *DSNF and Other Waste Form Degradation Abstraction*. ANL-WIS-MD-000004 REV 00. Las Vegas, Nevada: CRWMS M&O. ACC: MOL.20000223.0502.

CRWMS M&O 2000j. *Defense High Level Waste Disposal Container System Description Document*. SDD-DDC-SE-000001 REV 01. Las Vegas, Nevada: CRWMS M&O. ACC: MOL.20000823.0001.

DOE (U.S. Department of Energy) 1992. *Characteristics of Potential Repository Wastes*. DOE/RW-0184-R1. Volume 1. Washington, D.C.: U.S. Department of Energy, Office of Civilian Radioactive Waste Management. ACC: HQO.19920827.0001.

DOE 1998a. *Preliminary Design Concept for the Repository and Waste Package*. Volume 2 of *Viability Assessment of a Repository at Yucca Mountain*. DOE/RW-0508. Washington, D.C.: U.S. Department of Energy, Office of Civilian Radioactive Waste Management. ACC: MOL.19981007.0029.

DOE 1998b. "Design Specification." Volume 1 of *Preliminary Design Specification for Department of Energy Standardized Spent Nuclear Fuel Canisters*. DOE/SNF/REP-011, Rev. 1. Washington, D.C.: U.S. Department of Energy, Office of Spent Fuel Management and Special Projects. TIC: 241528.

DOE 1999a. "Design Specification." Volume 1 of *Preliminary Design Specification for Department of Energy Standardized Spent Nuclear Fuel Canisters*. DOE/SNF/REP-011, Rev. 3. Washington, D.C.: U.S. Department of Energy, Office of Spent Fuel Management and Special Projects. TIC: 246602.

DOE 1999b. *Shippingport LWBR (Th/U Oxide) Fuel Characteristics for Disposal Criticality Analysis*. DOE/SNF/REP-051, Revision 0. Washington, D.C.: U.S. Department of Energy, Office of Spent Fuel Management and Special Projects. TIC: 245631.

DOE 2000. *Quality Assurance Requirements and Description*. DOE/RW-0333P, Rev. 10. Washington, D.C.: U.S. Department of Energy, Office of Civilian Radioactive Waste Management. ACC: MOL.20000427.0422.

Heath, C. 1997. "Fifteen Foot High Level Waste Canister." Interoffice correspondence from C. Heath (CRWMS M&O) to D. Foust, May 13, 1997, DC.WMI.CAH.5/97.02. ACC: MOV.19970602.0021.

Hillner, E.; Franklin, D.G.; and Smee, J.D. 1998. *The Corrosion of Zircaloy-Clad Fuel Assemblies in a Geologic Repository Environment*. WAPD-T-3173. West Mifflin, Pennsylvania: Bettis Atomic Power Laboratory. TIC: 237127.

Nuclear Energy Agency 1998. *International Handbook of Evaluated Criticality Safety Benchmark Experiments*. NEA/NSC/DOC(95)03. Paris, France: Nuclear Energy Agency. TIC: 243013.

Östhols, E. and Malmström, M. 1995. "Dissolution Kinetics of ThO<sub>2</sub> in Acid and Carbonate Media." *Radiochimica Acta*, 68, (2), 113-119. München, Germany: R. Oldenbourg Verlag. TIC: 245120.

Parrington, J.R.; Knox, H.D.; Breneman, S.L.; Baum, E.M.; and Feiner, F. 1996. *Nuclides and Isotopes, Fifteenth Edition: Chart of the Nuclides*. San Jose, California: General Electric Company. TIC: 233705.

Spahiu, K. and Bruno, J. 1995. *A Selected Thermodynamic Database for REE to be Used in HLNW Performance Assessment Exercises*. SKB Technical Report 95-35. Stockholm, Sweden: Swedish Nuclear Fuel and Waste Management Company. TIC: 225493.

Taylor, W.J. 1997. "Incorporating Hanford 15 Foot (4.5 meter) Canister into Civilian Radioactive Waste Management System (CRWMS) Baseline." Memorandum from W.J. Taylor (DOE) to J. Williams (Office of Waste Acceptance and Storage and Transportation), April 2, 1997. ACC: HQP.19970609.0014.

Wilkins, D.R. and Heath, C.A. 1999. "Direction to Transition to Enhanced Design Alternative II." Letter from Dr. D.R. Wilkins and C.A. Heath (CRWMS M&O) to Distribution, June 15, 1999, LV.NS.JLY.06/99-026, with enclosures, "Strategy for Baselineing EDA II Requirements" and "Guidelines for Implementation of EDA II." ACC: MOL.19990622.0126; MOL.19990622.0127; MOL.19990622.0128.

YMP (Yucca Mountain Site Characterization Project) 1998. *Disposal Criticality Analysis Methodology Topical Report*. YMP/TR-004Q, Rev. 0. Las Vegas, Nevada: Yucca Mountain Site Characterization Office. ACC: MOL.19990210.0236.

Zimmer, E. and Merz E. 1984. Dissolution of Thorium-Uranium Mixed Oxides in Concentrated Nitric Acid. *Journal of Nuclear Materials*, 124, 64-67. Amsterdam, The Netherlands: Elsevier Science Publishers. TIC: 247214.

## 9.2 CODES, STANDARDS, REGULATIONS, AND PROCEDURES

AP-2.21Q, Rev. 0, ICN 0. *Quality Determinations and Planning for Scientific, Engineering, and Regulatory Compliance Activities*. Washington, D.C.: U.S. Department of Energy, Office of Civilian Radioactive Waste Management. ACC: MOL.20000802.0003.

AP-3.11Q, Rev. 1, ICN 1. *Technical Reports*. Washington, D.C.: U.S. Department of Energy, Office of Civilian Radioactive Waste Management. ACC: MOL.20000714.0549.

AP-3.15Q, Rev. 1, ICN 2. *Managing Technical Product Inputs*. Washington, D.C.: U.S. Department of Energy, Office of Civilian Radioactive Waste Management. ACC: MOL.20000713.0363.

AP-SI.1Q, Rev. 2, ICN 4. *Software Management*. Washington, D.C.: U.S. Department of Energy, Office of Civilian Radioactive Waste Management. ACC: MOL.20000223.0508.

AP-SV.1Q, Rev. 0, ICN 2. *Control of the Electronic Management of Information*. Washington, D.C.: U.S. Department of Energy, Office of Civilian Radioactive Waste Management. ACC: MOL.20000831.0065.

ASME (American Society of Mechanical Engineers) 1995. *1995 ASME Boiler and Pressure Vessel Code*. New York, New York: American Society of Mechanical Engineers. TIC: 245287.

ASTM A 276-91a. 1991. *Standard Specification for Stainless and Heat-Resisting Steel Bars and Shapes*. Philadelphia, Pennsylvania: American Society for Testing and Materials. TIC: 240022.

ASTM A 516/A 516M - 90. 1991. *Standard Specification for Pressure Vessel Plates, Carbon Steel, for Moderate- and Lower-Temperature Service*. Philadelphia, Pennsylvania: American Society for Testing and Materials. TIC: 240032.

ASTM A 240/A 240M-97a. 1997. *Standard Specification for Heat-Resisting Chromium and Chromium-Nickel Stainless Steel Plate, Sheet, and Strip for Pressure Vessels*. West Conshohocken, Pennsylvania: American Society for Testing and Materials. TIC: 239431.

ASTM B 811-90. 1991. *Standard Specification for Wrought Zirconium Alloy Seamless Tubes for Nuclear Reactor Fuel Cladding*. Philadelphia, Pennsylvania: American Society for Testing and Materials. TIC: 239780.

ASTM B 575-97. 1998. *Standard Specification for Low-Carbon Nickel-Molybdenum-Chromium, Low-Carbon Nickel-Chromium-Molybdenum, Low-Carbon Nickel-Chromium-Molybdenum-Copper and Low-Carbon Nickel-Chromium-Molybdenum-Tungsten Alloy Plate*,

*Sheet, and Strip*. West Conshohocken, Pennsylvania: American Society for Testing and Materials. TIC: 241816.

ASTM G 1-90 (Reapproved 1999). 1990. *Standard Practice for Preparing, Cleaning, and Evaluating Corrosion Test Specimens*. West Conshohocken, Pennsylvania: American Society for Testing and Materials. TIC: 238771.

NLP-2-0, Rev. 5, ICN 1. *Determination of Importance Evaluations*. Las Vegas, Nevada: CRWMS M&O. ACC: MOL.20000713.0360.

QAP-2-0, Rev. 5. *Conduct of Activities*. Las Vegas, Nevada: CRWMS M&O. ACC: MOL.19980826.0209.

### **9.3 SOURCE DATA**

MO0006J13WTRCM.000. Recommended Mean Values of Major Constituents in J-13 Well Water. Submittal date: 06/075/2000. Submit to RPC URN-0532

INTENTIONALLY LEFT BLANK

**APPENDIX A**

**SHIPPINGPORT LWBR DOE SNF CANISTER AND BASKET ASSEMBLY**





INTENTIONALLY LEFT BLANK

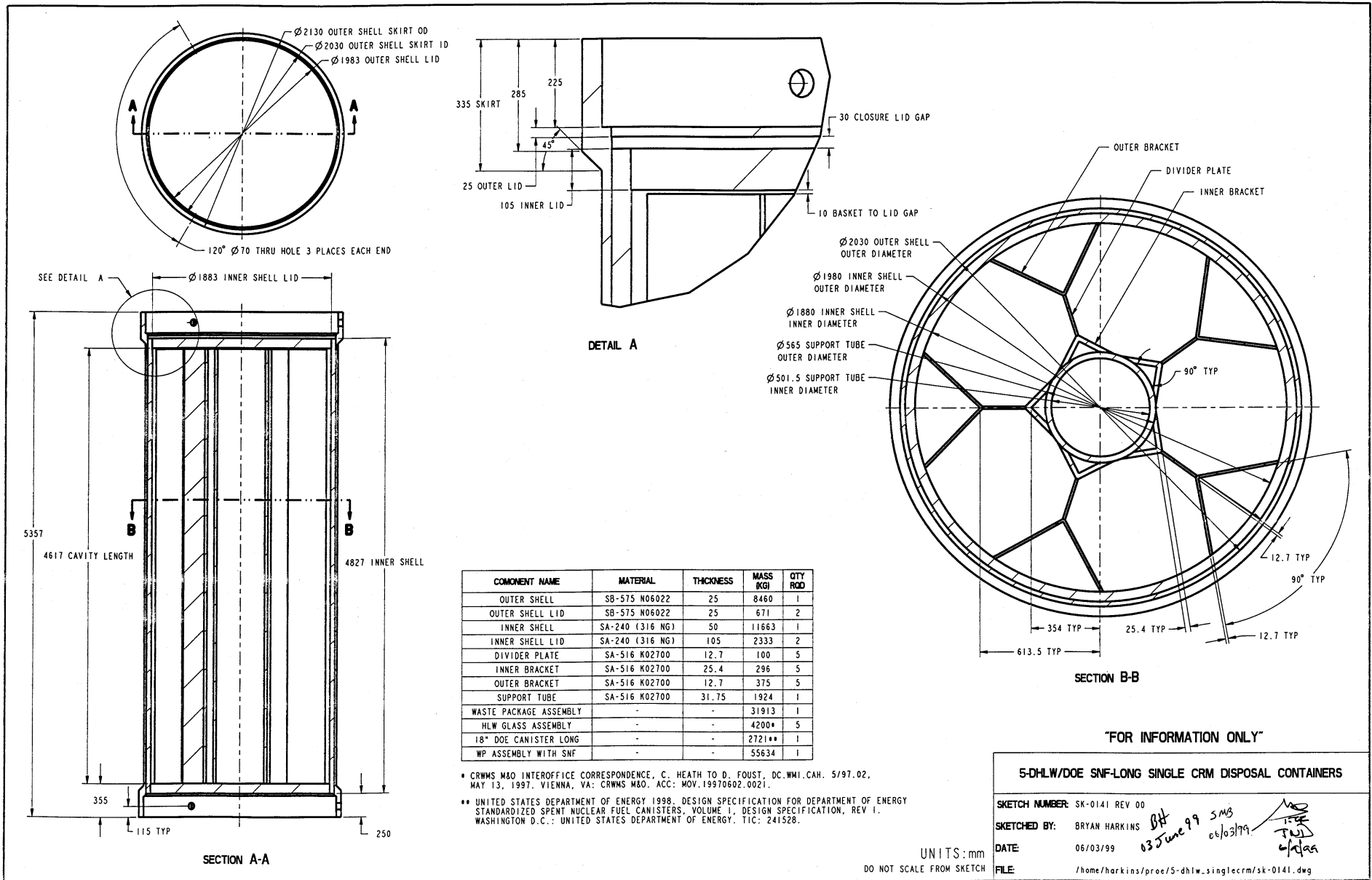
**APPENDIX B**

**5-DHLW/DOE SNF-LONG SINGLE CRM DISPOSAL CONTAINER**



# APPENDIX B

## 5-DHLW/DOE SNF-LONG SINGLE CRM DISPOSAL CONTAINER



INTENTIONALLY LEFT BLANK